THE ROLES OF THE LAMININ EXTRACELLULAR MATRIX AND MIGRATORY NEURAL CREST CELLS DURING OPTIC CUP MORPHOGENESIS

by

Chase Dallas Bryan

A dissertation submitted to the faculty of
The University of Utah
in partial fulfillment of the requirements for the degree of

Doctor of Philosophy

Department of Human Genetics

The University of Utah

May 2018

The University of Utah Graduate School

STATEMENT OF DISSERTATION APPROVAL

The dissertation of **Chase Dallas Bryan**

has been approved by the following supervisory committee members:

Kristen Kwan	, Chair	**01/31/2018** Date Approved
Monica Vetter	, Member	**01/31/2018** Date Approved
Charles Murtaugh	, Member	**01/31/2018** Date Approved
Rodney Stewart	, Member	**01/31/2018** Date Approved
Mark Metzstein	, Member	**01/31/2018** Date Approved

and by **Lynn Jorde** , Chair/Dean of

the Department/College/School of **Human Genetics**

and by David B. Kieda, Dean of The Graduate School.

ABSTRACT

The development of an organ involves establishment of its shape, which is often critical for proper function. Perhaps the most striking case where organ shape dictates function is in the vertebrate eye, where vision depends on many tissues taking on the correct shape, and becoming correctly oriented relative to all the other surrounding tissues. The basic shape of the eye is set up very early during embryogenesis, through development of the vertebrate optic cup. Disruptions to the early stages of optic cup morphogenesis can have profound effects on subsequent eye development and function. Therefore, understanding how the eye normally takes its shape during these early stages is critical to understand how the eye can become disrupted and cause vision loss or blindness. During optic cup morphogenesis, the developing eye is surrounded by a complex extracellular matrix, but the function of any given component of the extracellular matrix in this morphogenetic process has been unknown until now. Additionally, neural crest cells migrate around the optic cup during its development, but whether these cells are required for optic cup morphogenesis and how they shape the eye has remained mysterious until now. Here, we use the developing zebrafish optic cup to study the contribution of two extracellular matrix proteins during optic cup morphogenesis, laminin and nidogen. We find that both of these proteins are required for specific aspects of optic cup morphogenesis, and find that the neural crest which migrates around the developing eye is partially responsible for generating its extracellular matrix.

This dissertation is dedicated to my mother, Holly.

TABLE OF CONTENTS

LIST OF FIGURES

Figures

ACKNOWLEDGMENTS

I would like to thank Kristen Kwan for being such a wonderful mentor, teacher, and friend to me. I am endlessly grateful to have been given a chance to work with such a brilliant, thoughtful scientist. You have always had an open door and I remain constantly amazed at how supportive you are of your lab members and all you manage to accomplish every single day. I will greatly miss your excitement about the latest pieces of data I found or the newest restaurant we're all dying to eat at, and I especially thank you for helping open my palate for new foods. It was an honor to be your first doctoral trainee, and I hope your research group continues to thrive for many years.

I would also like to thank the members of my thesis committee, Monica Vetter, Charlie Murtaugh, Mark Metzstein, and Rodney Stewart. Thanks in part to your support and guidance, committee meetings were not daunting but were always helpful and kept me on track. I specifically chose you as mentors because I expected you to challenge me at every step of my training, and I am grateful for your willingness to do so in a way that helped me grow as a scientist.

Thanks to the entire Human Genetics department, both past and present. I was very excited to join this department thanks to its challenging but supportive environment. The research-in-progress and journal clubs we present are exceptionally helpful in training us to present to an audience with a wide variety of expertise, and the feedback we receive from the entire faculty is invaluable.

Thank you to George Eisenhoffer, Thomas Marshall and Jimmy Delalande. Your support and mentorship as I began my scientific career are the driving force that encouraged me to follow the path into academic science, and I am forever grateful for your guidance along the way.

Thank you to the members of the Kwan Lab. I feel so lucky to know such wonderful and brilliant people, and I am glad to call you all friends. Sarah Lusk, thank you for being like the annoying little sister I never had growing up. Macaulie Casey, thank you for joining the lab and dishing everything right back when someone messes with you. Thomas Brown, thank you for supporting my unpopular musical tastes. Brooke Froelich Murray, thank you for never letting me forget that my musical tastes are unpopular. Sydney Stringham, thank you for organizing us: we're all good friends, but thanks to your efforts we actually got together to do fun things together. Thank you to Keith Carney for being the added dose of sass that our lab desperately needed. Finally, thank you so much to Hannah Gordon. You were a wonderful friend even before you joined the lab, and it was so exciting to find out you would be a colleague as well. I'll always be grateful for your scientific passion and friendship.

I would like to thank all the friends I've made throughout my graduate career at the University of Utah. Thank you to Emily Wirick for being a great friend and labmate for the first several years of graduate school, we struggled and learned and grew together. Thank you to Erin Dickson, Brittany Fleming, Maggie Alexander, and Stephanie Meek, as well as the other close friends I made in the early days of graduate school. Thank you to Maria Elias, Kim Frizzell, Alex Locke, and Mark Smith for your unwavering friendship over the past few years, I feel lucky to know such wonderful and kind people.

Thank you to Jonathan Nelson for being a great friend and mentor during the latter stages of graduate school, your optimism and excitement about science were exceptionally helpful when progress slowed or when things got hard, and your hearty chuckle made every day brighter. Thank you to Ben Jussila for being a wonderful labmate and friend, I'm grateful for your willingness to always lend an ear or spend a night commiserating over difficult times. Thank you to Eric Bogenschutz for helping me embrace the exceptionally nerdy side of myself and for showing me the virtues of terrible cinema; I eagerly look forward to all future bad movies we can enjoy together. Thank you to Clay Carey for reminding me that I really do enjoy camping, I still think back fondly on our backpacking trips to southern Utah and how much I love this beautiful state. Thank you to Jacob Cooper and Jenna Goodrum for being such brilliant scientists and supportive friends, running and triathlon training are so much more fun with you two than by myself.

I want to thank Michelle Kossack for being a wonderful and supportive partner for the last several years. I am extremely lucky to have met you and I am excited to see what our future together holds.

Thank you to my brother Chad and my sister-in-law Sharlee for encouraging me to follow my dreams and stay excited about science. Thank you to my father Sam for igniting my passion for science and learning, I doubt I would be a scientist today were it not for your interest in trying to understand how the world works. Finally, to my mother Holly: you have been the most steadfast supporter of me following my dreams and encouraging me to be the absolute best I can be, I truly believe I could not have done this without your help and love. Thank you.

CHAPTER 1

INTRODUCTION

Developmental morphogenesis establishes the shape and structure of tissues and organs. Morphogenesis occurs through cellular and tissue-level movements, rearrangements and shape changes, in addition to any proliferation or cell death that occurs alongside these movements. While organ shapes may vary across species, the shapes those organs adopt within a species are largely consistent. With few exceptions, organs and the tissues that comprise them must adopt a stereotypical shape in order to function correctly. The morphogenetic programs that shape organs can differ widely and generate drastically different structures. For example, branching morphogenesis, required for lung, mammary and circulatory systems can give rise to vast arbors of branched tissues with extremely high surface areas. Other organs such as the brain and eye are generated through folding and rearrangements of entire epithelial sheets, which gives rise to exquisitely patterned and laminated structures which are critical for organ function. These epithelia are polarized along an apical-basal axis, and actomyosin constriction mediated tissue folding can occur at either end of this axis to drive shape changes in specific contexts. However, regulation of the site where constriction occurs is absolutely critical for laminated tissues like the vertebrate eye, where the proper orientation and positioning of multiple layers of cells is necessary for the organ to function correctly.

Apical constriction is the better characterized mechanism, and is responsible for folding events during gastrulation in sea urchin and *Drosophila* as well as during neural tube folding in vertebrates, reviewed in (Martin and Goldstein, 2014). Much less is known about basal constriction; it has primarily been characterized during the folding events that shape the zebrafish midbrain-hindbrain boundary and the medaka retina (Gutzman et al., 2015; Martinez-Morales et al., 2009). While both apical and basal constriction rely on actomyosin mediated constriction, their occurrence at opposite sides of the cell suggest mechanistic differences in regulation of where these events occur within the cell and the epithelial sheet. Both instances of basal constriction also appear to be regulated through adherence to the basal extracellular matrix (ECM), as disruptions to attachment to the ECM in either system leads to disruptions in basal constriction. Despite the importance of these epithelial constriction programs, little else is known about how they are controlled along the apical-basal axis.

Many molecules and programs that drive morphogenesis are intrinsic to the tissue undergoing morphogenesis. However, most organs develop in a complex environment comprised of many tissues and cell types, and interactions between these tissues are critical for their development. Interactions between developing epithelia and surrounding mesenchymal cells are observed throughout the embryo, and many of these interactions have been characterized in the developing mouse. While signaling molecules are frequently responsible for tissue-tissue communication and morphogenetic remodeling events, mesenchymal cells also regulate epithelial morphogenesis through modifications to the ECM. In the tooth placode, salivary gland, lung and kidney, specific ECM components are required for morphogenesis of the epithelia. These ECM proteins are

essential for development of the epithelium, as disruptions to their function through antibody blocking or genetic loss causes severe morphogenetic deficits in each of these organs. Intriguingly, the surrounding mesenchymal cells are the sole source of many of those ECM components which are critical for epithelial development.

There is a relative abundance of examples demonstrating that organ morphogenesis requires interactions with the ECM in addition to entirely separate tissues and cell types. Despite this, our understanding of how these interactions drive specific morphogenetic events is still quite lacking. Not only have many organs not been adequately described or investigated, but the specific molecules required for many morphogenetic movements are still not well known. We seek to understand how the optic cup, the embryonic precursor to the eye, forms during development and what molecules are required for its formation. To understand how the embryonic optic cup takes its complex shape and establishes the platform that will become the adult eye, we use the developing zebrafish (*Danio rerio*) to study this process. The zebrafish optic cup provides a unique system to study morphogenesis, where the effects of both intrinsic interactions with the ECM, as well as the contribution of outside tissues and molecules can be observed microscopically throughout development, and disrupted through genetic means.

Zebrafish optic cup morphogenesis

Optic cup morphogenesis in zebrafish occurs following the same general morphological principles as in other vertebrates, albeit much more rapidly than in most other vertebrate model systems (Kwan et al., 2012; Schmitt and Dowling, 1994). Optic

cup morphogenesis takes roughly 14 hours from start to finish in the zebrafish, whereas the same process can take days to weeks to occur in other vertebrates. Morphogenesis begins around 10 hours postfertilization (hpf), after the eye field has been specified within the anterior neural plate. The first stage of morphogenesis is bilateral evagination of the optic vesicles from the eye field of the developing brain, with eye field cells acquiring epithelial characteristics earlier than surrounding brain tissue (Ivanovitch et al., 2013). Evagination of the optic vesicle from the midline continues until approximately 16 hpf. As evagination continues, the optic vesicle begins to elongate in the posterior direction as cells within the optic vesicle begin to undergo a tissue-wide pinwheel movement; this series of movements occurs from approximately 12-14 hpf. During elongation, a furrow forms at the posterior interface between the optic vesicle and forebrain. The connection between the brain and optic vesicle continues to shrink as this furrow moves anteriorly, while the connection between the optic vesicle and forebrain constricts and forms the optic stalk. Around 16 hpf, the overlying ectoderm begins to thicken and form the lens placode. At this same time, the lateral layer of the optic vesicle buckles and begins to invaginate around the nascent lens placode. During invagination, cells in the lateral, lens-facing side of the optic vesicle begin to elongate and adopt the shape of neural retinal progenitor cells. Simultaneously, cells at the center of the medial, brain-facing layer of the optic vesicle begin to flatten; these will become the retinal pigment epithelium (RPE). Between 18-24 hpf, cells near the interface between medial and lateral layers of the optic vesicle move around the lateral margins of the optic vesicle to enter the neural retina; this process is called rim movement. During invagination, the ventral surface of the optic cup and optic stalk buckle centrally and begin forming the

choroid fissure, a thin, transient structure bounded by the nasal and temporal sides of the ventral neural retina. At 24 hpf, the lens placode has become semispherical and is beginning to pinch off the overlying ectoderm; this signals the end of optic cup morphogenesis. Once this process is complete, the optic cup is fully formed and is comprised of three separate tissues: the lens, neural retina, and RPE. One final movement of note occurs throughout the entirety of optic cup morphogenesis and continues after the lens separates from the ectoderm: anterior rotation. The optic vesicle initially is comprised of two layers oriented with the dorsal and ventral axes of the embryo. Throughout optic cup morphogenesis, these tissues will undergo rotation such that the initially dorsal layer becomes the anterior (nasal) side of the optic cup; the ventral layer will ultimately be oriented at the posterior (temporal) side.

Extracellular matrix in optic cup morphogenesis

A rich and complex extracellular matrix (ECM) surrounds the vertebrate optic cup throughout optic cup morphogenesis. The major components of this ECM are laminin-1, collagen IV, heparin sulfate proteoglycans, fibronectin, and nidogen. Each of these proteins has been observed surrounding optic cups from many vertebrate evolutionary lineages (Kwan, 2014). However, despite the evolutionary conservation of expression of these proteins around the eye, their function during optic cup morphogenesis is still largely unknown.

Extracellular matrices have many known functions. These protein rich matrices serve to provide structural rigidity and stability to the tissues they surround, and are critical for proper mechanotransduction to attached cells and tissues (Schwartz, 2010;

Vining and Mooney, 2017). While there are some components which are common to all extracellular matrices, their makeup can vary based on the tissues that generate them. The composition of the ECM can in turn regulate how cells and tissues respond to interactions with their environment, and different ECM compositions can elicit different responses within the same tissue (Klaas et al., 2016). ECMs also serve to sequester signaling molecules such as TGF-β, and the three-dimensional conformation of the matrix or mechanical load on the ECM regulates availability of these signaling molecules (Hinz, 2015). Binding to the ECM frequently serves as a survival signal for epithelia, and loss of contact with the ECM can cause cell death through a specialized apoptotic pathway called anoikis (Frisch and Francis, 1994). Finally, deposition of a basal ECM is critical for establishment of apicobasal polarity within an epithelial tissue.

Of the ECM proteins known to surround the developing optic cup, the function of laminin is the best understood. Laminin is arguably the most important component of the ECM, as many studies have implicated basal secretion of laminin as the initiating event which precedes formation of the basement membranes which surround all organs (Colognato and Yurchenco, 2000). Without laminin, other matrix components are disorganized and a functional basement membrane does not form (Jayadev and Sherwood, 2017). Several recent studies have established a role of laminin in very early optic cup evagination and during later stages of lens morphogenesis (Ivanovitch et al., 2013; Pathania et al., 2014; Semina et al., 2006). However, its role during the bulk of optic cup morphogenesis has remained unexplored. Chapter 2 of this dissertation describes in detail the necessity of laminin-α1 in establishing polarity within the optic vesicle and its roles in shaping the eye.

The contribution of other ECM components to optic cup morphogenesis is much less well understood. Fibronectin and collagen IV are particularly difficult to study, in part due their requirement during earlier stages of development; maternal deposition confounds loss of function studies, and disruptions to maternal and zygotic supplies impairs development long before optic cup morphogenesis occurs (Latimer and Jessen, 2010). However, this should not discount their roles in shaping the eye. Recent conditional deletion studies in mouse have demonstrated a role for fibronectin in lens morphogenesis and optic cup invagination (Huang et al., 2011), and zebrafish fibronectin mutants are microphthalmic and display anterior lens defects at later stages of eye development (Hayes et al., 2012). Nidogen, an ECM crosslinking protein, is required for retinal organoids to undergo optic cup morphogenesis *in vitro* (Eiraku et al., 2011), but its role during eye development *in vivo* has been overlooked until now. Chapter 3 of this dissertation demonstrates that nidogen is required for specific cellular movements during optic cup morphogenesis and proper basement membrane deposition surrounding the RPE.

Periocular mesenchyme in optic cup morphogenesis

The vertebrate eye forms in close proximity to multiple non-eye tissues, yet each of these tissues serves important roles in the development of the eye. Extraocular mesenchymal cells have long been noted to interact with the optic vesicle during its morphogenesis into the optic cup, but very little is known regarding what these cells provide to the developing eye. Work from chick optic vesicle explant cultures demonstrates that the mesenchyme is required for induction of the RPE, possibly through

TGF-β signaling (Fuhrmann et al., 2000). Studies in mouse have demonstrated a role for periocular mesenchyme in patterning and shaping the optic cup, but the underlying mechanism is unclear (Bassett et al., 2010). The periocular mesenchyme is a heterogeneous population comprised of neural crest and mesodermally derived mesenchyme, but a specific role for either cell type during optic cup morphogenesis remains unknown. Zebrafish *one-eyed pinhead* mutants display severe defects in mesoderm development; as the name suggests, they also display severe optic cup morphogenesis defects (Schier et al., 1997). This indicates a prominent role for the mesoderm in regulating eye development, possibly through modulation of Nodal signaling to the eye field. Recent work in zebrafish has suggested that the neural crest subset of periocular mesenchymal cells regulate Sonic Hedgehog signaling within the optic cup and may be involved in choroid fissure formation (Sedykh et al., 2017). Mesenchymal cells are also necessary for proper fusion of the choroid fissure at later stages of eye development, and fusion of the choroid fissure appears to be mediated in part through proteolysis of the basement membranes lining the structure (Hero, 1990; Hero et al., 1991; James et al., 2016; Lupo et al., 2011; Weiss et al., 2012). In other organ systems such as the lung and kidney, mesenchymal cells provide ECM components which are required for epithelial morphogenesis. Chapter 3 of this dissertation demonstrates that the neural crest cell population is absolutely necessary for optic cup development, and describes the roles for neural crest cells in regulating specific cellular movements during optic cup morphogenesis. We find that these movements are dependent on nidogen, an ECM protein which is not expressed in the optic vesicle but rather in the surrounding neural crest.

The role of apical polarity proteins in morphogenesis

Establishment of the apicobasal polarity axis is critical for the function of epithelial tissues and organs. For example, formation of an apical lumen is central to the development of many epithelial tissues such as the lung, mammary gland, and intestine. The apical surface is specified through a complex process and depends on directional, basal secretion of ECM proteins. The Par3/Par6/aPKC apical polarity complex is subsequently sequestered to the opposite side of the cell which establishes the apical surface (Denef et al., 2008). In other systems, proper recruitment of apical polarity proteins to their target surfaces is required for cellular and tissue morphogenesis (Horne-Badovinac et al., 2001; Jones and Metzstein, 2011). The optic cup is a polarized neuroepithelium, but it remains unclear whether establishment of the apical surface is required for morphogenesis of the eye. The apical complex protein aPKC is required for maintenance of retinal architecture at later stages of eye development (Horne-Badovinac et al., 2001), but maternal contributions of apical complex proteins have occluded their study at early stages of optic cup morphogenesis. Multiple ECM components surround the optic cup, and it remains unclear what components of the ECM are required to establish apicobasal polarity. Additionally, cell-ECM adhesions are mediated through integrin-containing focal adhesions as well as the dystrophin/dystroglycan complex, both of which have been shown to regulate tissue polarity (Akhtar and Streuli, 2013; Deng et al., 2003). We sought to determine how interactions with the ECM affect apical polarity within the optic cup, and how specific polarity proteins regulate morphogenesis of the eye. Chapter 2 of this dissertation details our findings regarding how loss of laminin affects apical polarity within the eye, and data presented in Chapter 4 demonstrate that

the apical polarity complex is not required for optic cup morphogenesis. These data implicate an invaluable role of the ECM in driving optic cup morphogenesis, and suggest that many of the cell biological processes that regulate morphogenesis occur downstream of cell-ECM adhesion.

Summary

Zebrafish optic cup morphogenesis is an excellent system in which many questions regarding the mechanisms organ morphogenesis can begin to be answered. How does any given component of the ECM govern organ morphogenesis and what tissue movements depend on that particular molecule? What processes or signaling events are regulated by adhesion to the matrix? Does one matrix component affect different sites within the same tissue differently? How do separate tissues interact with each other during development and contribute to the morphogenesis of their neighbors? Work presented here begins to address some of these questions in the context of optic cup morphogenesis. Chapter 2 describes my work in uncovering the role of the extracellular matrix protein laminin-α1. Chapter 3 describes my work in defining a role for the neural crest in optic cup morphogenesis through modification of the extracellular matrix. In Chapter 2 and Chapter 4 I investigate the cell biological responses to adhesion to the laminin extracellular matrix. Finally, Chapter 4 also describes my work in positional cloning of a new mutant which displays a unique, previously uncharacterized defect in optic cup morphogenesis.

References

Akhtar, N., Streuli, C.H., 2013. An integrin-ILK-microtubule network orients cell polarity and lumen formation in glandular epithelium. Nat. Cell Biol. 15, 17–27. https://doi.org/10.1038/ncb2646

Bassett, E.A., Williams, T., Zacharias, A.L., Gage, P.J., Fuhrmann, S., West-Mays, J.A., 2010. AP-2a knockout mice exhibit optic cup patterning defects and failure of optic stalk morphogenesis. Hum. Mol. Genet. 19, 1791–1804. https://doi.org/10.1093/hmg/ddq060

Colognato, H., Yurchenco, P.D., 2000. Form and function: The laminin family of heterotrimers. Dev. Dyn. 218, 213–234. https://doi.org/10.1002/(SICI)1097-0177(200006)218:2<213::AID-DVDY1>3.0.CO;2-R

Denef, N., Chen, Y., Weeks, S.D., Barcelo, G., Schüpbach, T., 2008. Crag regulates epithelial architecture and polarized deposition of basement membrane proteins in Drosophila. Dev. Cell 14, 354–364. https://doi.org/10.1016/j.devcel.2007.12.012

Deng, W.-M., Schneider, M., Frock, R., Castillejo-Lopez, C., Gaman, E.A., Baumgartner, S., Ruohola-Baker, H., 2003. Dystroglycan is required for polarizing the epithelial cells and the oocyte in Drosophila. Development 130, 173–184. https://doi.org/10.1242/dev.00199

Eiraku, M., Takata, N., Ishibashi, H., Kawada, M., Sakakura, E., Okuda, S., Sekiguchi, K., Adachi, T., Sasai, Y., 2011. Self-organizing optic-cup morphogenesis in three-dimensional culture. Nature 472, 51–56. https://doi.org/10.1038/nature09941

Frisch, S.M., Francis, H., 1994. Disruption of epithelial cell-matrix interaction induces apoptosis. J. Cell. Biol. 124, 619–626. https://doi.org/10.1083/jcb.124.4.619

Fuhrmann, S., Levine, E.M., Reh, T.A., 2000. Extraocular mesenchyme patterns the optic vesicle during early eye development in the embryonic chick. Development 127, 4599–4609.

Gutzman, J.H., Sahu, S.U., Kwas, C., 2015. Non-muscle myosin IIA and IIB differentially regulate cell shape changes during zebrafish brain morphogenesis. Dev. Biol. 397, 103–115. https://doi.org/10.1016/j.ydbio.2014.10.017

Hayes, J.M., Hartsock, A., Clark, B.S., Napier, H.R.L., Link, B.A., Gross, J.M., 2012. Integrin 5/Fibronectin1 and focal adhesion kinase are required for lens fiber morphogenesis in zebrafish. Mol. Biol. Cell 23, 4725–4738. https://doi.org/10.1091/mbc.E12-09-0672

Hero, I., 1990. Optic fissure closure in the normal cinnamon mouse: An ultrastructural study. Investig. Ophthalmol. Vis. Sci. 31, 197–216.

Hero, I., Farjah, M., Scholtz, C.L., 1991. The prenatal development of the optic fissure in

colobomatous microphthalmia. Investig. Ophthalmol. Vis. Sci. 32, 2622–2635.

Hinz, B., 2015. The extracellular matrix and transforming growth factor-β1: Tale of a strained relationship. Matrix Biol. 47, 54–65. https://doi.org/10.1016/j.matbio.2015.05.006

Horne-Badovinac, S., Lin, D., Waldron, S., Schwarz, M., Mbamalu, G., Pawson, T., Jan, Y.N., Stainier, D.Y.R., Abdelilah-Seyfried, S., 2001. Positional cloning of heart and soul reveals multiple roles for PKCλ in zebrafish organogenesis. Curr. Biol. 11, 1492–1502. https://doi.org/10.1016/S0960-9822(01)00458-4

Huang, J., Rajagopal, R., Liu, Y., Dattilo, L.K., Shaham, O., Ashery-Padan, R., Beebe, D.C., 2011. The mechanism of lens placode formation: A case of matrix-mediated morphogenesis. Dev. Biol. 355, 32–42. https://doi.org/10.1016/j.ydbio.2011.04.008

Ivanovitch, K., Cavodeassi, F., Wilson, S.W., 2013. Precocious acquisition of neuroepithelial character in the eye field underlies the onset of eye morphogenesis. Dev. Cell 27, 293–305. https://doi.org/10.1016/j.devcel.2013.09.023

James, A., Lee, C., Williams, A.M., Angileri, K., Lathrop, K.L., Gross, J.M., 2016. The hyaloid vasculature facilitates basement membrane breakdown during choroid fissure closure in the zebrafish eye. Dev. Biol. 419, 262–272. https://doi.org/10.1016/j.ydbio.2016.09.008

Jayadev, R., Sherwood, D.R., 2017. Basement membranes. Curr. Biol. 27, R207–R211. https://doi.org/10.1016/j.cub.2017.02.006

Jones, T.A., Metzstein, M.M., 2011. A novel function for the PAR complex in subcellular morphogenesis of tracheal terminal cells in Drosophila melanogaster. Genetics 189, 153–164. https://doi.org/10.1534/genetics.111.130351

Klaas, M., Kangur, T., Viil, J., Mäemets-Allas, K., Minajeva, A., Vadi, K., Antsov, M., Lapidus, N., Järvekülg, M., Jaks, V., 2016. The alterations in the extracellular matrix composition guide the repair of damaged liver tissue. Sci. Rep. 6, 1–12. https://doi.org/10.1038/srep27398

Kwan, K.M., 2014. Coming into focus: The role of extracellular matrix in vertebrate optic cup morphogenesis. Dev. Dyn. 243, 1242–1248. https://doi.org/10.1002/dvdy.24162

Kwan, K.M., Otsuna, H., Kidokoro, H., Carney, K.R., Saijoh, Y., Chien, C.-B., 2012. A complex choreography of cell movements shapes the vertebrate eye. Development 139, 359–372. https://doi.org/10.1242/dev.071407

Latimer, A., Jessen, J.R., 2010. Extracellular matrix assembly and organization during zebrafish gastrulation. Matrix Biol. 29, 89–96.

https://doi.org/10.1016/j.matbio.2009.10.002

Lupo, G., Gestri, G., O'Brien, M., Denton, R.M., Chandraratna, R.A.S., Ley, S. V, Harris, W.A., Wilson, S.W., 2011. Retinoic acid receptor signaling regulates choroid fissure closure through independent mechanisms in the ventral optic cup and periocular mesenchyme. Proc. Natl. Acad. Sci. U. S. A. 108, 8698–8703. https://doi.org/10.1073/pnas.1103802108

Martin, A.C., Goldstein, B., 2014. Apical constriction: Themes and variations on a cellular mechanism driving morphogenesis. Development 141, 1987–98. https://doi.org/10.1242/dev.102228

Martinez-Morales, J.R., Rembold, M., Greger, K., Simpson, J.C., Brown, K.E., Quiring, R., Pepperkok, R., Martin-Bermudo, M.D., Himmelbauer, H., Wittbrodt, J., 2009. Ojoplano-mediated basal constriction is essential for optic cup morphogenesis. Development 136, 2165–2175. https://doi.org/10.1242/dev.033563

Pathania, M., Semina, E. V., Duncan, M.K., 2014. Lens extrusion from laminin alpha 1 mutant zebrafish. Sci. World J. 2014. https://doi.org/10.1155/2014/524929

Schier, A.F., Neuhauss, S.C., Helde, K.A., Talbot, W.S., Driever, W., 1997. The one-eyed pinhead gene functions in mesoderm and endoderm formation in zebrafish and interacts with no tail. Development 124, 327–342.

Schmitt, E.A., Dowling, J.E., 1994. Early eye morphogenesis in the zebrafish, Brachydanio rerio. J. Comp. Neurol. 344, 532–42. https://doi.org/10.1002/cne.903440404

Schwartz, M.A., 2010. Integrins and extracellular matrix in mechanotransduction. Cold Spring Harb. Perspect. Biol. 2. https://doi.org/http://dx.doi.org/10.2147/CHC.S21829

Sedykh, I., Yoon, B., Roberson, L., Moskvin, O., Dewey, C.N., Grinblat, Y., 2017. Zebrafish zic2 controls formation of periocular neural crest and choroid fissure morphogenesis. Dev. Biol. 429, 92–104. https://doi.org/10.1016/j.ydbio.2017.07.003

Semina, E. V, Bosenko, D. V, Zinkevich, N.C., Soules, K.A., Hyde, D.R., Vihtelic, T.S., Willer, G.B., Gregg, R.G., Link, B.A., 2006. Mutations in laminin alpha 1 result in complex, lens-independent ocular phenotypes in zebrafish. Dev. Biol. 299, 63–77. https://doi.org/10.1016/j.ydbio.2006.07.005

Vining, K.H., Mooney, D.J., 2017. Mechanical forces direct stem cell behaviour in development and regeneration. Nat. Rev. Mol. Cell Biol. 18, 728–742. https://doi.org/10.1038/nrm.2017.108

Weiss, O., Kaufman, R., Michaeli, N., Inbal, A., 2012. Abnormal vasculature interferes with optic fissure closure in lmo2 mutant zebrafish embryos. Dev. Biol. 369, 191–198. https://doi.org/10.1016/j.ydbio.2012.06.029

CHAPTER 2

LOSS OF *LAMININ ALPHA 1* RESULTS IN MULTIPLE STRUCTURAL DEFECTS AND DIVERGENT EFFECTS ON ADHESION DURING VERTEBRATE OPTIC CUP MORPHOGENESIS

Reprinted with permission from: Chase D. Bryan, Chi-Bin Chien and Kristen M. Kwan (2016) Loss of *laminin alpha 1* results in multiple structural defects and divergent effects on adhesion during vertebrate optic cup morphogenesis. *Developmental Biology* 416.

Developmental Biology 416 (2016) 324–337

Contents lists available at ScienceDirect

Developmental Biology

journal homepage: www.elsevier.com/locate/developmentalbiology

Original research article

Loss of *laminin alpha 1* results in multiple structural defects and divergent effects on adhesion during vertebrate optic cup morphogenesis

Chase D. Bryan [a], Chi-Bin Chien [b,†], Kristen M. Kwan [a,*]

[a] Department of Human Genetics, University of Utah, Salt Lake City, UT 84112, USA
[b] Department of Neurobiology and Anatomy, University of Utah, Salt Lake City, UT 84112, USA

ARTICLE INFO

Article history:
Received 19 January 2016
Received in revised form
8 June 2016
Accepted 16 June 2016
Available online 20 June 2016

Keywords:
Eye morphogenesis
Laminin
Adhesion
Cell polarity
Retina
Lens

ABSTRACT

The vertebrate eye forms via a complex set of morphogenetic events. The optic vesicle evaginates and undergoes transformative shape changes to form the optic cup, in which neural retina and retinal pigmented epithelium enwrap the lens. It has long been known that a complex, glycoprotein-rich extracellular matrix layer surrounds the developing optic cup throughout the process, yet the functions of the matrix and its specific molecular components have remained unclear. Previous work established a role for laminin extracellular matrix in particular steps of eye development, including optic vesicle evagination, lens differentiation, and retinal ganglion cell polarization, yet it is unknown what role laminin might play in the early process of optic cup formation subsequent to the initial step of optic vesicle evagination. Here, we use the zebrafish *lama1* mutant (*lama1*^{UW1}) to determine the function of laminin during optic cup morphogenesis. Using live imaging, we find, surprisingly, that loss of laminin leads to divergent effects on focal adhesion assembly in a spatiotemporally-specific manner, and that laminin is required for multiple steps of optic cup morphogenesis, including optic stalk constriction, invagination, and formation of a spherical lens. Laminin is not required for single cell behaviors and changes in cell shape. Rather, in *lama1*^{UW1} mutants, loss of epithelial polarity and altered adhesion lead to defective tissue architecture and formation of a disorganized retina. These results demonstrate that the laminin extracellular matrix plays multiple critical roles regulating adhesion and polarity to establish and maintain tissue structure during optic cup morphogenesis.

1. Introduction

In vertebrates, the eye initially forms as an outpocketing of tissue from the prospective brain neuroepithelium. The newly formed optic vesicle then undergoes a series of complex cell and tissue movements – including elongation, rotation, and invagination – to form the optic cup, which is comprised of neural retina and retinal pigmented epithelium enwrapping the lens. The cellular processes – movements, divisions, tissue-tissue interactions, and shape changes – underlying these morphogenetic events are beginning to be elucidated via a combination of live imaging and quantitative histology (Chow and Lang, 2001; England et al., 2006; Fuhrmann, 2010; Heermann et al., 2015; Ivanovitch et al., 2013; Kwan et al., 2012; Martinez-Morales and Wittbrodt, 2009; Picker et al., 2009; Rembold et al., 2006; Yang, 2004). But while the cellular processes comprising optic cup formation are being described, we lack a comprehensive understanding of the molecular pathways controlling these critical movements.

A compelling molecular candidate for regulating optic cup morphogenesis is the extracellular matrix component laminin. It has been known for decades that in all vertebrates, a glycoprotein-rich layer surrounds the developing optic cup and lens, and that laminin is a significant component of this meshwork (Hendrix and Zwaan, 1975; Hilfer and Randolph, 1993; Kurkinen et al., 1979; McAvoy, 1981; Parmigiani and McAvoy, 1984; Peterson et al., 1995; Svoboda and O'Shea, 1987; Tuckett and Morriss-Kay, 1986; Wakely, 1977; Webster et al., 1983, 1984). Laminin proteins form heterotrimers comprised of α, β, and γ chains. There are multiple forms of each chain in vertebrates, although the laminin-111 species (the heterotrimer of lama1 (laminin-α1), lamb1 (laminin-β1), and lamc1 (laminin-γ1)) is considered to be the predominant isoform during early development (Colognato and Yurchenco, 2000; Miner and Yurchenco, 2004). In zebrafish, multiple laminin chains are expressed during the period of optic cup morphogenesis, but their functional roles during this process are largely unexplored.

* Correspondence to: Department of Human Genetics, EIHG 5100, University of Utah Medical Center, 15 North 2030 East, Salt Lake City, UT 84112, USA .
E-mail address: kristen.kwan@genetics.utah.edu (K.M. Kwan).
† Deceased.

http://dx.doi.org/10.1016/j.ydbio.2016.06.025

Functional roles for laminin have been elucidated primarily using *in vitro* cell culture systems. As a part of the extracellular matrix, laminin serves as an adhesive substrate, yet how it interacts *in vivo* with other ECM components to modulate adhesion and focal adhesion assembly is poorly understood. It is known that laminin impacts cell survival: loss of attachment can lead to anoikis, a specific form of programmed cell death (Frisch and Francis, 1994; Juliano et al., 2004). Laminin can also regulate cell migration, in particular lamellipodial protrusions (Adams and Watt, 1993; Daley and Yamada, 2013). Finally, laminin is often critical for establishing and maintaining epithelial cell polarity, by serving as an extrinsic cue to specify the basal surface (Martin-Belmonte and Mostov, 2008). A role for laminin in optic cup formation could affect any – or all – of these processes: it is unclear which might be crucial for the actual morphogenetic process.

In zebrafish, mutant analysis has revealed many roles for lama1, including in development of notochord, muscle, and brain structure, neurogenesis, neuronal migration, and axon guidance (Biehlmaier et al., 2007; Grant and Moens, 2010; Jiang et al., 1996; Karlstrom et al., 1996; Parsons et al., 2002; Paulus and Halloran, 2006; Pollard et al., 2006; Schier et al., 1996; Sittaramane et al., 2009; Sztal et al., 2012; Wolman et al., 2008). In the visual system, previous work has defined roles for different laminin chains in various steps of eye development, with most studies focusing on later stages after optic cup formation. Analysis of *lamb1* and *lamc1* mutants revealed coloboma, structural defects in the eye indicating failure of some aspect of choroid fissure development (Lee and Gross, 2007). *lama1* mutants display lens degeneration, as well as defects in development of the ocular anterior segment, including cornea and iris (Pathania et al., 2014; Semina et al., 2006; Zinkevich et al., 2006). Less is known, however, about earlier stages of eye development, specifically optic cup formation. Detailed analysis of the initiating event, optic vesicle evagination, indicates that laminin (specifically, the *lamc1* mutant was examined) plays a critical role in organizing, coordinating, and delimiting the polarized elongation of retinal progenitors just as the optic vesicle emerges (Ivanovitch et al., 2013). By the end of optic cup formation, *lamb1* and *lamc1* mutants appear to exhibit a "protruding lens" phenotype (Parsons et al., 2002), suggesting some defect in the process of optic cup morphogenesis, possibly invagination. However, the phenotype has not been studied in detail, and underlying cellular defects during optic cup formation have not been identified.

Taken together, these data suggest critical roles for laminin extracellular matrix proteins during eye development, yet much remains to be determined. What role does laminin play throughout optic cup morphogenesis? Are there specific tissue morphogenetic events that are dependent upon laminin? How does laminin regulate focal adhesion assembly, specifically during these morphogenetic events, and what other functions might laminin carry out? To address these questions, we are using the zebrafish mutant *bashful*^{UW1} (also called *lama1*^{UW1}), in which the *laminin alpha 1* (*lama1*) gene is disrupted (Paulus and Halloran, 2006; Semina et al., 2006). Using 4D timelapse imaging and visualization, we determine how loss of *lama1* affects optic cup morphogenesis beyond evagination. We examine focal adhesion assembly during optic cup formation, determine how this is disrupted by loss of *lama1*, and then investigate how loss of *lama1* affects several aspects of tissue morphogenesis, including cell survival, migration, shape changes, and polarity. Our data suggest that the laminin extracellular matrix is required for multiple specific morphogenetic events, acting through establishment of cell polarity and spatiotemporally-specific regulation of focal adhesion assembly.

2. Material and methods

2.1. Zebrafish

Embryos from *lama1*^{UW1} heterozygous incrosses were raised at 28.5–30 °C and staged according to time post fertilization and morphology (Kimmel et al., 1995). For all experiments, control embryos consisted of *lama1*^{UW1} wild type and heterozygous carrier siblings.

2.2. RNA synthesis and injections

Capped RNA was synthesized using pCS2 templates (pCS2-EGFP-CAAX, pCS2FA-H2A.F/Z-mCherry, pCS2FA-mCherry-CAAX, pCS2-EGFP-vinculin, pCS2-pard3-GFP), the mMessage mMachine SP6 kit (Ambion), purified (Qiagen RNeasy Mini Kit) and ethanol precipitated. 300–500 pg RNA (EGFP-CAAX, H2A.F/Z-mCherry, pard3-GFP) was injected into the cell of 1-cell stage embryos. For analysis of focal adhesion assembly, EGFP-vinculin and mCherry-CAAX (250 pg RNA each) were co-injected into the cell of 1-cell stage embryos.

2.3. Antibody staining

Embryos were fixed at the appropriate stage in 4% paraformaldehyde, permeabilized in TBST (TBS + 0.1% Triton X-100), and blocked in TBST + 2% BSA. Anti-laminin antibody (Sigma #L9393) was diluted 1:100, anti-vinculin antibody (Sigma #V4505) was diluted 1:100, anti-activated caspase-3 antibody (BD Pharmingen #559565) was diluted 1:200, anti-aPKC (PKC ζ (C-20) Santa Cruz Biotechnology #sc-216) was diluted 1:100, anti-fibronectin antibody (Sigma #F3648) was diluted 1:100. Alexa Fluor 488 goat anti-rabbit secondary (Life Technologies, A-11008) or Alexa Fluor 488 goat anti-mouse secondary (Life Technologies, A-11001) was co-incubated with 1 μM TOPRO-3 iodide (Life Technologies, T3605). Embryos were cleared in 70% glycerol for imaging.

2.4. Imaging

For timelapse imaging, embryos (12 hpf) were dechorionated, embedded in 1.6% low melting point agarose (in E2 + gentamycin) in DeltaT dishes (Bioptechs, #0420041500 C). E2 + gentamycin was overlaid, and the dish covered to prevent evaporation. Images were acquired using an Olympus FV1000 or Zeiss LSM710 laser scanning confocal microscope. 4-dimensional datasets were acquired: all datasets except for EGFP-vinculin imaging were acquired with the following parameters: 36 z-sections, 3.52 μm z-step, 40X water-immersion objective (1.15 NA). EGFP-vinculin 4-dimensional datasets (Fig. 3) were acquired with the following parameters: 63 z-sections, 2.1 μm z-step, 40X water-immersion objective (1.2 NA). For *in toto* eye imaging, time between z-stacks was 3.43 min (Fig. 1), 3.5 min (Fig. 3), 4.22 min and 4 min (Fig. 5 control and mutant, respectively), and 4.5 min (Fig. 6).

For Kaede photoconversion, Olympus Fluoview or Zeiss Zen software was used to expose a rectangular R. O. I. to 405 nm light for 15–20 s. Efficiency of photoconversion was assayed by loss of green and gain of red fluorescence in the R. O. I.

For all timelapse imaging experiments, datasets were acquired without knowledge of embryo genotype. After imaging was completed, embryos were de-embedded and genotyped. At least 3 timelapse datasets were acquired for all conditions presented.

2.5. Image processing and analysis

Image data were processed using ImageJ. Volume rendering was performed using Amira (Visage Imaging) or FluoRender (Wan

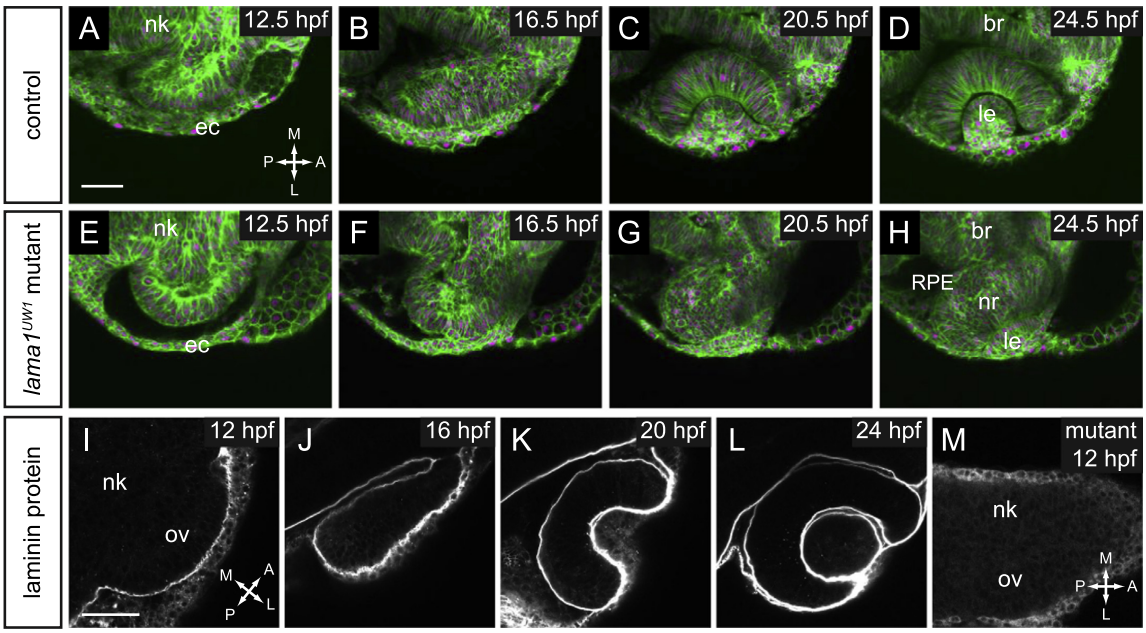

Fig. 1. Timelapse confocal microscopy reveals severe defects in optic cup formation in *lama1*^{UW1} mutant. (A-H) Single confocal slices from 4D datasets of optic vesicle morphogenesis, 12.5–24.5 hpf. EGFP-CAAX (membranes, *green*), H2A.F/Z-mCherry (nuclei, *magenta*). (A-D) Optic cup formation in control embryo. (E-H) Optic cup formation in *lama1*^{UW1} mutant embryo. Dorsal views; scale bar, 50 μm. (I-M) Localization of laminin protein. (I-L) In control embryos, laminin protein is found lining basal surfaces of developing eye and brain. (M) *lama1*^{UW1} mutant embryo reveals absence of laminin protein from early stages of optic vesicle development. *nk*, neural keel; *ov*, optic vesicle; *ec*, ectoderm; *br*, brain; *RPE*, retinal pigmented epithelium; *nr*, neural retina; *le*, lens. A, anterior; P, posterior; M, medial; L, lateral.

et al., 2009). Tissue volumes were measured using Amira after manual segmentation based on the membrane channel. Optic stalk cross section area was measured using Amira, after manual (slice by slice) segmentation of the interface between the retina and optic stalk.

2.5.1. Furrow angle measurements

Furrow angle was measured using the ImageJ angle tool. Within the z-stack, the slice containing the greatest optic vesicle area (representing the dorsal-ventral mid-point of the optic vesicle) was used for the measurement. A 25 μm radius circle was centered at the vertex of the optic stalk furrow. The first point of the angle was selected where the circle intersected with the neural keel, the second point of the angle was the vertex of the optic stalk furrow, and the third point of the angle was selected where the circle intersected with the optic vesicle (shown in Fig. 2F and G).

2.5.2. Invagination angle measurements

Invagination angle was also measured using the ImageJ angle tool. Within the z-stack, the slice containing the greatest lens area (representing the dorsal-ventral mid-point of the lens) was used for the measurement. The first point of the angle was selected at the center of the retina, just behind the lens, the second point of the angle (the vertex) was selected at one outer margin of retina, and the third point of the angle was selected at the other outer margin of the retina (Fig. 2P).

2.5.3. Focal adhesion quantification

Quantification of ECM adhesion using EGFP-vinculin was performed as follows: ratiometric analysis was performed on single confocal slices within the z-stack at the dorsal-ventral midpoint of the optic vesicle (14 hpf, for optic stalk furrow measurements), or at the dorsal-ventral midpoint of the lens (24 hpf, for lens-retina interface measurements). A 25 μm radius circle was centered at the vertex of the optic stalk furrow or deepest point of the lens-retina interface, then fluorescence intensity quantified along the basal surface within that circle (Fig. 3, yellow-bound regions). EGFP-vinculin fluorescence intensity was normalized to mCherry-CAAX intensity within the same area. Enrichment at the optic stalk furrow or lens-retina interface was determined by comparison to similar-sized regions at the brain midline (Fig. 3, blue-bound regions), a place where membrane components might be enriched, though not in an ECM-dependent manner, due to cell constriction at the apical surface.

Fig. 2. Quantitative analysis of *lama1*^{UW1} mutant phenotype. (A-E) Analysis of eye size at 24 hpf. (A-D) Volume renderings of control (A,B) and mutant (C,D) eyes. Neural retina + RPE (*blue*), lens (*yellow*). (A,C) Dorsal views. (B,D) Lateral views. *arrowhead*, choroid fissure; *asterisk*, choroid fissure missing in mutant. (E) Quantification of optic cup and lens volume in control and mutant eyes shows no significant difference in eye size. (F-H) Quantification of furrow angle during initial stages of optic stalk constriction. Single confocal section of control (F) and mutant (G) embryos, membrane channel (*gray*) at 14 hpf. A circle with a 25 μm radius was placed with its center at the vertex of the furrow, and angle was calculated by drawing radii to positions at which the circle intersected the optic vesicle and brain neuroepithelium. (H) Quantification of furrow angle demonstrates that the furrow exhibits a significantly larger angle in *lama1*^{UW1} mutants. (I-M) Visualization and quantification of optic stalk constriction. (I-L) 3D rendering of optic stalk cross-section (*orange*) over membrane channel (*gray*) at 24 hpf. (I,K) Dorsal views. (J,L) Face-on views of the optic stalk cross section. (M) Quantification of optic stalk cross section area shows that optic stalk constriction is impaired in *lama1*^{UW1} mutant embryos. (N-Q) Quantification of invagination angle. (N,O) Single confocal images of membrane channel (gray) in *lama1*^{UW1} control (N) and mutant (O) eyes at 24 hpf. Lines (*yellow*) were drawn to determine angle of invagination. (P) Schematic demonstrating how invagination angle (α) was determined. (Q) Quantification of invagination angle shows a severe defect in invagination in *lama1*^{UW1} mutant embryos. numbers at base of graph show embryos scored (one eye each);*$P < 0.001$, using the student's *t*-test.

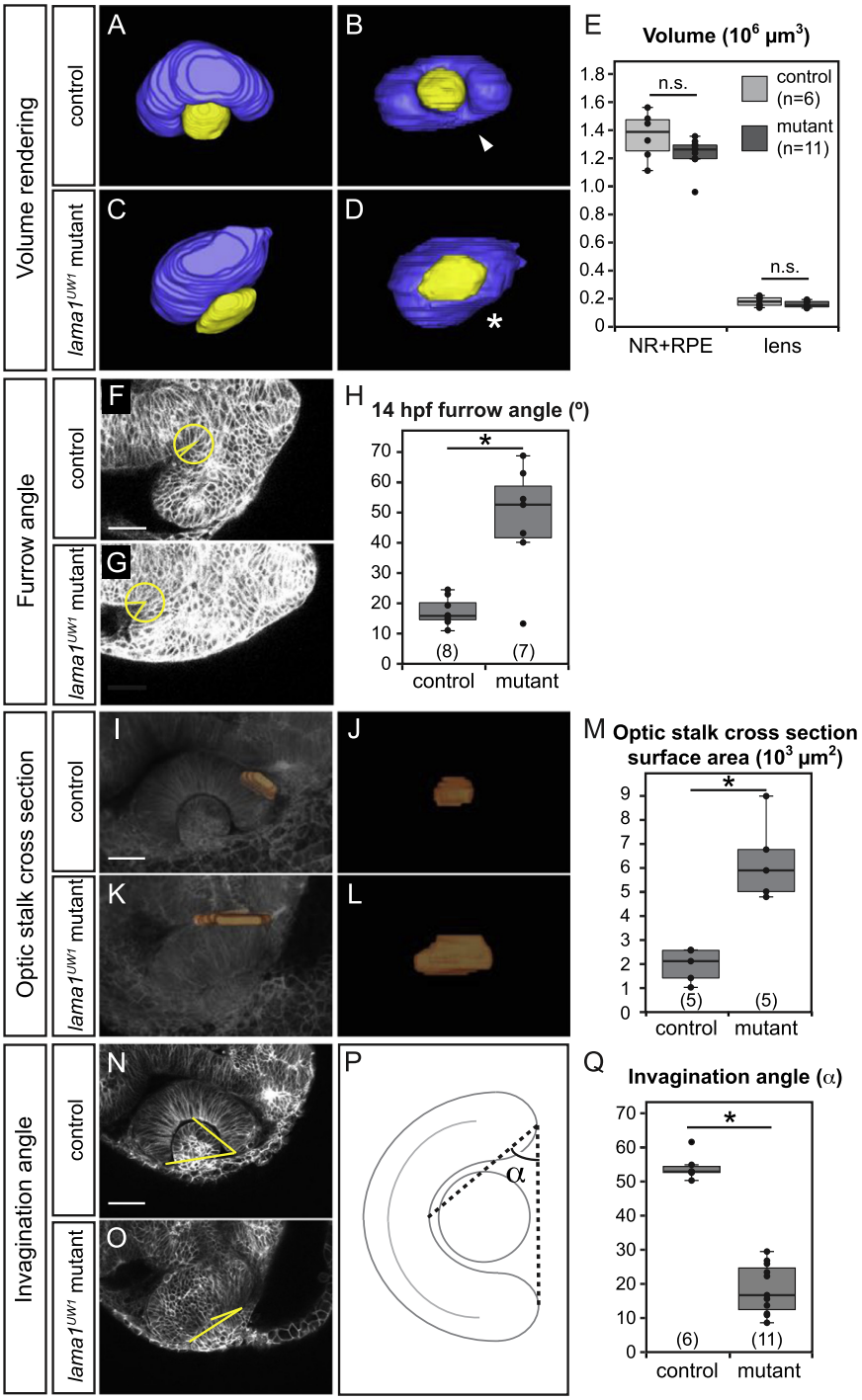
Volume rendering
control
lama1UW1 mutant
A
B
C
D
E
Volume (10^6 µm^3)
n.s.
control (n=6)
mutant (n=11)
n.s.
NR+RPE
lens
Furrow angle
F
G
H
14 hpf furrow angle (°)
(8)
(7)
control
mutant
Optic stalk cross section
I
J
K
L
M
Optic stalk cross section surface area (10^3 µm^2)
(5)
(5)
Invagination angle
N
O
P
α
Q
Invagination angle (α)
(6)
(11)

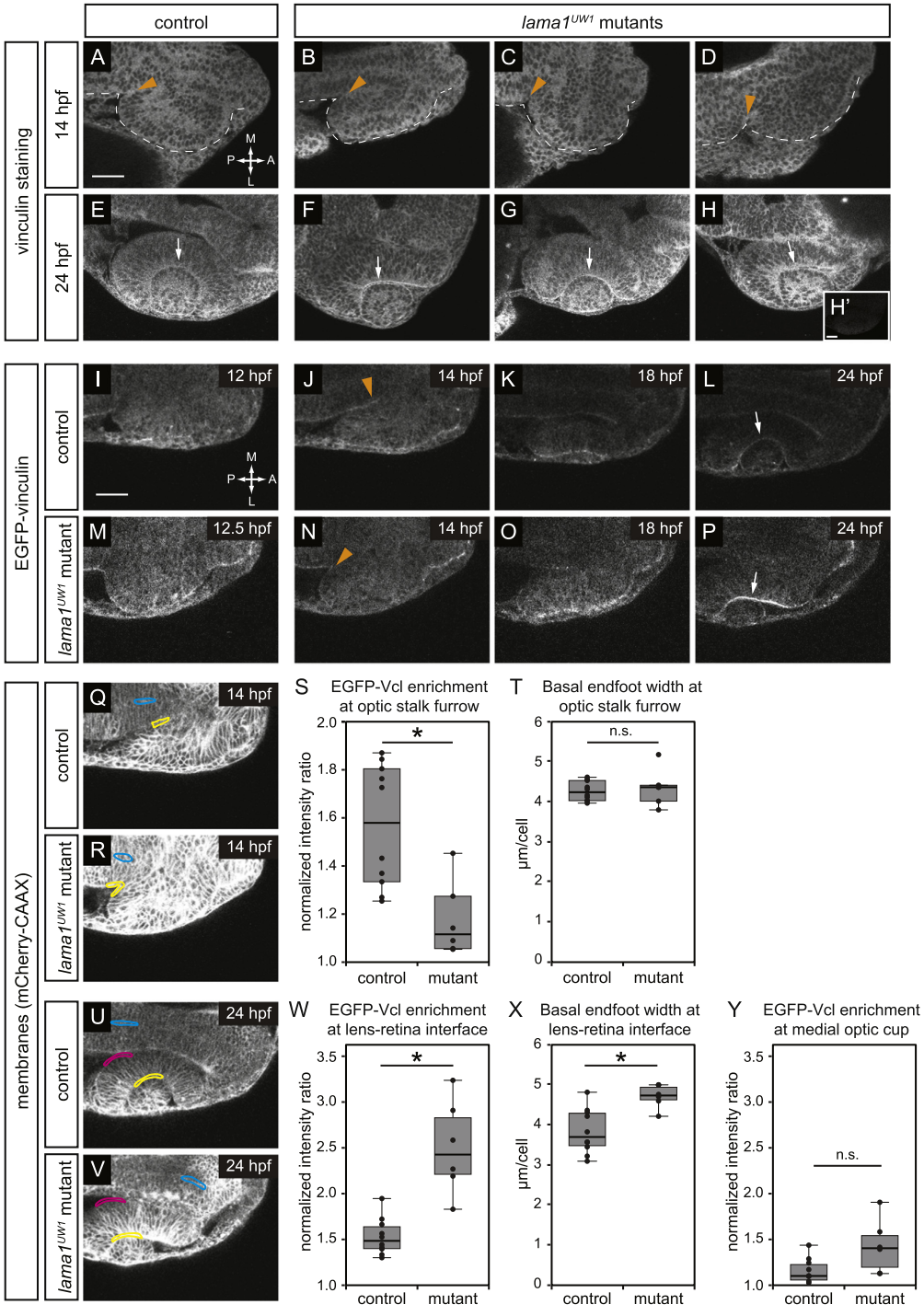
control
lama1UW1 mutants
vinculin staining
14 hpf
24 hpf
A
B
C
D
E
F
G
H
H'
M
P
A
L
EGFP-vinculin
control
lama1UW1 mutant
I 12 hpf
J 14 hpf
K 18 hpf
L 24 hpf
M 12.5 hpf
N 14 hpf
O 18 hpf
P 24 hpf
membranes (mCherry-CAAX)
Q 14 hpf
R 14 hpf
U 24 hpf
V 24 hpf
S EGFP-Vcl enrichment at optic stalk furrow
normalized intensity ratio
control
mutant
*
T Basal endfoot width at optic stalk furrow
µm/cell
n.s.
W EGFP-Vcl enrichment at lens-retina interface
X Basal endfoot width at lens-retina interface
Y EGFP-Vcl enrichment at medial optic cup

2.5.4. Basal endfoot width measurements

Basal endfoot width was measured using the same 25 μm radius circles used for measuring EGFP-vinculin enrichment. The number of cells in contact with the basal surfaces within the circles was counted, and basal surfaces lengths were measured using ImageJ. Average basal endfoot width was calculated by dividing the basal surface lengths by the number of cells in contact with the surface.

2.6. Box and whisker plots

Box and whisker plots were generated using the ggplot2 package in R. The band inside the box is the median. The upper and lower "hinges" correspond to the first and third quartiles. The upper whisker extends from the upper hinge to the highest value within (1.5* IQR), where IQR is the inter-quartile range. The lower whisker extends from the lower hinge to the lowest value within (1.5* IQR). Data points outside of the ends of the whiskers are outliers.

3. Results

3.1. lama1 is required for optic cup formation

In zebrafish, the optic cup forms 12–24 h post fertilization (hpf), during which time the flat, wing-like optic vesicle transforms into the organized optic cup with morphologically distinct neural retina, retinal pigmented epithelium (RPE), and lens. To determine whether laminin-α1 is required for optic cup formation, we examined the *bashful*^{UW1} (*bal*^{UW1}) mutant, which harbors a splice donor mutation in the *laminin-α1 (lama1)* gene, resulting in a protein truncation at amino acid 1424 followed by 60 additional amino acids translated from the intron (Paulus and Halloran, 2006; Semina et al., 2006). We refer to this allele as *lama1*^{UW1}. Mutant and sibling control embryos were labeled ubiquitously for membranes (EGFP-CAAX) and chromatin (H2A.F/Z-mCherry) using RNA injection at the 1-cell stage, and 4-dimensional timelapse confocal microscopy was performed from 12.5 to 24 hpf. This time period encompasses optic cup morphogenesis subsequent to optic vesicle evagination. Timelapse datasets reveal a striking disruption of optic cup morphogenesis (Fig. 1A-H; Movie S1, S2). At 12.5 hpf, the mutant optic vesicle appeared rounder and more symmetric along the anterior-posterior axis than the control (Fig. 1A and E). As optic cup morphogenesis proceeded, in control embryos, the neural retina progenitors elongated and took on a stereotypical columnar epithelial morphology, while RPE cells flattened. The lens invaginated from the overlying ectoderm and pinched off, forming its characteristic spherical shape (Fig. 1A-D, Movie S1). In *lama1*^{UW1} mutants, even though the RPE appeared to be present and flattened appropriately, the retina appeared disorganized, and the two tissues failed to enwrap the lens. The lens formed from the overlying ectoderm, though it was misshapen and ovoid (Fig. 1E-H, Movie S2). The failure of the neural retina and RPE to enwrap the lens leaves it exposed – similar to the "protruding lens" phenotype seen by stereomicroscope and reported previously for *lamb1* and *lamg1* mutants (Parsons et al., 2002). All phenotypes described throughout this manuscript appear to be 100% penetrant. Any apparent variability in phenotypes is related to the specific optical sections in the figures. For example, in mutant embryos, the retina still curves slightly around the lens in the dorsal domain; an optical section in the more dorsal domain will look as though invagination is less disrupted than in the central or ventral domains.

To determine when and where laminin protein is present, we performed antibody staining for the laminin protein heterotrimer (Fig. 1I-L). We found that laminin protein was present at all basal surfaces of the optic vesicle and lens throughout the stages of optic cup morphogenesis studied here. Therefore, laminin protein is found at the right time and place to be directly affecting optic cup morphogenesis. To determine how the *lama1*^{UW1} mutant allele affects laminin protein accumulation, antibody staining was performed on 12 hpf *lama1*^{UW1} mutants, when the optic vesicle has evaginated. We found that there was no detectable accumulation of laminin protein heterotrimer at the basal surface of the optic vesicle (Fig. 1M). Therefore, combined with the similar phenotype observed in the loss-of-function *lamb1* and *lamg1* mutants (Parsons et al., 2002), we consider this phenotype to be a loss-of-function for *lama1*.

3.2. Loss of lama1 leads to multiple defects in optic cup morphogenesis

We set out to quantitatively define the optic cup morphogenesis defects in *lama1*^{UW1} mutants. First, *lama1* mutants isolated in previous, large-scale screens were classified as having a small eye (Malicki et al., 1996). We sought to determine whether the defects in optic cup morphogenesis could be due to changes in eye size. To analyze eye size and shape, 3D volumes of the eye (neural retina+RPE and lens) were visualized and measured after manual segmentation of confocal z-stacks acquired of live embryos. Live imaging was used to avoid artifactual changes in volume due to fixation. The manually segmented volumes (Fig. 2A-D) revealed gross changes to the shape of the optic cup in *lama1*^{UW1} mutants: the domain of neural retina and RPE was flatter, the lens was ovoid rather than spherical, and the choroid fissure failed to form correctly (Fig. 2B and D; arrow marks choroid fissure in control embryo; asterisk marks missing choroid fissure in mutant). Volumes were measured to determine if there was a significant change in size: we found, somewhat surprisingly, that *lama1*^{UW1} mutants and control siblings had no significant difference in optic cup

Fig. 3. Focal adhesions are assembled in a specific spatiotemporal pattern, and are differentially disrupted by loss of lama1. (A-H) Antibody staining for the focal adhesion protein vinculin at 14 hpf (A-D) or 24 hpf (E-H), in control (A,E) or *lama1*^{UW1} mutant (B-D, F-H) embryos. (H') No primary anti-vinculin antibody control. *Orange arrowheads*, location of optic stalk furrow; *white arrows*, lens-retina interface; *dashed line*, outline of optic vesicle. (I-P) Single confocal slices from 4D datasets of EGFP-vinculin (*grayscale*) localization during optic cup morphogenesis, ~12–24 hpf. (I-L) EGFP-vinculin recruitment in control embryo is apparent at the optic stalk furrow (J, *orange arrowhead*), and lens-retina interface (L, *white arrow*). (*m*-P) EGFP-vinculin recruitment in *lama1*^{UW1} mutant embryo at the optic stalk furrow (N, *orange arrowhead*), and lens-retina interface (P, *white arrow*). Dorsal views; scale bar, 50 μm. A, anterior; P, posterior; M, medial; L, lateral. (Q-Y) Quantification of EGFP-vinculin recruitment at the optic stalk furrow and lens-retina interface. (Q,R,U,V) mCherry-CAAX (membranes, *gray*) localization in same single confocal slices as J,N,L,P, respectively. At the optic stalk furrow or lens-retina interface (Q,R,U,V; *yellow regions*), EGFP-vinculin fluorescence intensity was normalized to mCherry-CAAX. Enrichment was measured by comparing to normalized EGFP-vinculin fluorescence intensity at the midline (Q,R,U,V; *cyan regions*). A control medial optic cup domain (U,V; *magenta regions*) was quantified as a location where EGFP-vinculin recruitment was not noted; this domain was also compared to normalized EGFP-vinculin fluorescence intensity at the midline (U,V; *cyan regions*). (S) Quantification of EGFP-vinculin recruitment indicates decreased ECM adhesion at the optic stalk furrow in the *lama1*^{UW1} mutant. (T) Average basal endfoot width at the optic stalk furrow, based on counting the number of cells within the quantified region; no significant difference indicates that differences in cell morphology at that position (*e.g.* basal constriction) cannot strictly account for differences in apparent EGFP-vinculin recruitment. (W) Quantification of EGFP-vinculin recruitment indicates increased ECM adhesion at the lens-retina interface in the *lama1*^{UW1} mutant. (X) Average basal endfoot width at the lens-retina interface, based on counting the number of cells within the quantified region; *lama1*^{UW1} mutants have fewer cells with wider basal surfaces, indicating that increased cell number or constriction cannot account for apparent increased EGFP-vinculin recruitment at the mutant basal surface. (Y) Quantification of EGFP-vinculin recruitment at a control site in the medial optic cup where no enrichment of vinculin recruitment occurred in control or *lama1*^{UW1} mutants. Quantifications were performed on 10 control embryos and 6 mutant embryos (one eye scored per embryo); n.s., not significant;*$P < 0.005$, using a two-tailed *t*-test of unequal variance.

volume (Fig. 2E), suggesting that at this stage, defects in optic cup morphogenesis are not the result of gross gain or loss of tissue, and that the "small eye" phenotype observed in previous screens might arise later in development, possibly as a result of alterations in retinal neurogenesis.

Next, based on timelapse data, it appeared as though the optic stalk, the connection between the optic cup and the brain, failed to constrict in *lama1*^{UW1} mutants. Optic stalk constriction initiates through formation of a furrow at the posterior portion of the optic vesicle, resulting in a fold in the tissue, which then moves anteriorly. We measured the furrow angle in *lama1*^{UW1} control and mutant embryos, and found that the furrow was significantly more open in mutants than in control embryos (Fig. 2F-H, also see Methods). The open furrow suggests a failure of the tissue folding event that initiates optic stalk formation. To determine whether optic stalk constriction was indeed impaired in *lama1*^{UW1} mutants, we measured the cross-sectional area of the optic stalk at 24 hpf (Fig. 2I-M). The optic stalk cross section was reconstructed via manual segmentation of the interface of the optic cup and stalk (see Methods), and the surface area measured. We found that optic stalk constriction was significantly impaired in *lama1*^{UW1} mutants (Fig. 2M).

Finally, the protruding lens phenotype suggested that retinal invagination was impaired. The invagination angle (α) was measured in *lama1*^{UW1} control and mutant embryos as shown (Fig. 2N-P). We found that invagination was significantly impaired by loss of lama1 (Fig. 2Q).

We conclude that although optic cup size is normal, multiple steps of optic cup morphogenesis are impaired in *lama1*^{UW1} mutants, suggesting that under normal conditions, laminin regulates choroid fissure formation, optic stalk constriction, and optic cup invagination.

3.3. Loss of lama1 leads to spatiotemporally distinct effects on focal adhesion assembly

Laminin and other extracellular matrix molecules signal to cells through large protein complexes known as focal adhesions. Focal adhesions are assembled locally within the cell in response to matrix binding, in a mechanical tension-dependent manner. Although the extracellular matrix has been demonstrated to be present surrounding the entire optic vesicle (Hendrix and Zwaan, 1975; Hilfer and Randolph, 1993; Kurkinen et al., 1979; McAvoy, 1981; Parmigiani and McAvoy, 1984; Peterson et al., 1995; Svoboda and O'Shea, 1987; Tuckett and Morriss-Kay, 1986; Wakely, 1977; Webster et al., 1983, 1984), we wondered when and where focal adhesion assembly was occurring during optic cup morphogenesis. Determining spatiotemporal patterns of focal adhesion assembly during optic cup formation could help to reveal the specific morphogenetic events during which ECM adhesion and signaling might play a critical role.

We initially considered two possibilities: one result might be that focal adhesions are assembled uniformly around the optic vesicle throughout optic cup morphogenesis, reflecting the apparent uniform localization of ECM components such as laminin (Fig. 1I-L). Another possibility is that focal adhesions are assembled at particular sites during certain morphogenetic events, suggesting spatiotemporal specificity, and the simple presence of ECM might not be sufficient to trigger focal adhesion assembly. To begin to determine when and where focal adhesion assembly might be occurring during optic cup morphogenesis, we performed antibody staining for the focal adhesion protein vinculin, which is recruited to nascent focal adhesions in a tension-dependent manner (Carisey et al., 2013; Dumbauld et al., 2013; Grashoff et al., 2010; Humphries et al., 2007; Rubashkin et al., 2014). We initially assayed vinculin localization at two timepoints, 14 hpf and 24 hpf, to determine whether we could visualize sites of focal adhesion assembly, and whether these might be altered in *lama1*^{UW1} mutant embryos. At 14 hpf, weak, somewhat inconsistent recruitment of vinculin to the forming optic stalk region could be seen in control embryos, with no obvious difference in *lama1*^{UW1} mutant embryos (Fig. 3A-D, *orange arrowheads*). At 24 hpf, vinculin appeared to be weakly recruited to the lens-retina interface in control embryos (Fig. 3E), and surprisingly, appeared to be more strongly recruited in *lama1*^{UW1} mutant embryos (Fig. 3F-H, *white arrows*). These data suggest that rather than vinculin being recruited uniformly around the forming optic cup (reflecting the apparent uniform distribution of laminin and other ECM proteins), there might be spatiotemporal specificity to focal adhesion recruitment during optic cup morphogenesis.

While the antibody staining data were suggestive, these experiments were not quantitative, and variability in signal could be caused by minor differences in embryo clearing or embedding. Additionally, no other were timepoints were initially examined during optic cup morphogenesis. Therefore, we set out to assay focal adhesions quantitatively in live embryos. To this end, we used a fusion of EGFP to the focal adhesion protein vinculin, the same protein assayed by antibody staining. To facilitate quantification, RNA encoding EGFP-vinculin was coinjected into embryos along with mCherry-CAAX, a uniform membrane marker used for fluorescence normalization. We found that in control embryos, EGFP-vinculin reported focal adhesion assembly in a spatiotemporally specific manner, similar to what we observed via antibody staining. This further supports the idea that apparently uniform laminin protein distribution does not lead to uniform focal adhesion assembly. Notably, EGFP-vinculin was recruited to the optic stalk furrow at the onset of optic stalk constriction, and the lens-retina interface during invagination (Fig. 3I-L, Movie S3, S5). We then examined how adhesion might be disrupted by loss of lama1 (Fig. 3M-P), and found, surprisingly, distinct changes in vinculin recruitment during each morphogenetic event. In *lama1*^{UW1} mutant embryos, at the optic stalk furrow, EGFP-vinculin recruitment was diminished (Fig. 3N, Movie S4), but in contrast, EGFP-vinculin recruitment appeared increased at the lens-retina interface during invagination (Fig. 3P, Movie S6).

We quantified these results using ratiometric image analysis on selected regions of interest (ROIs) (Fig. 3Q,R,U,V), and determined EGFP-vinculin enrichment by normalizing to mCherry-CAAX signal, then comparing normalized signal in the ROI to a different control region, in which EGFP-vinculin and other membrane associated components might appear enriched due to apical cell constriction, but in a manner independent of ECM (also see Methods). Our measurements confirm that at the optic stalk furrow, focal adhesion recruitment was diminished in *lama1*^{UW1} mutants (Fig. 3S), suggesting that laminin promotes focal adhesion assembly at the onset of optic stalk constriction. In contrast, focal adhesion recruitment was increased at the lens-retina interface in *lama1*^{UW1} mutant optic cups (Fig. 3W), suggesting that under wildtype conditions, laminin acts to negatively regulate focal adhesion assembly during invagination, either directly or indirectly.

We were concerned that these measurements could be skewed by potential differences in cell morphology or number in the quantified region. It has been reported that constriction of the basal surface of retinal progenitor cells ("basal constriction") underlies optic cup invagination (Martinez-Morales et al., 2009), and such constriction might also occur during optic stalk furrow formation. Since vinculin recruitment to the basal surface is being quantified, a morphological difference in the basal surface between control and mutant embryos (for example, differences in cell crowding or density) might artifactually lead to an apparent change in focal adhesion recruitment. Therefore, we counted the number of cells within the region being quantified, and calculated

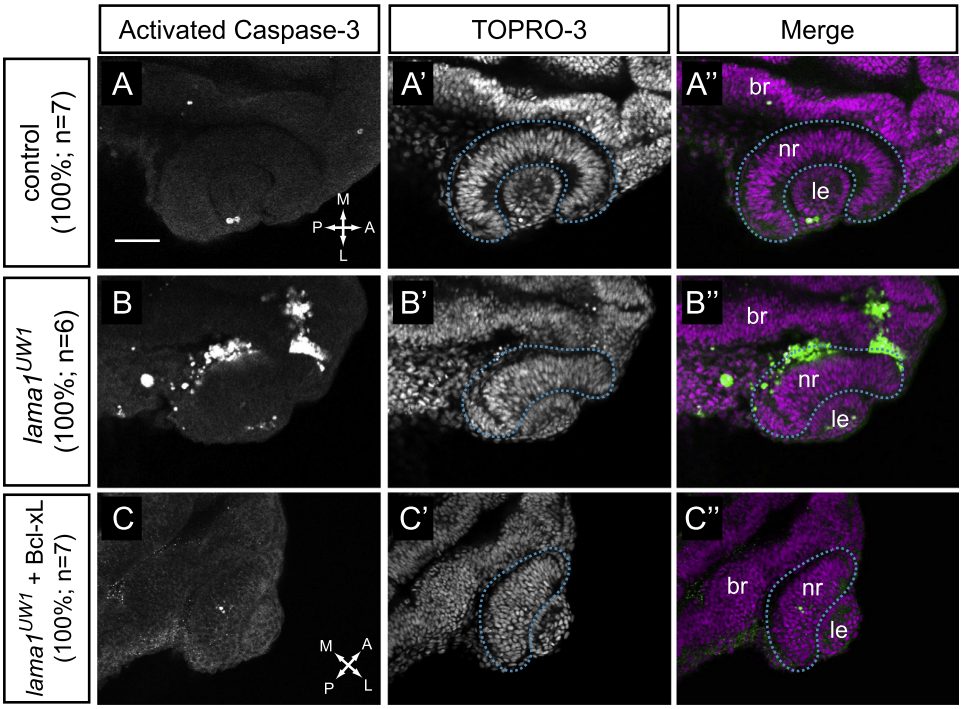

Fig. 4. Apoptosis is increased in *lama1*^{UW1} mutant embryos but is not the underlying cause of morphogenesis defects. (A-A″) Control embryos show little apoptotic cell death. (B-B″) *lama1*^{UW1} mutant embryos contain a significant number of dying cells. (C-C″) Injection of Bcl-xL RNA (100 pg) rescues apoptosis in *lama1*^{UW1} mutant embryos, however optic cup morphogenesis defects are still apparent. (A,B,C) Antibody staining for activated caspase-3. (A′,B′,C′) TOPRO-3 counterstain for nuclei. (A″, B″, C″) Merged images. *dashed blue line*, boundary of optic cup. Dorsal views; scale bar, 50 μm. *br*, brain; *nr*, neural retina; *le*, lens. A, anterior; P, posterior; M, medial; L, lateral.

an average basal endfoot width for control and *lama1*^{UW1} mutant embryos (Fig. S1). During optic stalk furrow formation, we found no significant difference between control and *lama1*^{UW1} mutant average basal endfoot width (Fig. 3T), suggesting that the significant loss of EGFP-vinculin recruitment in *lama1*^{UW1} mutant embryos cannot be due to a significant difference in the number of cells in the quantified region or basal surface cell morphology. During optic cup invagination, however, retinal progenitors in the *lama1*^{UW1} mutant have a larger average basal endfoot width, suggesting that basal constriction is impaired (Fig. 3X). This also suggests that the increased EGFP-vinculin signal observed at the lens-retina interface in the *lama1*^{UW1} mutant (Fig. 3W), cannot merely be due to cell constriction concentrating focal adhesion proteins at the basal surface, rather, there is increased EGFP-vinculin recruitment at the basal surface of each individual cell in the absence of lama1. Further evidence for specificity of these effects comes from quantification of the medial portion of the optic cup, a domain in which we failed to see obvious EGFP-vinculin recruitment (Fig. 3U and V; *magenta regions*). Quantification and normalization of EGFP-vinculin fluorescence in this area indicated very low levels of recruitment in control embryos (1.1-fold enrichment compared to 1.55-fold at the lens-retina interface), and there was no statistically significant difference between control and *lama1*^{UW1} mutant embryos (Fig. 3Y).

We conclude from these data that focal adhesions are assembled in a spatiotemporally specific manner in the early eye: laminin appears to surround the optic vesicle uniformly, yet vinculin is recruited only to a subset of sites where laminin is present. Further, loss of lama1 disrupts focal adhesion assembly in a divergent manner during the morphogenetic events we observed to be disrupted during optic cup morphogenesis, specifically optic stalk furrow formation and invagination (Fig. 2). Our data suggest that under normal conditions, laminin promotes vinculin recruitment and focal adhesion assembly during optic stalk constriction, but surprisingly, negatively modulates it during optic cup invagination. It is possible that this may be due to direct or indirect effects of loss of laminin, or functional differences in other ECM components present at different sites (see Discussion).

3.4. Cell death is not responsible for optic cup morphogenesis defects in lama1 mutants

In both *in vitro* and *in vivo* systems, attachment to the basement membrane or extracellular matrix is required for cell survival (Frisch and Francis, 1994; Juliano et al., 2004). We therefore determined whether loss of lama1 resulted in increased cell death in *lama1*^{UW1} mutants. Antibody staining for activated caspase-3, a marker of programmed cell death, was performed on *lama1*^{UW1} control and mutant embryos. We found that control embryos had little or no detectable cell death at 24 hpf (Fig. 4A-A″), with only a couple of cells positive for activated caspase-3 in the eye region, usually near the site of lens separation from the surface ectoderm. In contrast, *lama1*^{UW1} mutants contained large patches of dying, activated caspase-3-positive cells, which were found in more medial regions of the optic cup, arising from both within and outside of the optic cup (Fig. 4B-B″; *dashed blue lines* outline the optic cup). These cells could originate either from the optic vesicle or neural crest. Within the optic vesicle, notably, this is where focal adhesion assembly was diminished, near the medial optic vesicle, at the boundary between the optic vesicle and prospective

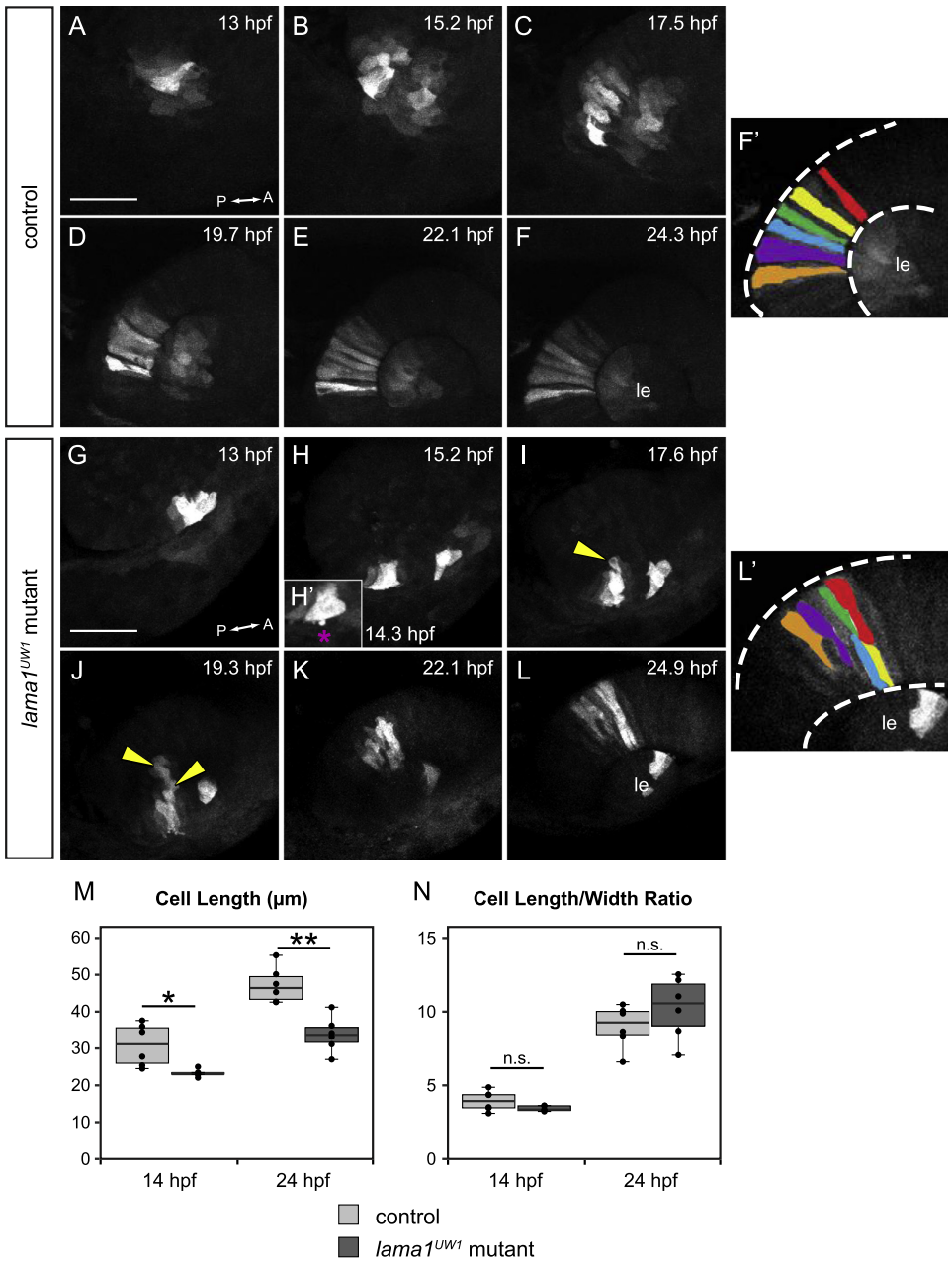

Fig. 5. Loss of motile cell behaviors does not underlie optic cup morphogenesis defects in *lama1*^{UW1} mutant embryos. Retinal progenitors expressing Kaede were exposed to 405 nm light, which converts Kaede from green to red fluorescence via an irreversible photocleavage. Images are maximum intensity projections from 4-dimensional datasets of the red (converted) channel. (A-F′) Images from a timelapse of a *lama1*^{UW1} control sibling embryo. (G-L′) Images from a timelapse of a mutant embryo. (H′) Zoomed image of single timepoint (14.3 hpf) showing a retinal progenitor extending a bleb (*magenta asterisk*) beyond the boundary of the optic vesicle. (F′, L′) Pseudocolor of marked retinal cells. Retinal progenitors in the control embryo extend across the entire width of the retina, while retinal progenitors in the *lama1*^{UW1} mutant embryo elongate, but do not span the width of the retina. Loss of apicobasal register marked by *arrowheads*. (M, N) Comparisons of length (M) or length/width ratio (N) of retinal progenitors in *lama1*^{UW1} mutant or control embryos. While retinal progenitors are longer in control embryos than mutants, the length/width ratio is not significantly different. $^{*}P < 0.02$;$^{**}P < 0.001$; n.s. = not significant. Dorsal views; scale bar, 50 μm. *le*, lens; dashed lines, retina margins. A, anterior; P, posterior.

brain tissue (Fig. 3J,N,S). Conversely, at the basal retina (the lens-retina interface), where focal adhesion assembly was not lost in *lama1*^{UW1} mutants (Fig. 3L, P and W), we did not see increased cell death (Fig. 4B-B″), suggesting that maintenance of adhesion could be protective against cell death. These results suggest that, similar to other epithelial tissues, optic cup cells are sensitive to loss of extracellular matrix adhesion, and respond by undergoing cell death.

The significant amount of cell death in *lama1*^{UW1} mutants led us to ask whether this could be responsible for the morphogenetic defects observed in optic cup formation. To test this, we injected RNA encoding the apoptosis inhibitor Bcl-xL (Sidi et al., 2008) into 1-cell stage embryos, to determine whether suppression of cell death is sufficient to rescue the morphogenetic defects in *lama1*^{UW1} mutants. We found that expression of Bcl-xL suppressed apoptosis (note almost complete lack of activated caspase-3 positive cells in *lama1*^{UW1} mutants). However, gross morphogenetic defects were still apparent (Fig. 4C-C″), and *lama1*^{UW1} mutant optic cups still failed to undergo invagination, with the neural retina and RPE failing to enwrap the misshapen, ovoid lens.

We also attempted to suppress cell death in *lama1*^{UW1} mutant embryos with a commonly used p53 morpholino oligonucleotide. However, this was ineffective, and high levels of cell death remained (data not shown). Although many cell death pathways are p53-dependent, anoikis, caused by loss of matrix attachment, can be independent of p53 signaling (Chiarugi and Giannoni, 2008; Guadamillas et al., 2011). Therefore, we conclude that laminin is normally required for cell survival and loss of lama1 leads to anoikis (either directly or indirectly), but this is not responsible for the gross optic cup morphogenesis defects observed.

3.5. *lama1 mutants display normal motile cell behaviors, but tissue-level structural defects arise during invagination*

Laminin has been demonstrated to influence single cell behavior and cell migration in a variety of systems (Adams and Watt, 1993; Daley and Yamada, 2013). We therefore sought to visualize single cell behaviors underlying optic cup formation, and whether they are affected by loss of lama1. To visualize single cell behaviors, we utilized the photoactivatable fluorophore Kaede (Ando et al., 2002). In its native state, Kaede emits green fluorescence (excitation maximum 508 nm), but when exposed to UV light, the protein undergoes an irreversible photocleavage and subsequently emits red fluorescence (excitation maximum 572 nm). By photoconverting small groups of cells expressing cytoplasmic Kaede, we were able to watch their individual behavior and movement throughout the process of optic cup morphogenesis using 4D timelapse confocal microscopy.

Using the Kaede photoconversion strategy, we found that retinal progenitors in both *lama1*^{UW1} control and mutant embryos appeared polarized and displayed active lamellipodial-like protrusions (Fig. 5A-L; Movie S7, S8). These protrusions were observed to extend and retract from both ends of the cell and persisted for a significant period of optic cup morphogenesis, ceasing only ~20 hpf, at which point the retinal progenitors lengthened and assumed their stereotypical elongated columnar epithelial morphology. In both control and mutant embryos, retinal progenitors appeared to carry out the same elongation behavior: though absolute cell length was longer in controls than mutants (Fig. 5M), length/width ratio was not significantly different at either 14 or 24 hpf (Fig. 5N). Protrusive activity was observed in both control and mutant embryos, but with one notable difference: in control embryos, active lamellipodial-like protrusions never extended beyond the boundary of the optic vesicle. In *lama1*^{UW1} mutant embryos, we sometimes observed protrusions that extended beyond the boundary of the optic vesicle. These protrusions did not exhibit a characteristic lamellipodial-like morphology, but rather appeared more bleb-like (Fig. 5H′, *magenta asterisk*). These were reminiscent of protrusions that extended beyond the limit of the optic vesicle in *lamg1* mutants and morphants during evagination (Ivanovitch et al., 2013). These data suggest that despite the change in overall tissue morphology, the ability to produce motile cell behaviors and undergo cell elongation is not dependent upon lama1.

Despite normal cellular behaviors, a separate, structural phenotype was observed. In control embryos, retinal progenitors aligned with their neighbors, such that their apical and basal ends were in register with each other throughout the course of optic cup morphogenesis (Fig. 5A-F′). In this way, the retina maintained its pseudostratified monolayer structure prior to the onset of neurogenesis. In *lama1*^{UW1} mutant embryos, however, retinal progenitors failed to maintain apicobasal register: though cells were in register during the first part of optic cup morphogenesis, they appeared to sort into separate domains during invagination (Fig. 5G-L′). At the end of optic cup formation, marked retinal progenitors failed to span the width of the retina (Fig. 5L′). This may be better visualized when moving through a confocal z-stack of *lama1*^{UW1} control and mutant optic cups at 24 hpf (Movies S9, S10). In control embryos, retinal progenitor cells were oriented with their long axes pointing toward the lens (Fig. 1D, Movie S9). In contrast, in *lama1*^{UW1} mutant embryos, cells appeared to be organized into multiple domains; cells in some domains appeared to be oriented with their long axes not pointing toward the lens (Fig. 1H, Movie S10). Therefore, lama1 is required to maintain correct retinal structure and orientation of progenitor elongation through optic cup invagination, though it does not appear to be required for retinal progenitors to produce protrusive cell behaviors and elongate.

3.6. *Apicobasal polarity is disrupted in lama1 mutants*

Laminin has been demonstrated to be critical for establishing and maintaining epithelial polarity both *in vitro* and *in vivo* (Martin-Belmonte and Mostov, 2008). At early stages of zebrafish optic vesicle evagination, ZO-1, a component of tight junctions, is localized to the apical surface, opposite the laminin staining that surrounds the optic vesicle (Ivanovitch et al., 2013). It was shown that during optic vesicle evagination, laminin is important for establishing apicobasal polarity: in the *lamg1* mutant (*sleepy*^{m86}), ZO-1 was mislocalized to what should be the presumptive basal surface, in addition to the apparent apical surface (Ivanovitch et al., 2013). In that study, however, polarity was assayed specifically during optic vesicle evagination stages; it is unknown how epithelial polarity and structure might change throughout the process of optic cup morphogenesis in the presence or absence of laminin.

Therefore, we first assayed polarity at the completion of optic cup morphogenesis (24 hpf), in both *lama1*^{UW1} control and mutant embryos. To do this, antibody staining was performed for a marker of the apical surface, atypical protein kinase C (aPKC). We found that in control embryos, aPKC was localized to a single apical surface, at the interface between the neural retina and retinal pigmented epithelium (Fig. 6A, *green arrowhead*). In *lama1*^{UW1} mutant embryos, however, localization of aPKC was disrupted. Though polarity was disrupted with 100% penetrance, the exact number of apical domains present was variable (Fig. 6B-D): in addition to the correct apical domain (*green arrowheads*), multiple ectopic domains of aPKC localization were found (*yellow arrowheads*), as well as ectopic puncta (*magenta asterisks*). The ectopic domains and puncta were scattered throughout the retina. Similar results were obtained using an antibody against the tight junction protein ZO-1 (data not shown). These observations suggest that

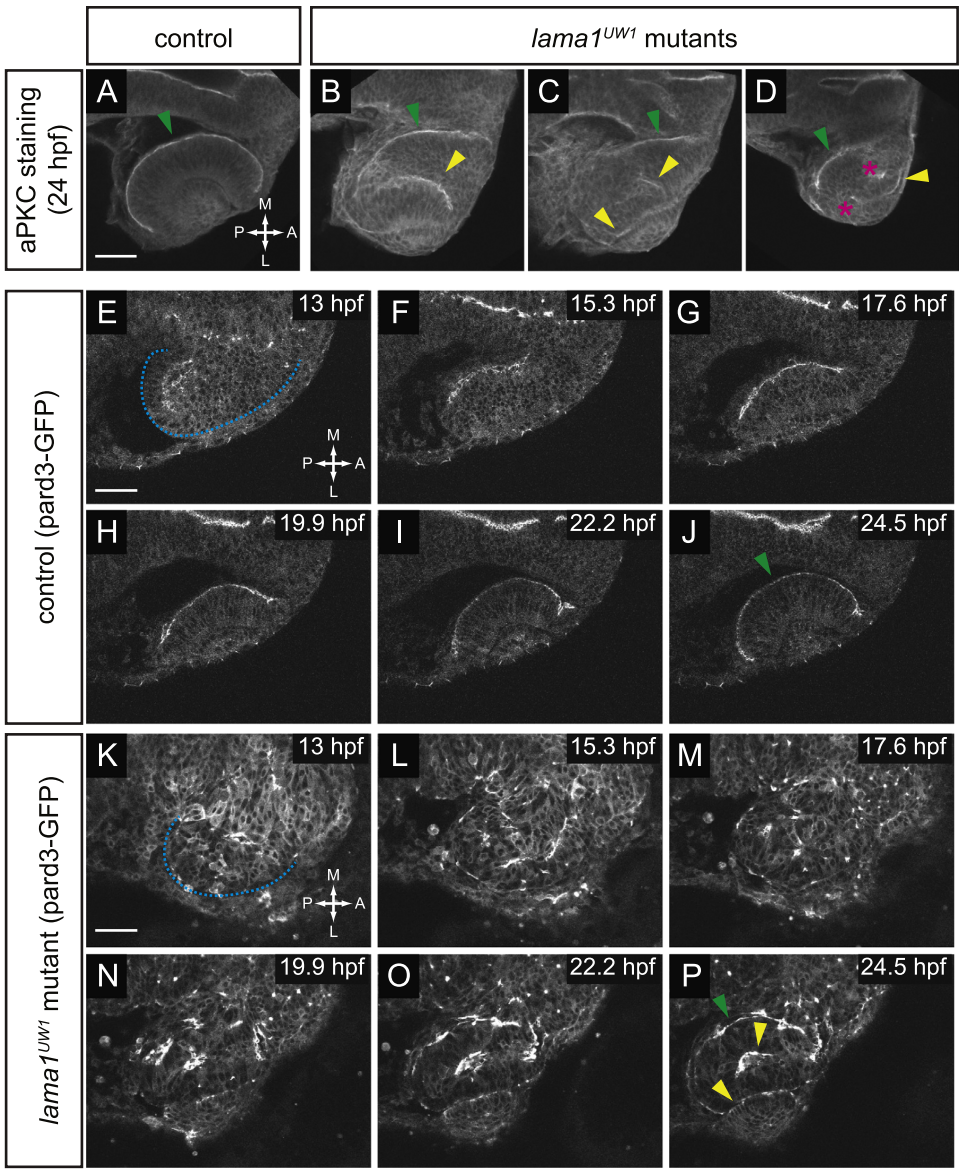

Fig. 6. Apicobasal polarity is disrupted from the earliest stages of optic vesicle morphogenesis. (A-D) Antibody staining for aPKC in control (A) and *lama1*^{UW1} mutant embryos (B-D) reveals disruption of polarity at 24 hpf. *green arrowheads*, correct apical domain. *yellow arrowheads*, ectopic apical domains. *asterisks*, ectopic puncta. (E-P) Single confocal sections from 4D datasets of apical domain dynamics (marked by pard3-GFP) in a *lama1*^{UW1} control embryo (E-J), or a mutant embryo (K-P). In *lama1*^{UW1} mutant embryos, pard3-GFP localization is disrupted similar to aPKC. *dashed blue line* marks outline of optic vesicle. *green arrowheads*, correct apical domain. *yellow arrowheads*, ectopic apical domains. Dorsal views; scale bar, 50 μm. A, anterior; P, posterior; M, medial; L, lateral.

early defects in cell polarity that are caused by loss of laminin proteins may persist through optic cup morphogenesis, resulting in multiple, randomly positioned apical domains in the optic cup.

To determine how these multiple domains might arise and change over time, we took a 4-dimensional live imaging approach (Fig. 6E-P, Movie S11, S12), visualizing the apical surface using pard3-GFP, a fusion of the zebrafish homolog of the polarity protein pard3 to GFP (Geldmacher-Voss et al., 2003). Embryos were injected at the one-cell stage with RNA encoding pard3-GFP.

At 13 hpf, in control embryos, pard3-GFP marked a coherent, single apical surface lining the lumen of the optic vesicle (the interface between the two layers of the optic vesicle) (Fig. 6E). As optic cup morphogenesis proceeded, the single apical domain remained intact, extending along the forming retina-RPE interface as the optic vesicle elongated and subsequently underwent invagination (Fig. 6E-J, Movie S11). At 24 hpf, the apical localization of pard3-GFP is very similar to that of aPKC (Fig. 6A,J). Thus, the apical domain that initially demarcates the layers of the optic

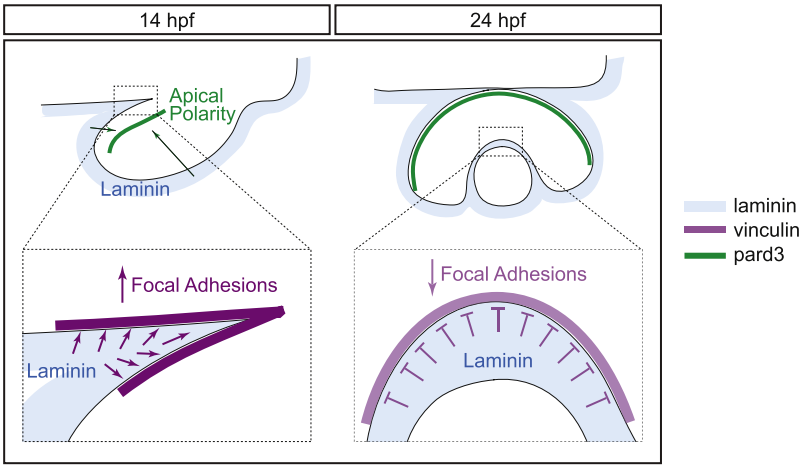

Fig. 7. Model of laminin function during optic vesicle morphogenesis. During optic vesicle morphogenesis, lama1 is required for establishment of apicobasal polarity, but also has spatiotemporally specific effects on focal adhesions. During optic stalk constriction, lama1 promotes focal adhesion assembly, but during optic cup invagination, lama1 inhibits it. *blue*, laminin; *magenta*, vinculin; *green*, pard3.

vesicle comes to form the interface between the retinal pigmented epithelium and neural retina in the optic cup.

In the *lama1*^{UW1} mutant, we found that apicobasal polarity was severely disrupted throughout optic cup morphogenesis. At 13 hpf, the optic vesicle was already slightly misshapen (similar to Fig. 1E). Apical identity was disrupted: pard3-GFP was found with a diffuse cytoplasmic localization and also in puncta scattered randomly throughout cells of the optic vesicle (Fig. 6K). As optic cup morphogenesis proceeded, the diffuse cytoplasmic pard3-GFP fluorescence gradually disappeared (by 22.2 hpf, Fig. 6O). Coherent domains of pard3-GFP fluorescence appeared to form and coalesce stochastically (Fig. 6K-P, Movie S12). By the end of optic cup morphogenesis, pard3-GFP localization resolved into multiple apical domains, similar to what we observed by aPKC antibody staining (Fig. 6B-D,P). In the particular embryo shown in Fig. 6P, pard3-GFP was observed at both the correct location (the interface between the neural retina and retinal pigmented epithelium, *green arrowhead*), as well as at ectopic locations: at the interface between the neural retina and lens, and also in a domain extending into the middle of the retina (*yellow arrowheads*). We conclude that laminin is required for epithelial polarity: in the absence of lama1, cell polarity is disrupted throughout the process of optic cup morphogenesis, with cells randomly designating apical identity and self-organizing stochastically to generate multiple apical domains.

4. Discussion

It has been long known that a rich extracellular matrix layer surrounds the eye throughout the process of optic cup morphogenesis (Hendrix and Zwaan, 1975; Hilfer and Randolph, 1993; Kurkinen et al., 1979; McAvoy, 1981; Parmigiani and McAvoy, 1984; Peterson et al., 1995; Svoboda and O'Shea, 1987; Tuckett and Morriss-Kay, 1986; Wakely, 1977; Webster et al., 1983, 1984), yet in most cases, the function of specific matrix components in regulating the morphogenetic process remains unclear. Here, we demonstrate that laminin extracellular matrix regulates spatiotemporally specific focal adhesion assembly, cell survival, cellular protrusions, and cell polarity during optic cup morphogenesis. Programmed cell death, likely anoikis due to the loss of substrate attachment, is clearly induced, yet it appears to be separate from the morphogenetic phenotypes, as inhibition of cell death does not rescue optic cup formation. Previous work focusing on optic vesicle evagination demonstrated that laminin is critical for tissue organization, establishing cell polarity, and delimiting protrusive activity (Ivanovitch et al., 2013). Here, we have extended those observations to determine the role of laminin through the process of optic cup formation, using a combination of genetics and 4-dimensional live imaging. Future work will aim to determine the specific molecular mechanisms by which laminin controls these diverse cellular processes.

Although the complex extracellular matrix layer has been described to surround the developing eye in every vertebrate organism tested to date, how this affects focal adhesion assembly – the output of functional extracellular matrix engagement – has been unclear. Using vinculin antibody staining and 4D live imaging of EGFP-vinculin, we find that rather than reflecting the apparent uniform distribution of laminin around the optic vesicle, focal adhesions are assembled in a spatiotemporally specific manner, primarily during optic stalk constriction and optic cup invagination. Further, removal of lama1 results in surprisingly divergent effects: focal adhesion assembly is decreased during optic stalk furrow formation, but increased during optic vesicle invagination. We propose that the changes in adhesion disrupt both morphogenetic processes. While we would have predicted that focal adhesions might be decreased by loss of laminin, the increase during invagination is more surprising. We hypothesize that differential interactions between ECM components and receptors may underlie the apparently variable role of laminin in modulating adhesion.

Our experiments do not indicate whether these effects due to loss of laminin are direct or indirect. Laminin is not, of course, the only extracellular matrix component present lining the basal surface of the developing eye. In all vertebrates examined to date, laminin, fibronectin, and collagen surround the developing optic vesicle and lens, in addition to the host of other glycoproteins also found in the complex matrix. Their specific functions in optic cup morphogenesis are unclear, though loss of one component may impact the expression and function of other components. Our initial experiments indicate that loss of lama1 results in disruption of the uniform fibronectin matrix around the anterior lens of the

optic cup at 24 hpf, though no gross changes around the rest of the optic vesicle or cup are apparent at either 14 hpf or 24 hpf (data not shown). Thus, although loss of fibronectin in the *lama1*^{UW1} mutant does occur in a spatiotemporally specific manner, obvious changes in fibronectin localization are not found in regions where vinculin recruitment is affected, specifically at the optic stalk furrow or lens-retina interface. There is a possibility that loss of laminin leads to more subtle changes in ECM structure, for example, fibronectin fibril assembly; future experiments will address these possibilities. It is known that vinculin is recruited to focal adhesions in a manner that is facilitated by tissue tension and ECM stiffness (Pasapera et al., 2010). We speculate that during optic cup invagination, laminin may serve to limit the stiffness and higher order assembly of collagen and fibronectin networks, thereby limiting vinculin recruitment and focal adhesion assembly under normal conditions.

One other structural defect we observed is that of the oblong lens (Fig. 1). Instead of invaginating and forming a spherical structure, the lens has a flattened, ovoid shape. The lens volume is unchanged (Fig. 2E), so specification and proliferation are unlikely to be affected. We hypothesize that an intact laminin extracellular matrix is required to establish uniform circumferential tension around the invaginating lens: loss of adhesion to the laminin matrix between the prospective lens and retina results in a loss of tension in the anterior-posterior axis, resulting in the oblong lens. In addition, it is known that laminin is required for later steps of lens development: lama1 mutants display lens degeneration or extrusion (Pathania et al., 2014; Semina et al., 2006). It is possible that these early defects in establishment of the proper lens structure directly impact these later phenotypes. It has been previously reported that at later stages, focal adhesions are decreased in the anterior segment of *lama1* mutant embryos (Semina et al., 2006); this decrease could be initiated early due to loss of both laminin and fibronectin (data not shown).

We propose the following model for laminin activity during optic cup formation (Fig. 7). In wild type embryos, laminin surrounds the optic vesicle throughout morphogenesis stages. Epithelial polarity is established by the end of evagination, and the single, coherent apical domain (separating the two layers of the optic vesicle) is reshaped as the optic vesicle undergoes elongation and invagination to form the optic cup. Focal adhesions are assembled during optic stalk furrow formation and at the lens-retina interface during invagination. Laminin promotes focal adhesion assembly during optic stalk constriction, but may negatively modulate it during optic cup invagination.

The analyses performed here, as well as detailed cellular analyses performed by other groups, have begun to inform a detailed functional role for laminin in optic cup morphogenesis. In the future, it will be important to both dissect the specific functions of each extracellular matrix component and determine how each affects the function of others in this complex morphogenetic process.

Author contributions

C. D. B., C.-B. C., and K. M. K. conceived of the experiments and developed the concepts. C. D. B. and K. M. K. performed experiments and data analysis, and C. D. B. and K. M. K. prepared and edited the manuscript prior to submission.

Acknowledgments

We are grateful to Mary Halloran, Brian Link, Alexander Reugels, Adam Navis, and Michel Bagnat for reagents. Thanks to Jennifer Gutzman and members of the Chien and Kwan Labs for useful discussions, and Mark Metzstein and Charlie Murtaugh for critical reading of the manuscript. This work was initially supported by a postdoctoral fellowship to K. M. K. from the American Cancer Society, and subsequently by grants to K. M. K. from the Knights Templar Eye Foundation, a March of Dimes Basil O'Connor Starter Scholar Award, and NEI/NIH (R01 EY025378, R01 EY025780). C. D. B. was supported by the University of Utah Developmental Biology Training Grant (NIH T32HD007491).

Appendix A. Supporting information

Supplementary data associated with this article can be found in the online version at http://dx.doi.org/10.1016/j.ydbio.2016.06.025.

References

Adams, J.C., Watt, F.M., 1993. Regulation of development and differentiation by the extracellular matrix. Development 117, 1183–1198.
Ando, R., Hama, H., Yamamoto-Hino, M., Mizuno, H., Miyawaki, A., 2002. An optical marker based on the UV-induced green-to-red photoconversion of a fluorescent protein. Proc. Natl. Acad. Sci. USA 99, 12651–12656.
Biehlmaier, O., Makhankov, Y., Neuhauss, S.C., 2007. Impaired retinal differentiation and maintenance in zebrafish laminin mutants. Invest. Ophthalmol. Vis. Sci. 48, 2887–2894.
Carisey, A., Tsang, R., Greiner, A.M., Nijenhuis, N., Heath, N., Nazgiewicz, A., Kemkemer, R., Derby, B., Spatz, J., Ballestrem, C., 2013. Vinculin regulates the recruitment and release of core focal adhesion proteins in a force-dependent manner. Curr. Biol. 23, 271–281.
Chiarugi, P., Giannoni, E., 2008. Anoikis: a necessary death program for anchorage-dependent cells. Biochem. Pharmacol. 76, 1352–1364.
Chow, R.L., Lang, R.A., 2001. Early eye development in vertebrates. Annu Rev. Cell Dev. Biol. 17, 255–296.
Colognato, H., Yurchenco, P.D., 2000. Form and function: the laminin family of heterotrimers. Dev. Dyn. 218, 213–234.
Daley, W.P., Yamada, K.M., 2013. ECM-modulated cellular dynamics as a driving force for tissue morphogenesis. Curr. Opin. Genet Dev. 23, 408–414.
Dumbauld, D.W., Lee, T.T., Singh, A., Scrimgeour, J., Gersbach, C.A., Zamir, E.A., Fu, J., Chen, C.S., Curtis, J.E., Craig, S.W., Garcia, A.J., 2013. How vinculin regulates force transmission. Proc. Natl. Acad. Sci. USA 110, 9788–9793.
England, S.J., Blanchard, G.B., Mahadevan, L., Adams, R.J., 2006. A dynamic fate map of the forebrain shows how vertebrate eyes form and explains two causes of cyclopia. Development 133, 4613–4617.
Frisch, S.M., Francis, H., 1994. Disruption of epithelial cell-matrix interactions induces apoptosis. J. Cell Biol. 124, 619–626.
Fuhrmann, S., 2010. Eye morphogenesis and patterning of the optic vesicle. Curr. Top. Dev. Biol. 93, 61–84.
Geldmacher-Voss, B., Reugels, A.M., Pauls, S., Campos-Ortega, J.A., 2003. A 90-degree rotation of the mitotic spindle changes the orientation of mitoses of zebrafish neuroepithelial cells. Development 130, 3767–3780.
Grant, P.K., Moens, C.B., 2010. The neuroepithelial basement membrane serves as a boundary and a substrate for neuron migration in the zebrafish hindbrain. Neural Dev. 5, 9.
Grashoff, C., Hoffman, B.D., Brenner, M.D., Zhou, R., Parsons, M., Yang, M.T., McLean, M.A., Sligar, S.G., Chen, C.S., Ha, T., Schwartz, M.A., 2010. Measuring mechanical tension across vinculin reveals regulation of focal adhesion dynamics. Nature 466, 263–266.
Guadamillas, M.C., Cerezo, A., Del Pozo, M.A., 2011. Overcoming anoikis–pathways to anchorage-independent growth in cancer. J. Cell Sci. 124, 3189–3197.
Heermann, S., Schutz, L., Lemke, S., Krieglstein, K., Wittbrodt, J., 2015. ye morphogenesis driven by epithelial flow into the optic cup facilitated by modulation of bone morphogenetic protein. Elife, 4.
Hendrix, R.W., Zwaan, J., 1975. The matrix of the optic vesicle-presumptive lens interface during induction of the lens in the chicken embryo. J. Embryol. Exp. Morphol. 33, 1023–1049.
Hilfer, S.R., Randolph, G.J., 1993. Immunolocalization of basal lamina components during development of chick otic and optic primordia. Anat. Rec. 235, 443–452.
Humphries, J.D., Wang, P., Streuli, C., Geiger, B., Humphries, M.J., Ballestrem, C., 2007. Vinculin controls focal adhesion formation by direct interactions with talin and actin. J. Cell Biol. 179, 1043–1057.
Ivanovitch, K., Cavodeassi, F., Wilson, S.W., 2013. Precocious acquisition of neuroepithelial character in the eye field underlies the onset of eye morphogenesis. Dev. Cell 27, 293–305.
Jiang, Y.J., Brand, M., Heisenberg, C.P., Beuchle, D., Furutani-Seiki, M., Kelsh, R.N., Warga, R.M., Granato, M., Haffter, P., Hammerschmidt, M., Kane, D.A., Mullins, M.C., Odenthal, J., van Eeden, F.J., Nusslein-Volhard, C., 1996. Mutations affecting neurogenesis and brain morphology in the zebrafish, Danio rerio. Development 123, 205–216.

Juliano, R.L., Reddig, P., Alahari, S., Edin, M., Howe, A., Aplin, A., 2004. Integrin regulation of cell signalling and motility. Biochem. Soc. Trans. 32, 443–446.
Karlstrom, R.O., Trowe, T., Klostermann, S., Baier, H., Brand, M., Crawford, A.D., Grunewald, B., Haffter, P., Hoffmann, H., Meyer, S.U., Muller, B.K., Richter, S., van Eeden, F.J., Nusslein-Volhard, C., Bonhoeffer, F., 1996. Zebrafish mutations affecting retinotectal axon pathfinding. Development 123, 427–438.
Kimmel, C.B., Ballard, W.W., Kimmel, S.R., Ullmann, B., Schilling, T.F., 1995. Stages of embryonic development of the zebrafish. Dev. Dyn. 203, 253–310.
Kurkinen, M., Alitalo, K., Vaheri, A., Stenman, S., Saxen, L., 1979. Fibronectin in the development of embryonic chick eye. Dev. Biol. 69, 589–600.
Kwan, K.M., Otsuna, H., Kidokoro, H., Carney, K.R., Saijoh, Y., Chien, C.B., 2012. A complex choreography of cell movements shapes the vertebrate eye. Development 139, 359–372.
Lee, J., Gross, J.M., 2007. Laminin beta1 and gamma1 containing laminins are essential for basement membrane integrity in the zebrafish eye. Invest. Ophthalmol. Vis. Sci. 48, 2483–2490.
Malicki, J., Neuhauss, S.C., Schier, A.F., Solnica-Krezel, L., Stemple, D.L., Stainier, D.Y., Abdelilah, S., Zwartkruis, F., Rangini, Z., Driever, W., 1996. Mutations affecting development of the zebrafish retina. Development 123, 263–273.
Martin-Belmonte, F., Mostov, K., 2008. Regulation of cell polarity during epithelial morphogenesis. Curr. Opin. Cell Biol. 20, 227–234.
Martinez-Morales, J.R., Rembold, M., Greger, K., Simpson, J.C., Brown, K.E., Quiring, R., Pepperkok, R., Martin-Bermudo, M.D., Himmelbauer, H., Wittbrodt, J., 2009. ojoplano-mediated basal constriction is essential for optic cup morphogenesis. Development 136, 2165–2175.
Martinez-Morales, J.R., Wittbrodt, J., 2009. Shaping the vertebrate eye. Curr. Opin. Genet. Dev. 19, 511–517.
McAvoy, J.W., 1981. The spatial relationship between presumptive lens and optic vesicle/cup during early eye morphogenesis in the rat. Exp. Eye Res. 33, 447–458.
Miner, J.H., Yurchenco, P.D., 2004. Laminin functions in tissue morphogenesis. Annu. Rev. Cell Dev. Biol. 20, 255–284.
Parmigiani, C., McAvoy, J., 1984. Localisation of laminin and fibronectin during rat lens morphogenesis. Differentiation 28, 53–61.
Parsons, M.J., Pollard, S.M., Saude, L., Feldman, B., Coutinho, P., Hirst, E.M., Stemple, D.L., 2002. Zebrafish mutants identify an essential role for laminins in notochord formation. Development 129, 3137–3146.
Pasapera, A.M., Schneider, I.C., Rericha, E., Schlaepfer, D.D., Waterman, C.M., 2010. Myosin II activity regulates vinculin recruitment to focal adhesions through FAK-mediated paxillin phosphorylation. J. Cell Biol. 188, 877–890.
Pathania, M., Semina, E.V., Duncan, M.K., 2014. Lens extrusion from Laminin alpha 1 mutant zebrafish. Sci. World J. 2014, 524929.
Paulus, J.D., Halloran, M.C., 2006. Zebrafish bashful/laminin-alpha 1 mutants exhibit multiple axon guidance defects. Dev. Dyn. 235, 213–224.
Peterson, P.E., Pow, C.S., Wilson, D.B., Hendrickx, A.G., 1995. Localisation of glycoproteins and glycosaminoglycans during early eye development in the macaque. J. Anat. 186 (Pt 1), 31–42.
Picker, A., Cavodeassi, F., Machate, A., Bernauer, S., Hans, S., Abe, G., Kawakami, K., Wilson, S.W., Brand, M., 2009. Dynamic coupling of pattern formation and morphogenesis in the developing vertebrate retina. PLoS Biol. 7, e1000214.
Pollard, S.M., Parsons, M.J., Kamei, M., Kettleborough, R.N., Thomas, K.A., Pham, V. N., Bae, M.K., Scott, A., Weinstein, B.M., Stemple, D.L., 2006. Essential and overlapping roles for laminin alpha chains in notochord and blood vessel formation. Dev. Biol. 289, 64–76.
Rembold, M., Loosli, F., Adams, R.J., Wittbrodt, J., 2006. Individual cell migration serves as the driving force for optic vesicle evagination. Science 313, 1130–1134.
Rubashkin, M.G., Cassereau, L., Bainer, R., DuFort, C.C., Yui, Y., Ou, G., Paszek, M.J., Davidson, M.W., Chen, Y.Y., Weaver, V.M., 2014. Force engages vinculin and promotes tumor progression by enhancing PI3K activation of phosphatidylinositol (3,4,5)-triphosphate. Cancer Res. 74, 4597–4611.
Schier, A.F., Neuhauss, S.C., Harvey, M., Malicki, J., Solnica-Krezel, L., Stainier, D.Y., Zwartkruis, F., Abdelilah, S., Stemple, D.L., Rangini, Z., Yang, H., Driever, W., 1996. Mutations affecting the development of the embryonic zebrafish brain. Development 123, 165–178.
Semina, E.V., Bosenko, D.V., Zinkevich, N.C., Soules, K.A., Hyde, D.R., Vihtelic, T.S., Willer, G.B., Gregg, R.G., Link, B.A., 2006. Mutations in laminin alpha 1 result in complex, lens-independent ocular phenotypes in zebrafish. Dev. Biol. 299, 63–77.
Sidi, S., Sanda, T., Kennedy, R.D., Hagen, A.T., Jette, C.A., Hoffmans, R., Pascual, J., Imamura, S., Kishi, S., Amatruda, J.F., Kanki, J.P., Green,D.R.,, J.P., D'Andrea, A.A., Look, A.T., 2008. Chk1 suppresses a caspase-2 apoptotic response to DNA damage that bypasses p53, Bcl-2, and caspase-3. Cell 133, 864–877.
Sittaramane, V., Sawant, A., Wolman, M.A., Maves, L., Halloran, M.C., Chandrasekhar, A., 2009. The cell adhesion molecule Tag1, transmembrane protein Stbm/Vangl2, and Lamininalpha1 exhibit genetic interactions during migration of facial branchiomotor neurons in zebrafish. Dev. Biol. 325, 363–373.
Svoboda, K.K., O'Shea, K.S., 1987. An analysis of cell shape and the neuroepithelial basal lamina during optic vesicle formation in the mouse embryo. Development 100, 185–200.
Sztal, T.E., Sonntag, C., Hall, T.E., Currie, P.D., 2012. Epistatic dissection of laminin-receptor interactions in dystrophic zebrafish muscle. Hum. Mol. Genet 21, 4718–4731.
Tuckett, F., Morriss-Kay, G.M., 1986. The distribution of fibronectin, laminin and entactin in the neurulating rat embryo studied by indirect immunofluorescence. J. Embryol. Exp. Morphol. 94, 95–112.
Wakely, J., 1977. Scanning electron microscope study of the extracellular matrix between presumptive lens and presumptive retina of the chick embryo. Anat. Embryol. (Berl.) 150, 163–170.
Wan, Y., Otsuna, H., Chien, C.B., Hansen, C., 2009. An interactive visualization tool for multi-channel confocal microscopy data in neurobiology research. IEEE Trans. Vis. Comput. Graph 15, 1489–1496.
Webster Jr., E.H., Silver, A.F., Gonsalves, N.I., 1983. Histochemical analysis of extracellular matrix material in embryonic mouse lens morphogenesis. Dev. Biol. 100, 147–157.
Webster Jr., E.H., Silver, A.F., Gonsalves, N.I., 1984. The extracellular matrix between the optic vesicle and presumptive lens during lens morphogenesis in an anophthalmic strain of mice. Dev. Biol. 103, 142–150.
Wolman, M.A., Sittaramane, V.K., Essner, J.J., Yost, H.J., Chandrasekhar, A., Halloran, M.C., 2008. Transient axonal glycoprotein-1 (TAG-1) and laminin-alpha1 regulate dynamic growth cone behaviors and initial axon direction in vivo. Neural Dev. 3, 6.
Yang, X.J., 2004. Roles of cell-extrinsic growth factors in vertebrate eye pattern formation and retinogenesis. Semin. Cell Dev. Biol. 15, 91–103.
Zinkevich, N.S., Bosenko, D.V., Link, B.A., Semina, E.V., 2006. laminin alpha 1 gene is essential for normal lens development in zebrafish. BMC Dev. Biol. 6, 13.

Figure S1

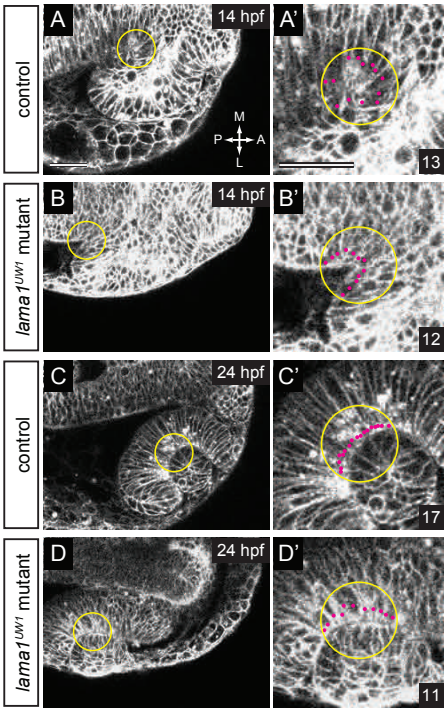

Supplementary Fig S1. Method for measuring basal endfoot width. (A-B′) At 14 hpf, a 25 µm radius circle (*yellow*) was centered at the vertex of the optic stalk furrow. (C-D′) At 24 hpf, a 25 µm circle (*yellow*) was centered at the deepest point of the lens-retina interface. In all cases, basal surface length was measured using ImageJ. Within the circle, the number of cells in contact with the basal surface was counted (*magenta dots*). Average basal endfoot width was calculated by dividing the basal surface length by the number of cells in contact with it. (A-D) Single confocal sections for measurements. (A′-D′) Zoomed images. Numbers in bottom right insets are numbers of cells in contact with the basal surface in that image. Dorsal views; scale bar, 50 µm. A, anterior; P, posterior; M, medial; L, lateral.

CHAPTER 3

CRANIAL NEURAL CREST CELLS REGULATE OPTIC CUP MORPHOGENESIS THROUGH MODIFICATIONS TO THE EXTRACELLULAR MATRIX

Abstract

The interactions between a developing organ and its surrounding environment are critical in regulating its proper development. The vertebrate eye undergoes morphogenesis in close proximity to multiple tissues, and reciprocal signaling and mechanical crosstalk between each tissue is important for their development. Epithelial-mesenchymal interactions are critical for the development of many organs; mesenchymal cells have been observed in close proximity to the eye throughout optic development, and while previous work has demonstrated that mutations which affect the periocular mesenchyme can cause morphogenetic defects within the optic cup, specific roles of the periocular mesenchyme have remained elusive. While it has long been known that the periocular mesenchyme is comprised of cells derived from both the neural crest and the mesoderm, no specific role has been identified for either cell population during optic cup morphogenesis, and the molecular nature of these tissues' interactions with the eye are not well understood. Here, we utilize the zebrafish *tfap2a;foxd3* double mutant which displays a very strong loss of neural crest cells to determine the role of the neural crest

during optic cup morphogenesis. Using timelapse microscopy and four-dimensional cell tracking, we show that the neural crest is required for cell movements throughout the optic vesicle, and loss of the neural crest impairs optic cup morphogenesis. We demonstrate that neural crest cells are required for proper basement membrane formation around the developing retinal pigment epithelium, and that these neural crest cells express the extracellular matrix protein nidogen. Strikingly, ectopically expressing nidogen in the absence of neural crest cells partially restores optic cup morphogenesis. These results demonstrate that the neural crest is required for proper formation of the ocular extracellular matrix, which in turn drives optic cup morphogenesis.

Introduction

Vertebrate eye development begins with specification of the eye field, followed by a series of tissue movements that together comprise optic cup morphogenesis (Hilfer, 1983; Schmitt and Dowling, 1994; Schook, 1980; Walls, 1942). Initially, a pair of optic vesicles evaginate bilaterally from the developing forebrain; the optic vesicles will give rise to the neural retina and retinal pigment epithelium (RPE). These vesicles subsequently elongate, and the connection between the vesicle and brain is constricted, generating the optic stalk. Multiple tissue rearrangements occur during invagination, the final stage of optic cup morphogenesis: the optic vesicles buckle and begin to take on a hemispherical shape to accommodate the lens as it invaginates toward the vesicles from the overlying ectoderm, and the optic fissure forms along the ventral side of the optic vesicle and optic stalk. Lineage tracing and live imaging experiments performed in zebrafish have enabled cellular-level analysis of the morphogenetic movements that

occur during these stages of eye development. These experiments revealed that during invagination, a subset of cells that arise on the medial layer of the optic vesicle migrate around the rim of the vesicle and eventually take up residence within the lateral layer, contributing to the neural retina; those which remain on the medial layer will flatten and comprise the RPE (Heermann et al., 2015; Kwan et al., 2012; Li et al., 2000; Picker et al., 2009; Sidhaye and Norden, 2017). However, despite all that is known regarding the movements that occur during vertebrate optic cup morphogenesis, the molecular and cellular mechanisms that regulate specific movements are still not well understood. Additionally, the optic vesicle undergoes morphogenesis in a complex environment containing multiple extraocular tissues, including the overlying ectoderm where the lens will develop, as well as the periocular mesenchyme (POM). While several of these tissues are known to contribute to optic cup morphogenesis, much is yet to be learned about how these interactions shape the eye.

Mesenchymal cells have been shown to contribute to numerous morphogenetic programs and the development of multiple epithelial organs, and these contributions are frequently driven by mesenchymally-derived growth factors and signaling molecules. During mouse tooth placode morphogenesis, the nearby mesenchymal cell population is induced to express multiple morphogens including BMPs, WNTs, and FGFs which signal to the epithelium; this signaling regulates several stages of dental placode morphogenesis (Thesleff, 2003). In the mouse salivary gland, mesenchymal cell expression of Fgf10 is necessary and sufficient for directional morphogenesis of the salivary gland epithelium (Wells et al., 2013). Similar signaling-mediated interactions have been described in other organs and model systems. However, epithelial-mesenchymal communication is not

limited to signaling molecules: mesenchymal cells also affect morphogenesis through modifications to the extracellular matrix (ECM) that surrounds developing epithelia. Mesenchymal cells can drive morphogenesis through cleavage and destruction of ECM via proteolysis: for example, mesenchymally-expressed MMP-2 is required for branching morphogenesis in the developing mouse lung (Kheradmand et al., 2002). Conversely, mesenchymal cells can promote morphogenesis through deposition of new ECM components such as laminin and nidogen, reviewed in Nelson and Larsen (2015).

Previous work has indicated a role for epithelial-mesenchymal interactions during optic cup morphogenesis, although the exact role and molecular nature of these interactions are largely unknown. The POM is a heterogeneous cell population in close proximity to the optic cup, comprised of neural crest cells and mesodermally-derived mesenchyme (Johnston et al., 1979), and multiple tissues in the mature eye are derived in part from these mesenchymal cell populations (Williams and Bohnsack, 2015). In addition to their contributions to structures within the mature eye, disruptions to transcription factors expressed in the POM during optic cup morphogenesis such as *ap2a*, *pitx2* or *zic2* lead to severe eye malformations (Bassett et al., 2010; Bohnsack et al., 2012; Sedykh et al., 2017). For example, during mouse optic cup morphogenesis, the transcription factor AP-2α is expressed in the periocular mesenchyme and lens ectoderm and is absent from the optic vesicle. Despite this, AP-2α-null mice display severe patterning and morphogenesis defects within the optic stalk, neural retina, and RPE (Bassett et al., 2010). These defects may arise as a result of aberrant signaling: mouse *ap2a* mutants exhibit disruptions to Hedgehog signaling within the optic cup, a phenotype also observed in zebrafish *zic2* mutants (Sedykh et al., 2017). Experiments in

chick explants suggest that POM-derived TGF-β signaling is crucial for specifying RPE cell fate, as well as the correct position of the developing lens in the overlying ectoderm (Fuhrmann et al., 2000; Grocott et al., 2011). These data suggest a critical role for the POM in regulating optic cup morphogenesis, possibly through regulating direct or indirect signaling to the optic cup. Interestingly, communication between these tissues appears to be bidirectional: the developing optic vesicle is known to signal to the migratory neural crest, in part through retinoic acid and PDGF signaling (Bohnsack et al., 2012; Eberhart et al., 2008; Lupo et al., 2011). In zebrafish *rx3* mutants, eye specification fails to occur; these embryos subsequently display aberrant craniofacial neural crest migration (Langenberg et al., 2008), indicating that the eye is at least partially responsible for proper anterior neural crest migration. However, many of the molecules that mediate these bidirectional epithelial-mesenchymal interactions during optic cup morphogenesis have yet to be discovered.

In other organ systems, mesenchymal cells are known to drive morphogenetic events through modifications to the ECM. A complex ECM has long been known to surround the developing optic vesicle throughout optic cup morphogenesis (Hendrix and Zwaan, 1975; Kwan, 2014; Peterson et al., 1995; Svoboda and O'Shea, 1987; Tuckett and Morriss-Kay, 1986), yet the specific functions of many of the components of this ECM are still unknown. Attachment to the ECM is often required for survival signaling, and loss of this attachment can lead to cell death through anoikis (Frisch and Francis, 1994). The ECM also provides structural integrity to epithelia (Halfter et al., 2015; Miner and Yurchenco, 2004; Shawky and Davidson, 2015). Despite this broad knowledge about ECM function, only recently have specific roles of fibronectin (Hayes et al., 2012; Huang

et al., 2011) and laminin (Bryan et al., 2016; Ivanovitch et al., 2013; Sidhaye and Norden, 2017) during optic cup morphogenesis been elucidated, and both of these ECM proteins are expressed by the optic vesicle itself. POM cells could modify the ocular ECM by expressing ECM-degrading proteins such as metalloproteases, or structural ECM proteins such as nidogens: both are expressed by mesenchymal cells during morphogenesis of other organs. The roles of many ECM proteins during optic cup morphogenesis, especially those which may be produced by mesenchymal cells, have not been studied in detail, and their functions during this process remain a mystery.

The POM likely regulates multiple aspects of optic cup morphogenesis, yet many questions remain about the nature of the interactions between the POM and the developing eye. What is the specific contribution of the neural crest versus the mesodermal mesenchyme? In this study, we sought to characterize the role of the neural crest in regulating morphogenesis of the developing optic cup. When and where do neural crest cells interact with the optic vesicle during optic cup morphogenesis? Is the neural crest cell population required for optic cup morphogenesis? Are there tissue or cellular morphogenetic events within the developing eye that depend on the neural crest? At a molecular level, how do neural crest cells interact with and regulate behaviors within the optic cup? Here we demonstrate that loss of neural crest cells, via 2 independent genetic methods, impairs optic cup morphogenesis. Using 4-dimensional timelapse imaging and computational methods, we pinpoint the specific cell movements within the optic cup that are dependent on the neural crest. Finally, we uncover a key molecular effector of neural crest crosstalk with the eye: our results indicate that neural crest cells regulate optic cup morphogenesis through deposition of a crucial modulator of ECM structure.

Results

Neural crest is in contact with the optic vesicle throughout optic cup morphogenesis

In zebrafish, optic cup morphogenesis occurs from 10-24 hours postfertilization (hpf), during which the optic vesicles undergo a series of stereotypical movements and shape changes to become the organized optic cup, comprised of the neural retina, retinal pigment epithelium (RPE), and the lens. To begin to determine when and how the neural crest cell population might affect optic cup morphogenesis, we sought to first identify when and where neural crest cells interact with the developing eye tissues. To visualize both eye tissues and neural crest, we crossed two transgenic zebrafish lines: *Tg(bactin2:EGFP-CAAX)*^{z200}, in which GFP ubiquitously labels cell membranes, and *Tg(sox10:memRFP)*^{vu234} (Kirby et al., 2006), in which neural crest cell membranes are marked with membrane-bound RFP. Using embryos from this cross we performed timelapse imaging during optic cup morphogenesis, from 12.5 hpf-24.5 hpf (Fig 3.1, Movies S1, S2). We find that as early as 12.5 hpf, neural crest cells are already in contact with the posterior margin of the optic vesicle (Fig 3.1A, A'). Initially, neural crest cells migrate anteriorly in the space between the prospective brain and optic vesicle (Fig 3.1B, Movie S1); beginning around 16 hpf, the developing optic stalk is gradually enwrapped by neural crest cells (Fig 3.1B', Movie S2). Neural crest cells also migrate laterally and ventrally to encompass the posterior and ventral sides of the optic cup, and the neural crest has entered the optic fissure and is migrating toward the space between the neural retina and lens by 24.5 hpf (Fig 3.1D'). By the end of optic cup morphogenesis, neural crest-derived cells have encapsulated the RPE side of the optic cup (Fig 3.1D).

Neural crest cells are required for proper optic cup morphogenesis

Multiple studies have suggested there may be developmental crosstalk between the developing eye and the neural crest (Bohnsack et al., 2012; Eberhart et al., 2008; Grocott et al., 2011; Langenberg et al., 2008; Sedykh et al., 2017). As we see neural crest cells in contact with the optic vesicles at early stages of eye development, we sought to determine whether the neural crest cells are required for proper optic cup morphogenesis. To test the requirement for neural crest, we used two independent genetic models, both of which exhibit a widespread depletion of neural crest.

The zebrafish *tfap2a;foxd3* double mutant has been demonstrated to exhibit a strong loss of neural crest cells (Arduini et al., 2009; Wang et al., 2011). We crossed adult *tfap2a*^{ts213}*;foxd3*^{zdf10} heterozygote carriers to two transgenic lines: *Tg(bactin2:EGFP-CAAX)* and *Tg(sox10:memRFP)*. Crossing these two transgenic/double heterozygote lines enabled us to visualize the optic cup as well as to assay the presence of any remaining neural crest cells in the *tfap2a;foxd3* double mutant. At 24 hpf, *tfap2a;foxd3* mutants display several optic cup morphogenesis defects. At the dorsal/ventral midpoint of the optic cup, the nasal side of the neural retina remains flatter than in sibling control embryos and fails to completely enwrap the lens, indicative of a defect in optic cup invagination (Fig 3.2A, B, G). The optic fissure, a cleft structure which runs along the ventral side of the optic stalk and into the optic cup where it is bounded by nasal and temporal margins in the ventral retina, is also disrupted in *tfap2a;foxd3* double mutants. Control embryos display two very closely apposed margins (Fig 3.2H) while the margins in *tfap2a;foxd3* mutants are wideset, indicative of a defect in optic fissure formation (Fig 3.2I). At 24 hpf, *tfap2a;foxd3* double mutants show a

dramatic reduction of *sox10:memRFP*-positive cells in the vicinity of the optic cup (Fig 3.2E, L) compared to wildtype controls (Fig 3.2D, K), with a notable absence on the nasal side of the optic cup (Fig 3.2L). Since incrosses of *tfap2a;foxd3* heterozygote adults yield both single as well as double mutant genotypes, we characterized *tfap2a* and *foxd3* single mutants as well. Neither single mutant displays as severe optic cup morphogenesis defects as the double mutant (Fig S3.1A, B, E), likely due to the presence of more remaining neural crest cells in either single mutant compared to the double mutant (Fig S3.1C, D).

As a second means of testing the requirement for neural crest cells in optic cup morphogenesis, we assayed optic cup morphogenesis in *alyron*^{z24} (*paf1*) mutants where neural crest development is severely impaired (Cretekos and Grunwald, 1999). Although ubiquitously expressed, disruptions to components of the Paf1 complex result in severe reductions in neural crest gene expression, coupled with developmental defects in neural crest derived tissues (Akanuma et al., 2007; Langenbacher et al., 2011; Nguyen et al., 2010). We observe that optic cup invagination is even more severely disrupted in *paf1* mutants when compared to wildtype controls and *tfap2a;foxd3* mutants (Fig 3.2C, G). We also visualized neural crest in *paf1* mutants and saw a reduction in *sox10:memRFP*-positive cells surrounding the optic cup at 24 hpf (Fig 3.2F, M), similar to the neural crest loss seen in the *tfap2a;foxd3* double mutant. However, as *paf1* and other members of the Paf1 complex are expressed ubiquitously (Nguyen et al., 2010; Thisse and Thisse, 2004), it is possible that *paf1* also plays a role in development of the optic vesicle itself, which could account for the more severe morphogenesis defects we observe in the *paf1* mutants. Thus, further analysis on the role of neural crest in optic cup morphogenesis was carried

out solely using the *tfap2a;foxd3* double mutant.

Previous studies have implicated a role for the periocular mesenchyme in closure of the optic fissure along the ventral side of the retina and optic stalk (Hero, 1990; Hero et al., 1991; James et al., 2016; Lupo et al., 2011; Weiss et al., 2012). Consistent with these data, we see optic fissure defects and gaps in ocular pigmentation (coloboma) in *tfap2a;foxd3* double mutants at 52hpf (Fig 3.2 O, P). However, the previous studies have focused largely on the stages surrounding optic fissure fusion, during which the POM do appear to play an active role. Therefore, by assaying at 24 hpf, our data demonstrate that the neural crest is additionally required for the earlier stages of optic cup morphogenesis and optic fissure formation.

TGF-β signaling is unaffected by loss of neural crest, while Pax2a expression is expanded

The finding that neural crest cells are required for early stages of optic cup morphogenesis raised the possibility that neural crest cells were providing a signaling cue to the developing optic cup. Work performed in chick optic vesicle explants demonstrated that periocular mesenchyme cells are necessary for proper RPE specification and development; this requirement could be bypassed through treatment with the TGF-β family member Activin (Fuhrmann et al., 2000). Additional experiments have suggested that neural crest cells repress lens specification through TGF-β signaling to ensure proper positioning of the lens (Grocott et al., 2011). Thus, we sought to determine whether the neural crest is necessary for proper TGF-β signaling to the developing eye in zebrafish. Using an antibody against phospho-Smad3 to detect

locations of active TGF-β signaling, we did not detect any differences in phospho-Smad3 localization between wildtype (Fig 3.3A, C) and mutant optic cups (Fig 3.3B, D; Fig S3.2A-D) at 24 hpf. This result indicates that the neural crest subpopulation of POM is not required for proper TGF-β signaling to the developing optic cup in zebrafish.

As we observed morphogenetic anomalies in anterior and ventral portions of the optic cup in *tfap2a;foxd3* double mutants, we hypothesized that the neural crest might be required for some aspect of optic cup patterning. Using an antibody against Pax2a, a transcription factor expressed in the ventronasal optic cup and optic stalk (Fig 3.3E, G), we found that Pax2a expression is expanded into the RPE layer in *tfap2a;foxd3* double mutants, in cells located more dorsally or temporally than observed in wildtype eyes (Fig 3.3F, H). This expansion was consistently observed in *tfap2a;foxd3* double mutants as well as both *tfap2a* and *foxd3* single mutants (Fig S3.2 E-H). The specificity of expansion of Pax2a into portions of the RPE, but not into ectopic portions of the neural retina, suggests that these defects might be due to alterations of cellular movements within the optic cup as opposed to widespread optic patterning defects.

Neural crest cells are required for proper cell movements within the optic vesicle

The optic cup invagination and choroid fissure formation defects at 24 hpf suggested that cell movements within the optic cup were disrupted in the *tfap2a;foxd3* double mutant. We therefore sought to pinpoint any cell movements disrupted by loss of neural crest to determine how widespread any movement defects are; this in turn could give us clues regarding the nature of the molecular interaction between the optic vesicle

and neural crest. Since we observed defects in invagination, we focused on the cellular movements that occur during this process. We focused on two movements which are executed by cells that reside on the medial layer of the optic vesicle that appear to interact with the neural crest. The first involves RPE movement and flattening during optic cup morphogenesis, while the second, rim involution, involves a subset of optic vesicle cells that migrate around the optic cup rim into the prospective neural retina from the opposite layer of the optic vesicle, where the RPE will develop (Heermann et al., 2015; Kwan et al., 2012; Picker et al., 2009; Sidhaye and Norden, 2017). In mutant optic cups, we consistently observed an expansion of Pax2a expression into the RPE layer, while Pax2a is normally absent from this region in wildtype embryos; failure of Pax2a-expressing cells to undergo rim movement into the neural retina could result in their residing in the RPE layer of the optic cup. Therefore, we hypothesized that rim involution might be disrupted in the absence of neural crest cells. To test this possibility, as well as to determine how widespread the cell movements are which depend on the neural crest, we performed live imaging and 4-dimensional cell tracking of cells within optic cups of wildtype and *tfap2a;foxd3* double mutant embryos (Fig 3.4).

As we saw obvious invagination defects on the nasal side of 24 hpf *tfap2a;foxd3* double mutant optic cups, we began by retrospectively tracking those cells from their final positions at 24 hpf, and visualizing the movements of cells into that portion of the optic cup. The differences between wildtype and *tfap2a;foxd3* mutant nasal RPE cells are most apparent, with a clear change in trajectory shape. While the nasal RPE population arises in the same position in both genotypes, wildtype nasal RPE cells continually move toward the anterior and lateral sides of the embryo (Fig 3.4C-C’’’, Movie S3). In contrast,

the *tfap2a;foxd3* nasal RPE cell population only moves in a straight, anterior direction until 19.5 hpf when they make a sudden, 90-degree turn in the lateral direction (Fig 3.4D-D’’’, Movie S4).

The effects we observe in the temporal retina are somewhat subtler, but still detectable through cell tracking. We find that both wildtype (Fig 3.4E-E’’’, Movie S5) and *tfap2a;foxd3* double mutant nasal retinal cells (Fig 3.4F-F’’’, Movie S6) arise in equivalent domains (Kwan et al., 2012) and follow a similar trajectory during optic cup morphogenesis, with one key difference: while wildtype retinal cells undergo a lateral turn away from the midline around 17.75 hpf (Movie S5), that same turn is delayed in the *tfap2a;foxd3* mutant until approximately 19.5 hpf (Movie S6).

To test how widespread the alterations to optic vesicle cell movements are, we tracked cells which contribute to the temporal retina. Despite a lack of gross morphological defects in the temporal side of the optic cup, we found differences between wildtype and *tfap2a;foxd3* double mutants on this side of the optic vesicle as well. In wildtype embryos, the cells that undergo rim involution on the temporal side of the optic cup begin to migrate around the rim of the optic cup at approximately 20 hpf, with noticeable movement back into the neural retina visible by 22 hpf (Fig 3.4G-G’’’, Movie S7). In the *tfap2a;foxd3* double mutant, these same cells either do not begin migrating around the rim until 22 hpf, or do not migrate into the neural retina at all by 24 hpf (Fig 3.4 H-H’’’, Movie S8).

These results reveal that the neural crest is responsible for regulating cell movements widely throughout the optic vesicle, and underscore the power of individual cell tracking. Even despite there being no obvious gross morphological defects in the

temporal hemisphere of the optic cup, using this technique, we can identify movement deficits. The global aberrations to cell movements we observe within the optic cups of *tfap2a;foxd3* double mutants demonstrate that the neural crest is required for RPE movements and rim involution throughout the optic cup during invagination.

The extracellular matrix protein nidogen is expressed in neural crest cells surrounding the optic cup

Having demonstrated a requirement for neural crest cells in driving cell movements within the developing optic cup, we sought to determine the molecular mechanism by which the neural crest could promote those cell movements. Recent work has demonstrated that retinal invagination is dependent on the laminin extracellular matrix (Bryan et al., 2016; Sidhaye and Norden, 2017) and that rim involution specifically is altered when attachments to the ECM are disrupted (Sidhaye and Norden, 2017). As we have demonstrated that rim involution is disrupted in the *tfap2a;foxd3* double mutant, we hypothesized that the neural crest could be modifying the ECM to drive this movement.

In mouse, the ECM protein nidogen has previously been shown to be expressed by mesenchymal cells in the vicinity of both kidney and lung during their development, but not by the epithelial portions of these organs. Intriguingly, inhibition of nidogen/laminin interactions through blocking antibodies in primary organ culture or loss of function mutations *in vivo* impairs branching morphogenesis of the lung, as well as tubular morphogenesis in the developing kidney (Bader et al., 2005; Ekblom et al., 1994; Kadoya et al., 1997; Willem et al., 2002). Further, the combination of laminin-1, nidogen,

and the TGF-β factor nodal was sufficient to support optic cup morphogenesis in mouse retinal organoids (Eiraku et al., 2011). *In vivo*, laminin transcripts are expressed within the developing optic vesicle during optic cup morphogenesis (Dong and Chung, 1991; Lee and Gross, 2007; Pollard et al., 2006; Semina et al., 2006). In mouse, nidogen expression has been observed in the POM and invaginating lens (Dong and Chung, 1991), and published zebrafish *in situ* hybridizations suggested that both *nidogen 1b* and *nidogen 2a* were expressed in the cranial neural crest (Kudoh et al., 2001; Thisse and Thisse, 2004; Zhu et al., 2017). However, the role of nidogen during optic cup morphogenesis has never been investigated *in vivo*. Because the specific periocular cell populations expressing nidogens had not been completely defined, we sought to determine with cellular resolution the expression of the four zebrafish *nidogen* genes in and around the developing eye. Using *Tg(sox10:GFP)*^{ba4} transgenics, we found that both *nid1b* and *nid2a* are expressed in *sox10:GFP*-positive neural crest cells migrating around the developing optic cup (Fig 3.5). We also observed both *nid1b* and *nid2a* expressed in the overlying ectoderm as well as the developing lens at 18 and 24 hpf, while both are notably absent from the neural retina and RPE. At these same times, *nid1a* is expressed solely in the developing somites (Fig S3.3A, E, I); while *nid2b* is detected diffusely throughout the head (Fig S3.3D, H, L).

Antibody staining in wildtype embryos revealed that nidogen protein is detected around cells which appear to be migrating between the brain and the optic vesicle at 18 hpf (Fig 3.6A, A'), and is detectable in the basement membranes surrounding the RPE, neural retina, and lens at 24 hpf (Fig 3.6C-C''). As neural crest cells would be the only source for nidogen protein for the basement membrane surrounding the RPE,

tfap2a;foxd3 double mutants that lack these cells also lack nidogen protein between the brain and RPE (Fig 3.6B, B', D, D'), while the basement membranes surrounding the lens and retina are unaffected (Fig 3.6D''). These data suggest that neural crest cells deposit the nidogen proteins found in the basement membrane surrounding the developing RPE.

To determine whether loss of neural crest affected other components of the extracellular matrix, we also investigated whether localization or expression of the ECM components laminin-1 or fibronectin were altered in the *tfap2a;foxd3* double mutant. Antibody staining for laminin (Fig S3.4A-D) and fibronectin (Fig S3.4E-H) revealed no obvious differences between wildtype and double mutant embryos, indicating that loss of neural crest in the *tfap2a;foxd3* mutant specifically affects the localization of nidogen along the surface of the RPE.

The basement membrane around the developing RPE is disrupted in *tfap2a;foxd3* double mutants

Several loss-of-function studies in mouse have demonstrated that nidogen is required for proper formation of basement membranes around the kidney, heart, lung and limbs (Bader et al., 2005; Böse et al., 2006; Ekblom et al., 1994; Kadoya et al., 1997). Although we did not see any effects on expression or localization of other components of the basement membrane in the neural crest mutants under light microscopy, we sought directly visualize the assembled basement membranes around the eye which would allow us to detect any differences in ECM ultrastructure. Using transmission electron microscopy, we visualized the basement membranes at the basal surfaces of the brain and

RPE, as well as the neural retina and lens in 24 hpf control (Fig 3.7A-D) and *tfap2a;foxd3* double mutant embryos (Fig 3.7E-H). We observed specifically localized defects in the *tfap2a;foxd3* double mutant in the basement membrane surrounding the RPE (Fig 3.7F); this basement membrane appeared disorganized and not as well defined as the same structure in controls (Fig 3.7B). Somewhat surprisingly, although neural crest cells migrate in the space between the brain and the optic vesicle, the basement membrane lining the developing forebrain appears normal in *tfap2a;foxd3* double mutants and is undistinguishable from control embryos (Fig 3.7A, E), suggesting that neural crest cells are specifically required for formation of the basement membrane surrounding the RPE. The basement membranes lining the neural retina (Fig 3.7C, G) and lens (Fig 3.7D, H) also appeared normal in the *tfap2a;foxd3* double mutants compared to wildtype controls, as expected due to the nidogen produced by the lens placode. These results confirm that neural crest cells are required for proper formation of the basement membrane surrounding the RPE, possibly through deposition of nidogen which is absent from this surface in the *tfap2a;foxd3* double mutant.

Dominant-interfering nidogen disrupts optic cup morphogenesis

The basement membrane loss we observed around the RPE in the *tfap2a;foxd3* mutant was reminiscent of the basement membrane loss observed in several organs in mouse models where nidogen was disrupted, either through loss of function mutations or through disruptions to laminin-nidogen complex formation. This observation, coupled with the finding that *nid1b* and *nid2a* are expressed by neural crest cells during optic cup morphogenesis, suggested a functional role for nidogen in optic cup morphogenesis.

Nidogen's interactions with laminins and other ECM components have been well characterized *in vitro*, and because previous studies have reported genetic compensation in instances where some but not all nidogens were disrupted (Bader et al., 2005; Böse et al., 2006; Zhu et al., 2017), we elected to use a dominant-interference strategy to disrupt nidogen function using a well characterized truncated form of nidogen, Nd-III. This truncated form of nidogen lacks the G1 and G2 domains required for collagen IV and heparin sulfate proteoglycan binding, but retains the laminin binding domain (Fox et al., 1991; Reinhardt et al., 1993). Nd-III acts in a dominant-negative fashion by inhibiting bridging between laminin and other extracellular matrices, and preventing full length nidogen from binding to laminin (Pujuguet et al., 2000). Using the Tol2kit (Kwan et al., 2007) we generated transgenic zebrafish which expressed lyn-mCherry as an expression reporter, as well as a 2A peptide upstream of either full-length zebrafish *nid1a* (Fig 3.8A, WT-Nid1a), or a truncated form of *nid1a* based on the mouse Nd-III fragment (Fig 3.8A, DI-Nid1a). By generating heat-shock inducible transgenes, we were able to control the timing when WT-Nid1a and DI-Nid1a would be expressed, and by driving lyn-mCherry from the same transcript, we were able to visualize all cells that expressed the transgene (see Materials and Methods for full transgenic nomenclature).

We previously observed neural crest cells arriving at the optic vesicle as early as 12 hpf (Fig 3.1). Therefore we performed heat-shocks from 12-13 hpf to induce WT-Nid1a or DI-Nid1a expression at the onset of neural crest migration around the optic vesicle. We crossed zebrafish containing *hs:WT-Nid1a* or *hs:DI-Nid1a* transgenes with *Tg(bactin2:EGFP-CAAX)* transgenics, which enabled us to image the optic cups of *hs:WT-Nid1a* transgene-positive embryos which had not been heat-shocked (Fig 3.8B,

B') as a control. We found that ubiquitous overexpression of WT-Nid1a slightly, but significantly impaired invagination compared to control embryos (Fig 3.8C, C', E), and we noted that lens morphogenesis is also subtly altered such that the lens is not completely spherical. However, overexpressing DI-Nid1a substantially impaired invagination, resulting in striking phenotypes including a severely flattened neural retina and ovoid lens (Fig 3.8 D, D', E). To ensure these phenotypes were due to effects on the optic cup itself and not due to a disruption to neural crest migration, we generated double transgenics with *sox10:GFP* and either *hs:WT-Nid1a* or *hs:DI-Nid1a* to visualize neural crest cells in the presence of WT-Nid1a or DI-Nid1a. We find that neither overexpression of WT-Nid1a or DI-Nid1a affects neural crest migration (Fig 3.8F, G). We therefore conclude that DI-Nid1a strongly impairs optic cup morphogenesis, possibly through direct effects on the optic vesicle and not indirectly through the neural crest cells themselves.

Nidogen can partially rescue *tfap2a;foxd3* double mutant optic cup phenotypes

Nidogen expression in the neural crest, coupled with the phenotypes we observed when we ubiquitously overexpressed DI-Nid1a, suggested that disruptions to the nidogen matrix might be the underlying cause of the morphogenesis defects we observed in mutants where neural crest cells are lost.

We sought to understand if the optic cup morphogenesis defects we observed in the *tfap2a;foxd3* mutants are indeed due to a lack of nidogen which would be deposited by neural crest cells. To test this, we sought to ubiquitously overexpress WT-Nid1a in

tfap2a;foxd3 mutants where there would be no neural crest cells present to deposit nidogen. In effect, we wanted to determine whether WT-Nid1a could rescue optic cup morphogenesis, fully or in part, in *tfap2a;foxd3* double mutants. We generated *tfap2a;foxd3* mutants that contained both the *EGFP-CAAX* transgene, as well as the *hs:WT-Nid1a* transgene. In these embryos, we could visualize the optic cups of both undisturbed embryos, as well as those that were heat-shocked from 12-13 hpf. In control, nonheat-shocked embryos (Fig 3.9A-B'), we observed the usual invagination defects in *tfap2a;foxd3* mutants compared to their wildtype siblings (Fig 3.9E). Much to our surprise, wildtype and *tfap2a;foxd3* mutant embryos that were heat-shocked from 12-13 hpf looked phenotypically similar (Fig 3.9C-D') and we did not detect a difference when comparing their levels of invagination (Fig 3.9E). From this experiment, we conclude that optic cup morphogenesis depends on nidogen, and that ectopic expression of nidogen from the optic cup and surrounding tissues can partially rescue mutant phenotypes caused by loss of nidogen producing cells.

Discussion

Interactions with neural crest cells drive optic cup morphogenesis

Crosstalk between developing tissues is critical for proper morphogenesis of multiple tissues and their subsequent function. This theme is seen throughout organogenesis, with epithelial-mesenchymal interactions being of particular importance. Developing epithelia frequently require surrounding mesenchyme in order to adopt their mature, functional shapes: the lung, kidney, salivary gland, and tooth placode are but a few examples where these interactions are critical (Bader et al., 2005; Ekblom et al.,

1994; Kadoya et al., 1997; Thesleff, 2003). A complex, dynamic mesenchyme is known to surround the developing eye, and mesenchymal cells contribute to later-developing optic tissues such as the hyaloid vasculature and structures within the anterior segment (James et al., 2016; Soules and Link, 2005). Disruptions to the periocular mesenchyme have profound effects on the developing optic cup, such as morphogenetic defects that stretch from the neural retina into the optic stalk and optic fissure (Bassett et al., 2010; Lupo et al., 2011), but many of these analyses have been unable to resolve specifically when or where defects arise within the optic cup. Additionally, the periocular mesenchyme is comprised of both neural crest and mesodermally-derived mesenchymal cells (Gage et al., 2005; Johnston et al., 1979), and much has yet to be learned about the specific molecular contributions from either tissue during early optic cup development. Here, using the zebrafish *tfap2a;foxd3* double mutant, which displays a near complete loss of neural crest cells (Arduini et al., 2009; Wang et al., 2011), we conclusively demonstrate that the neural crest subpopulation of the periocular mesenchyme is critical for morphogenesis of the optic cup. Through live imaging experiments, we visualize neural crest cells and see that they migrate around the optic vesicle throughout much of optic cup morphogenesis, and are required for cellular movements within the optic vesicle. In particular, RPE cell movements and rim involution depend on the presence of neural crest cells.

The periocular mesenchyme has long been observed in close proximity with the developing optic cup, but its specific functions have remained elusive. One possible mechanism mesenchymal cells may use to drive optic cup morphogenesis is by modulating the signaling received by the optic vesicle during its development. Zebrafish

zic2a;2b double mutants display disruptions to the periocular neural crest, in addition to molecular and morphological hallmarks of expanded Hedgehog signaling within the optic cup (Sedykh et al., 2017). Dampening of Hh signaling in these mutants reduces the frequency of optic cup morphogenesis defects, suggesting that the neural crest could serve as a negative regulator of Hh signaling to the eye, possibly through decreasing Hh ligand availability via alterations to the ECM; alternately, zic2a/2b may regulate Hh via some function intrinsic to the optic cup itself. In chick, periocular mesenchyme is required for RPE development: optic vesicle explants cultured without any periocular mesenchyme do not develop RPE (Fuhrmann et al., 2000). RPE specification could be achieved without mesenchymal cells through treatment with Activin, a TGF-β family member, suggesting that the POM serves as a source for TGF-β signaling to the optic cup. We did not observe a difference in TGF-β signaling in the optic cup in *tfap2a;foxd3* double mutants (using pSmad3 as a readout); additionally, neural crest cells are not required for the development of RPE in zebrafish, as we observed obvious pigmentation of *tfap2a;foxd3* mutant eyes at 52 hpf. These results suggest two possibilities: RPE development could be regulated through different mechanisms in the zebrafish versus the chick, or the mesodermal mesenchyme is sufficient for TGF-β signaling to the optic cup and to drive RPE development in the absence of neural crest cells in zebrafish. Evidence indicates the latter possibility is more likely: zebrafish *one-eyed pinhead* mutants display a severe disruption to mesoderm development, and as the name suggests, present with severe optic cup morphogenesis defects and unpigmented eyes (Schier et al., 1997). A differential role for the mesenchymal populations would not be surprising: even among neural crest cells, differences arise between the cranial and trunk populations. In the

future, it will be interesting to dissect the specific roles of the mesodermal mesenchyme in optic cup morphogenesis.

Neural crest cells promote morphogenesis through the ECM protein nidogen

Several studies have implicated the ECM surrounding the optic vesicle as a key player in driving optic cup morphogenesis. Loss of fibronectin from the lens ectoderm impairs lens placode formation and morphogenesis in the mouse (Huang et al., 2011). Zebrafish mutants lacking fibronectin display lens morphogenesis defects as early as 2 dpf, although it has been hypothesized that maternal deposition of fibronectin may mask earlier requirements for fibronectin during optic cup morphogenesis (Hayes et al., 2012). In retinal organoid culture, the minimal mixture of components needed to elicit optic cup morphogenesis is nodal, a TGF-β ligand, and the ECM components laminin-1 and nidogen (Eiraku et al., 2011). The roles of laminin in early eye development have recently been described: laminin is required for proper adhesion of cells within the optic vesicle to the ECM, and disruptions to these adhesions impairs establishment of apicobasal polarity and subsequent morphogenesis (Bryan et al., 2016; Ivanovitch et al., 2013; Nicolás-Pérez et al., 2016; Sidhaye and Norden, 2017).

The role of nidogen in optic cup morphogenesis has remained elusive until now, although its roles in other organ systems have been previously investigated. While nidogens are ubiquitous components of basement membranes, the mesenchymal cells in the embryonic lung and kidney are those tissues' sole source of nidogens (Ekblom et al., 1994; Kadoya et al., 1997; Senior et al., 1996). Disruptions to nidogen function, either

through blocking antibodies or loss-of-function mutations, impedes epithelial morphogenesis of the lung, kidney and developing limb (Bader et al., 2005; Böse et al., 2006; Ekblom et al., 1994; Kadoya et al., 1997). Here, we demonstrate that neural crest cells produce the nidogen which is deposited along the basal surface of the RPE, and that neural crest cells are required for formation of the basement membrane along this surface. Impairing nidogen function, either through loss of neural crest cells or through expression of a dominant-interfering form of Nid1a, lead to defects in optic cup morphogenesis. Intriguingly, overexpression of full-length Nid1a also causes slight defects in optic cup invagination, suggesting that an optimal level of nidogen is required for proper ECM function. Consistent with this, loss of the nidogen-binding site in the laminin γ1 chain results in higher penetrance of renal defects than when both nidogen 1 and 2 are lost (Bader et al., 2005; Willem et al., 2002); this was predicted to be due to an increase of free nidogen incapable of binding to laminin, which could sequester other components of the ECM and interfere with other matrix interactions (Bader et al., 2005).

How the addition of nidogen to the ECM surrounding the optic cup promotes the morphogenetic movements required for optic cup morphogenesis is unclear. While both laminin and fibronectin were still detectable around the RPE in the absence of neural crest cells, we did not detect a normal basement membrane at this site. This finding is consistent with mouse nidogen mutants that show similar basement membrane defects around the developing kidney, lung, and heart, despite retention of other ECM components (Bader et al., 2005). Proper attachment to the ECM is required for many aspects of optic cup morphogenesis including RPE cell movements and rim involution (Bryan et al., 2016; Hayes et al., 2012; Martinez-Morales et al., 2009; Sidhaye and

Norden, 2017), two processes which we show to be disrupted in the absence of neural crest. We predict that through deposition of nidogen into the ECM, neural crest cells generate a permissive environment which enables timely migration of the optic vesicle cells which move around the rim of the optic vesicle and into the developing neural retina. Disruptions to nidogen function, either through loss of neural crest cells or through expression of a dominant-interfering form of nidogen, lead to defects in optic cup morphogenesis. It will be interesting to investigate whether the developing optic cup can still properly adhere to the ECM which remains in the absence of neural crest cells, as basement membrane assembly is likely required for adhesions to form at the correct time and place during optic cup morphogenesis. Further, growth factors and signaling molecules such as FGFs and BMPs are regulated through deposition into the ECM, and correct assembly of the basement membrane may be required to properly regulate these signaling pathways during optic cup morphogenesis; these will be interesting signaling pathways to investigate in the context of disrupted basement membrane assembly.

Materials and methods

Zebrafish lines

Embryos from the following mutant and transgenic lines were raised at 28.5°C and staged according to hours postfertilization and morphology (Kimmel et al., 1995).

- Mutant alleles: *tfap2a*^{ts213}*;foxd3*^{zdf10} (Arduini et al., 2009); *nid1b*^{sa13713} and *nid2a*^{sa15802} (Kettleborough et al., 2013). The *alyron*^{z24} allele contains a C to A transversion in the coding sequence of the *paf1* gene, resulting in a premature stop mutation at tyrosine 281 (Y281*) (Mick Jurynec and David Grunwald, personal

communication).

- Transgenic alleles: *Tg(sox10:memRFP)* ^{vu234} (Kirby et al., 2006), *Tg(sox10:GFP)*^{ba4} (Dutton et al., 2008), *Tg(bactin2:EGFP-CAAX)*^{z200}, *Tg(hsp70:lyn-mCherry-2A-WT-Nid1a)*^{z202}*, Tg(hsp70:lyn-mCherry-2A-DI-Nid1a)*^{z203}.

Construction of Nid1a transgenic lines

Tg(hsp70:lyn-mCherry-2A-WT-Nid1a), a.k.a. *hs:WT-Nid1a* and *Tg(hsp70:lyn-mCherry-2A-DI-Nid1a),* a.k.a. *hs:DI-Nid1a* were generated using Gateway (Invitrogen) recombination. IMAGE Clone ID 8000296 (GE Dharmacon) was used as the template to PCR amplify cDNAs encoding wildtype and dominant-interfering Nid1a; these were ligated into pCS2FA prior to Gateway cloning. PCR primers were used to introduce the PTV-2A peptide (Provost et al., 2007) on the 5' end, and the SV40 late poly-adenylation signal on the 3' end of the zebrafish *nid1a* cDNA. Gateway 3' entry clones were generated via BP recombination and subsequently LR recombined into the pDEST-Tol2-CG2 destination vector which contains an *myl7:EGFP* expression cassette as a transgenesis marker (Kwan et al., 2007). Plasmid DNA (25 pg) was microinjected along with 50 pg mRNA encoding Tol2 transposase into single-cell wildtype embryos and screened for *myl7:EGFP* expression. Fluorescent embryos were raised to adulthood and outcrossed to generate stable transgenic lines.

Heat-shocks

Embryos were transferred from a 28.5°C incubator and immediately overlaid with fresh, preheated 39°C E3. Embryos were incubated at 39°C for one hour on an Echotherm heating plate (Torrey Pines Scientific). Embryos were then transferred back to a 28.5°C incubator and grown to the indicated stage.

Allele identification/genotyping

All mutant alleles were PCR genotyped using either CAPS or dCAPS techniques (Neff et al., 1998). *tfap2a*^{ts213}: Forward (5'-CGCTCAGGTCTTATAAATAGGCTACTAATAATGTTAC-3'), Reverse (5'-CTGAGAGGTGGCTATTTCCCGTTAAGATTCG-3'), mutant allele is cut with BlpI. *foxd3*^{zdf10}: dCAPS Forward (5'-CGACTGCTTCGTCAAGATCCCACGGGAACCGGGCAACCCGGGCAAAGGCAACTACTGGACCCTCGACCCCCAGTCGGAAAATAT-3'), Reverse (5'-CAGGGGGAATGTACGGGTACTGC-3'), mutant allele is cut with SspI. *paf1*^{z24}: Forward (5'-GTTCAGAGGTATGATGGATGAGG-3'), Reverse (5'-GTATGCAGCTTTATGAAAACACTC-3'), wildtype band is cut with NspI. *nid1b*^{sa13713}: Forward (5'-ATCTGGGCAGTCCTGAAGGAATCGCC-3'), dCAPS Reverse (5'-GCACATTCTGGAGCTCATTCTGATTCTGATTTTAAACGTTCGCGCTGCTCTACTTTAGCGTGTTTTAGCCGTGTCATGCATTGGT-3'), wildtype allele is cut with KpnI. *nid2a*^{sa15802}: Forward (5'-GACTTGCATTTCCAGTTACTCAGAATAAATATCTGTCTAGAC-3'), dCAPS

Reverse (5'-CGGCCGTTGCCGTAAAAGCCGGAGTTGCAGTGACAGCAGAAGCCGGTGGAATGATCTGTACAGTGAGCGTTTAGACTGCAGT-3'), mutant allele is cut with ScaI.

RNA synthesis and injections

Capped mRNAs were synthesized using linearized pCS2 templates (pCS2-EGFP-CAAX, pCS2FA-H2A.F/Z-mCherry), the mMessage mMachine SP6 kit (Ambion), purified (Qiagen RNeasy Mini Kit) and ethanol precipitated. One-cell stage embryos were microinjected with 150-250 pg of each mRNA. EGFP-CAAX mRNA was injected to visualize cell membranes, H2A.F/Z-mCherry mRNA was injected to visualize nuclei.

Antibody staining

Embryos were fixed at the indicated stage in 4% paraformaldehyde, permeabilized in PBST (PBS+0.5% Triton X-100), and blocked in PBST + 2% bovine serum albumin. Antibodies and concentrations are as follows: anti-Pax2a (Genetex GTX128127), 1:200; anti-pSmad3 (Abcam, ab52903), 1:200; anti-Nidogen/Entactin (Abcam, ab14511), 1:100; anti-Laminin 1 (Sigma, L9393), 1:100; anti-Fibronectin (Sigma, F3648), 1:100; anti-GFP (Invitrogen, A10262), 1:200. Secondary antibodies used were Alexa Fluor 488 goat anti-mouse (Life Technologies, A-11001), Alexa Fluor 488 goat anti-rabbit (Life Technologies, A-11008), Alexa Fluor 488 goat anti-chicken (Invitrogen A-11039) and incubated at 1:200. Nuclei were detected by incubation with 1 μM TOPRO-3 iodide (Life Technologies, T3605). Embryos were cleared through a series of 30%/50%/70% glycerol (in PBS) for imaging.

In situ hybridization

Embryos were fixed at the indicated stage in 4% paraformaldehyde overnight at 4°C and dehydrated in 100% methanol. Color *in situ* hybridizations were performed similar to (Thisse and Thisse, 2008). Fluorescent *in situ* hybridizations were carried out as described previously (Lauter et al., 2014; Leerberg et al., 2017). Anti-GFP labeling and detection was performed after *in situ* hybridization and tyramide signal amplification.

In situ probes were synthesized from linearized pBluescript II SK+ templates (pBSII-Nid1a, pBSII-Nid1b, pBSII-Nid2a, pBSII-Nid2b) using T3 or T7 polymerases and DIG labeling mix (Roche, 11277073910). All four probe sequences were synthesized (IDT gBlocks) and ligated into pBluescript II SK+.

Light microscopy

For timelapse imaging, 12 hpf embryos were embedded in 1.6% low-melt agarose (in E3) in DeltaT dishes (Bioptechs, #0420041500 C), E3 was overlaid and the dish covered to prevent evaporation. For antibody stained or fluorescent *in situ* hybridization imaging, embryos were embedded in 1% low-melt agarose (in PBS) in Pelco glass-bottom dishes (Ted Pella, #14027), PBS was overlaid to prevent evaporation.

Confocal images were acquired using a Zeiss LSM710 laser scanning confocal microscope. For timelapse imaging, datasets were acquired using the following parameters: 63 z-sections, 2.10 μm z-step, 40x water-immersion objective (1.2 NA). Time between z-stacks was 2.5 minutes. For all timelapse and antibody imaging, datasets were acquired without knowledge of embryo genotype. Embryos were de-embedded and genotyped after imaging was completed.

Brightfield images were acquired using an Olympus SZX16 stereomicroscope with either an Olympus DP26 or UC90 camera.

Transmission electron microscopy

Embryos (24 hpf) were fixed, stained and embedded using the microwave-assisted tissue processing protocol described in (Czopka and Lyons, 2011). Tails were dissected from embryos prior to fixation and used for genotyping.

Our tissue sampling and analytical techniques have been described previously in detail (Anderson et al., 2011a, 2011b; Lauritzen et al., 2013; Marc et al., 2014, 2013).

The tissues were osmicated for 60 minutes in 0.5% OsO4 in 0.1 M cacodylate buffer, processed in maleate buffer for en bloc staining with uranyl acetate, and processed for resin embedding. The epoxy resin bloc with zebrafish tissue was sectioned in the horizontal plane at 70–90 nm onto polyvinyl formal resin coated gold slot grids for transmission electron microscopy (TEM) (Lauritzen et al., 2013; Marc and Jones, 2002).

Each TEM section was imaged on a JEOL JEM-1400 transmission electron microscope at 20,000x and stored in 16- and 8-bit versions, as well as image pyramids of optimized tiles for web visualization with the Viking viewer (Anderson et al., 2011a, 2011b). Each image was captured as an array of image tiles at roughly 500-800 tiles/slice with 15% overlap.

Image processing and analysis

Images were processed using ImageJ. Volume rendering was performed using FluoRender (Wan et al., 2009). For lateral view 3D rendering of the optic cup, the

ectoderm was digitally erased in ImageJ prior to visualization in FluoRender. Invagination angles were measured as previously described (Bryan et al., 2016) and shown in Fig 3.2G. Individual cell tracking was performed as described in (Kwan et al., 2012) using LongTracker; nuclei were visualized using H2A.F/Z-mCherry.

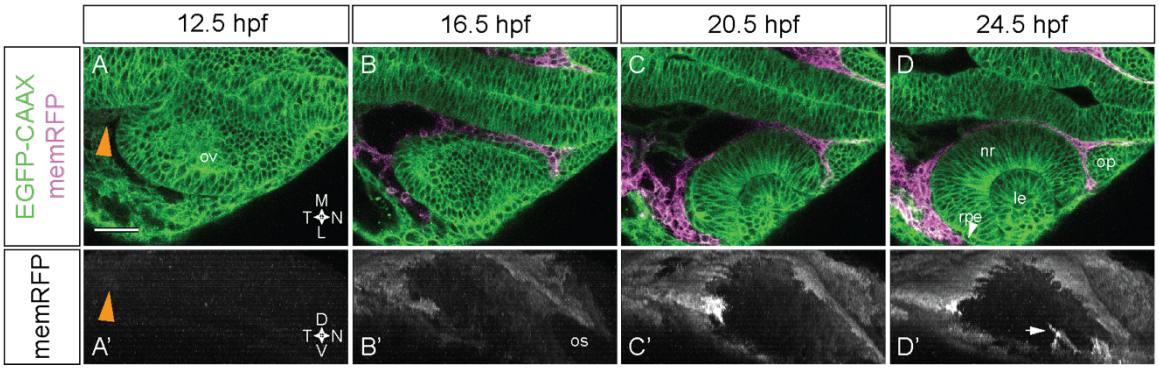

Figure 3.1. Neural crest is in contact with the optic vesicle throughout optic cup morphogenesis. Live imaging time series from 12.5-24.5 hpf of a *Tg(bactin2:EGFP-CAAX);Tg(sox10:memRFP)* double transgenic embryo. (A-D) Dorsal view, single confocal sections from a 4D dataset. (A'-D') Lateral view, 3D rendering of the RFP channel from the same dataset as shown in (A-D). Orange arrowheads in A, A' indicate neural crest cells beginning to express memRFP. White arrowhead in D indicates retinal pigment epithelium between neural crest and neural retina. White arrow in D' indicates neural crest-derived cells entering the optic fissure. Scale bar, 50 μm. ov, optic vesicle; os, optic stalk; nr, neural retina; rpe, retinal pigment epithelium; le, lens; op, olfactory placode. M, medial; L, lateral; D, dorsal; V, ventral; N, nasal; T, temporal.

Figure 3.2. Optic cup morphogenesis is disrupted in neural crest mutants. (A-F) Dorsal view, single confocal sections of 24 hpf *Tg(sox10:memRFP)*-positive control (A, D), *tfap2a;foxd3* double mutant (B, E), and *paf1* mutant embryos. Sections shown are at the dorsal/ventral midpoint of the lens. EGFP-CAAX was used to visualize optic cup morphology: embryos in A/D and B/E were also *Tg(bactin2:EGFP-CAAX)*-positive, while the *paf1* mutant shown in C/F was injected with mRNA encoding EGFP-CAAX. White outline in (E) shows the boundaries of the optic cup and lens, as shown in (B). White arrowheads in (B, C) denote the nasal retina failing to fully enwrap the lens in *tfap2a;foxd3* and *paf1* mutants, respectively. (G) Quantification of invagination angles, measured as shown in the inset diagram. *P<0.0001 using the student's t-test. (H-M) Lateral view, 3D renderings of the embryos shown above in (A-F). Blue dashed lines mark the margins of the optic fissure. Note the wideset margins of the optic fissure in the *tfap2a;foxd3* mutant in (I); no discernable margins are visible in the *paf1* mutant at 24 hpf. White asterisks in (L, M) indicate regions of missing neural crest cells. (N, O) Brightfield images of 52 hpf control and *tfap2a;foxd3* double mutant embryos. Red arrows in (I, J, O) indicate coloboma. (P) Quantification of coloboma percentages across three clutches of *tfap2a;foxd3* double heterozygote incrosses. Scale bars: 50 μm in (A), 100 μm in (N). M, medial; L, lateral; D, dorsal; V, ventral; N, nasal; T, temporal.

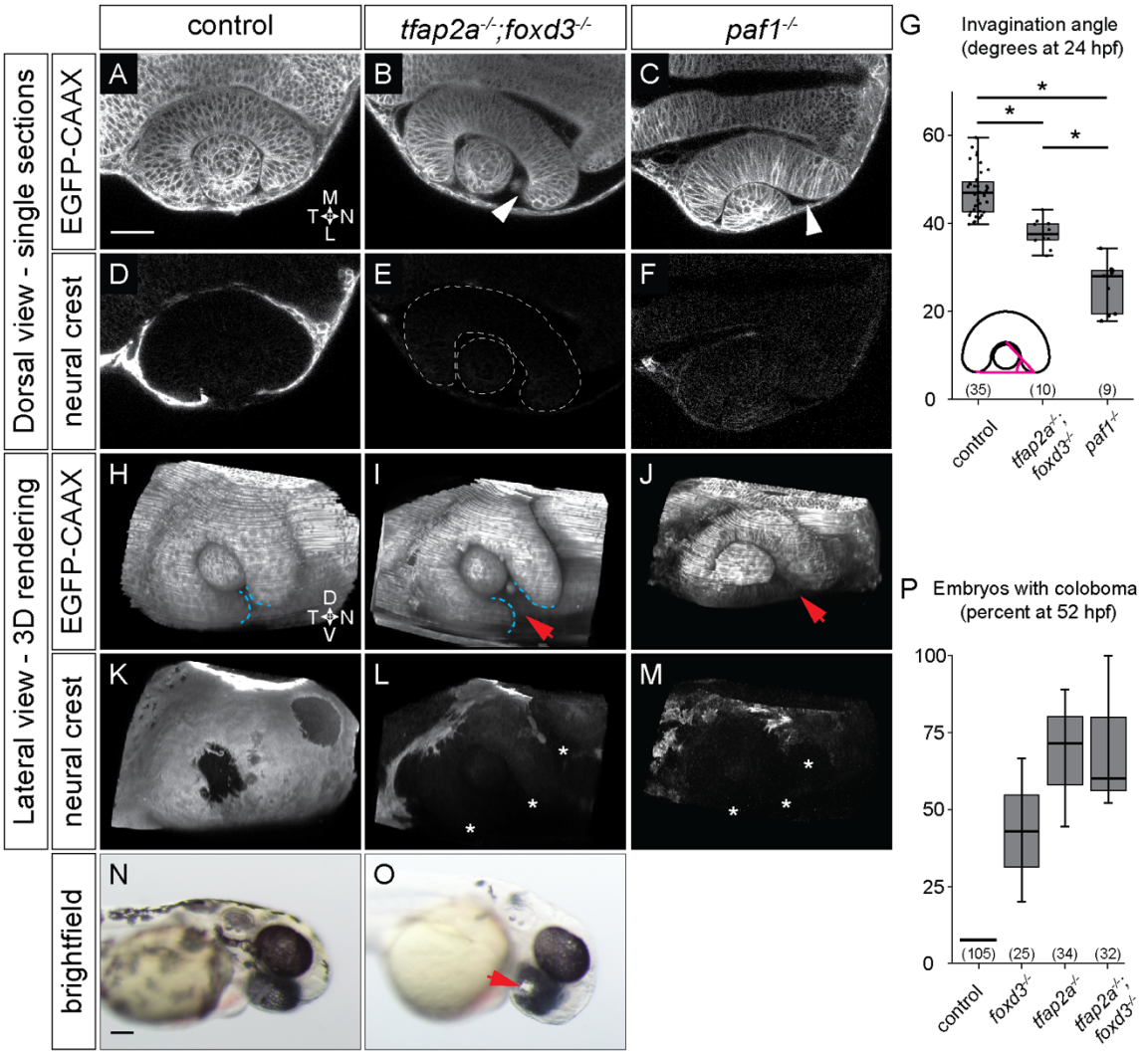
control
tfap2a-/-;foxd3-/-
paf1-/-
Dorsal view - single sections
Lateral view - 3D rendering
EGFP-CAAX
neural crest
EGFP-CAAX
neural crest
brightfield
A
B
C
D
E
F
H
I
J
K
L
M
N
O
M
T
N
L
D
T
N
V
G
Invagination angle
(degrees at 24 hpf)
60
40
20
0
(35)
(10)
(9)
control
tfap2a-/-;
foxd3-/-
paf1-/-
P
Embryos with coloboma
(percent at 52 hpf)
100
75
50
25
0
(105)
(25)
(34)
(32)
control
foxd3-/-
tfap2a-/-
tfap2a-/-;
foxd3-/-

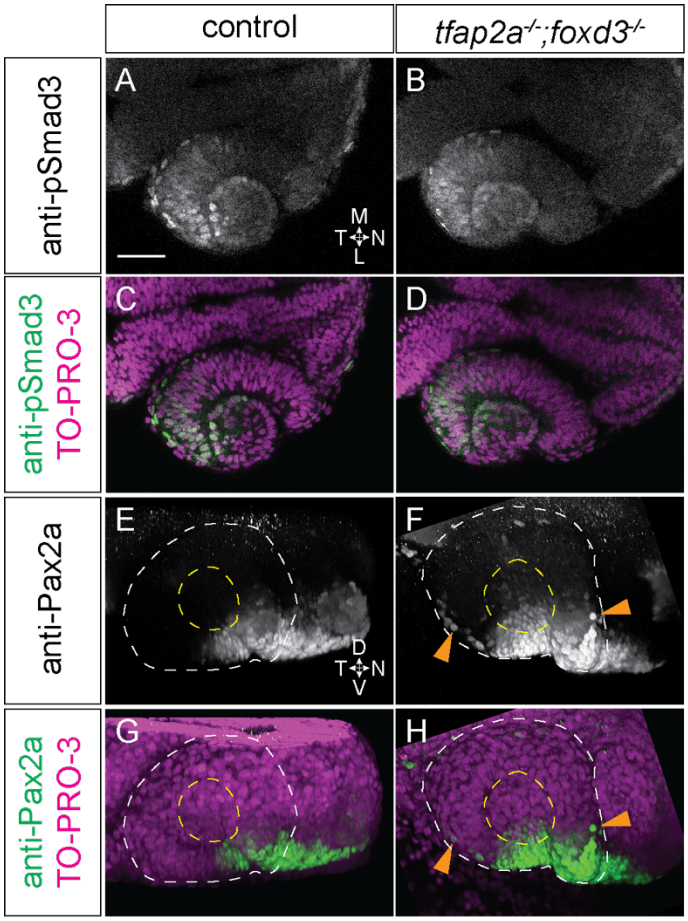

Figure 3.3. At 24 hpf, *tfap2a;foxd3* mutants display normal TGF-beta signaling, while Pax2a expression expands into the RPE. (A-D) Dorsal view, single confocal sections of 24 hpf control (A, C) and *tfap2a;foxd3* double mutant (B,D) optic cups stained with anti-phospho-Smad3. Sections shown are at the dorsal/ventral lens midpoint. (E-H) Lateral view, 3D renderings of 24 hpf control (E, G) and *tfap2a;foxd3* double mutant (F,H) optic cups stained with anti-Pax2a. White dashed circles denote the boundary of the optic cup, yellow dashed circles display the boundary of the lens. Orange arrowheads in (F, H) indicate RPE cells which ectopically express Pax2a. Nuclei were counterstained with TO-PRO-3 (magenta); merges shown in (C, D, G, H). M, medial; L, lateral; D, dorsal; V, ventral; N, nasal; T, temporal.

Figure 3.4. Cell movements throughout the optic cup are disrupted in *tfap2a;foxd3* double mutants. Live imaging time series of optic cup morphogenesis from 12.5-24.5 hpf of *Tg(bactin2:EGFP-CAAX)* wildtype and *tfap2a;foxd3* double mutant embryos. All images display the EGFP-CAAX channel to visualize cell membranes; embryos were also injected with mRNA encoding H2A.F/Z-mCherry to facilitate visualization of nuclei. (A-B’’’) Dorsal view, single confocal sections from wildtype (A-A’’’) and *tfap2a;foxd3* double mutant (B-B’’’) 4D datasets. (C-H’’’) Average projections of membrane channel through ~60 μm centered at the dorsal/ventral midpoint of the optic vesicle with indicated cell trajectories (nasal RPE, nasal retina, or temporal retina) overlaid. Trajectories were generated by adding nuclear signal selections over time. Scale bar, 50 μm. M, medial; L, lateral; N, nasal; T, temporal.

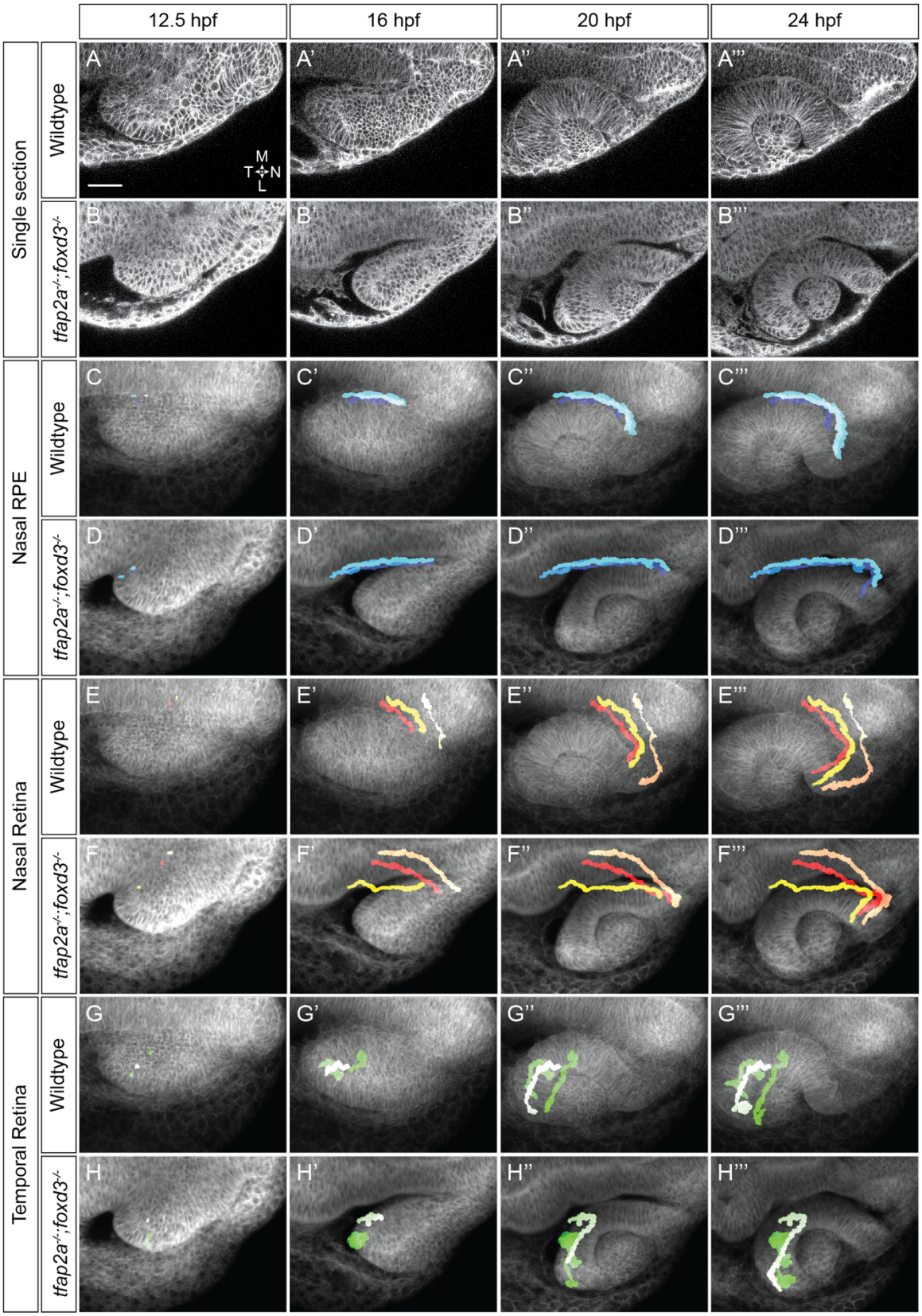
12.5 hpf
16 hpf
20 hpf
24 hpf
Single section
Nasal RPE
Nasal Retina
Temporal Retina
Wildtype
tfap2a-/-;foxd3-/-
A
A'
A''
A'''
B
B'
B''
B'''
C
C'
C''
C'''
D
D'
D''
D'''
E
E'
E''
E'''
F
F'
F''
F'''
G
G'
G''
G'''
H
H'
H''
H'''
M
T
N
L

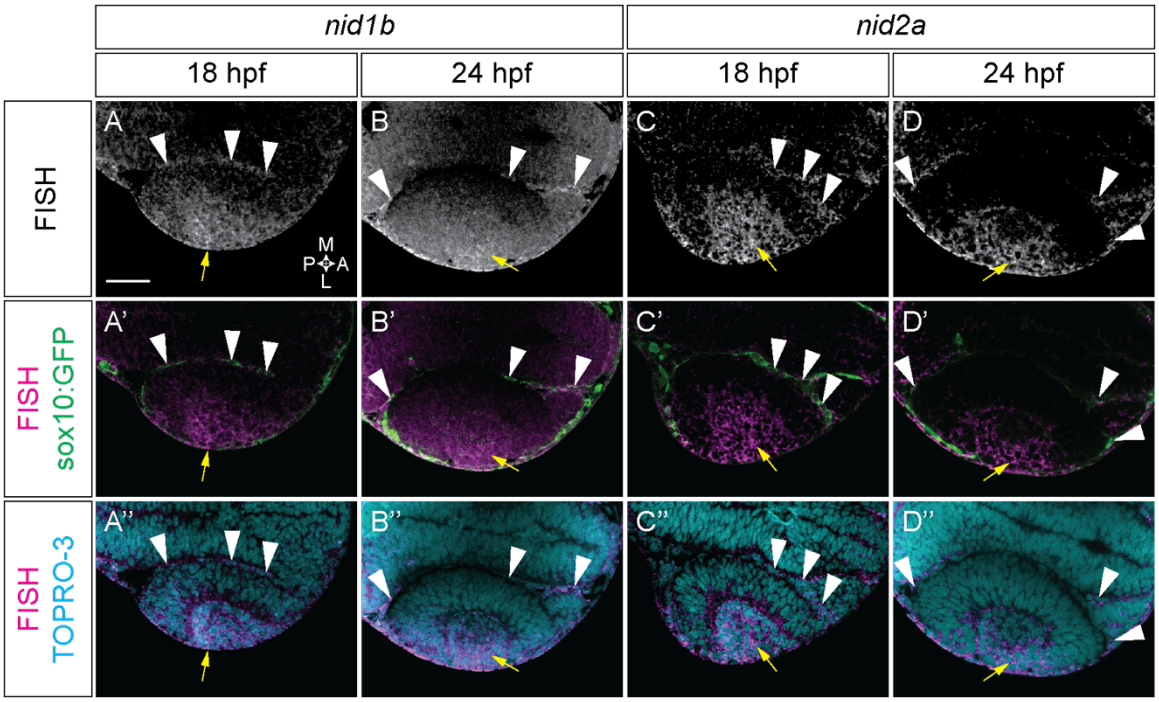

Figure 3.5. Nidogen 1b and 2a are expressed in the neural crest and developing lens. *In situs* were performed in *Tg(sox10:GFP)* embryos at 18 (A-A'', C-C'') and 24 hpf (B-B'', D-D''). (A-D) Fluorescence *in situ* hybridization with probes against *nid1b* (A,B) and *nid2a* (C,D). (A'-D') FISH merged with sox10:GFP expression (green) to visualize colocalization between FISH and GFP+ neural crest cells (white arrowheads). GFP signal was amplified after hybridization using an anti-GFP antibody. (A''-D'') FISH merged with nuclei counterstained with TO-PRO-3. Yellow arrows denote lens expression in each case. Dorsal view, single confocal sections. Scale bar, 50 μm.

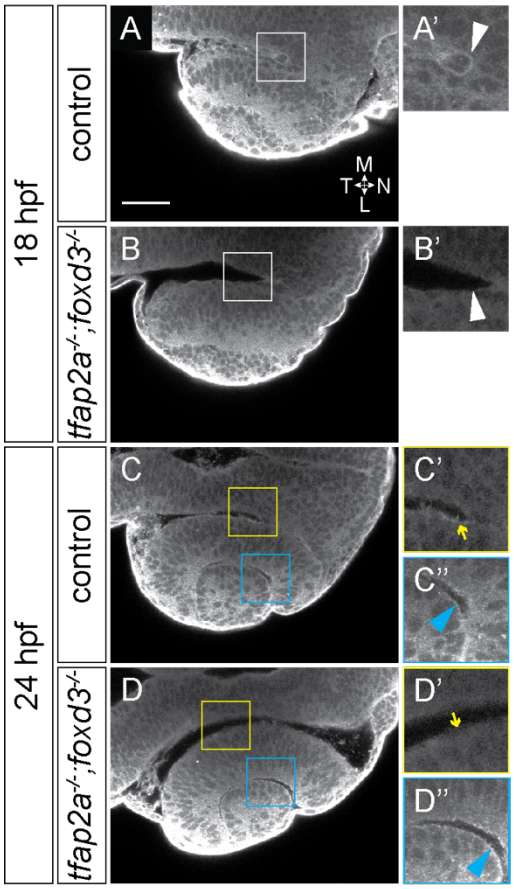

Figure 3.6. Nidogen protein is absent from the RPE side of the optic cup in *tfap2a;foxd3* double mutants. At 18 hpf, nidogen protein is detected by immunofluorescence in neural crest cells between the brain and developing RPE in the optic stalk furrow (A, magnified in A'). This expression is missing in *tfap2a;foxd3* double mutant embryos at 18 hpf and there are no cells visible in the same space (B, magnified in B'). At 24 hpf in control embryos, a nidogen ECM surface is detectable on along both the RPE (yellow box in C, yellow arrow in C') and at the lens-retina interface (C, C'', blue arrowhead). In 24 hpf *tfap2a;foxd3* double mutants, nidogen is not detectable along the RPE (D', yellow arrow), but is still present in the ECMs at the lens-retina interface (D'', blue arrowhead). Dorsal view, single confocal sections. Scale bar, 50 μm.

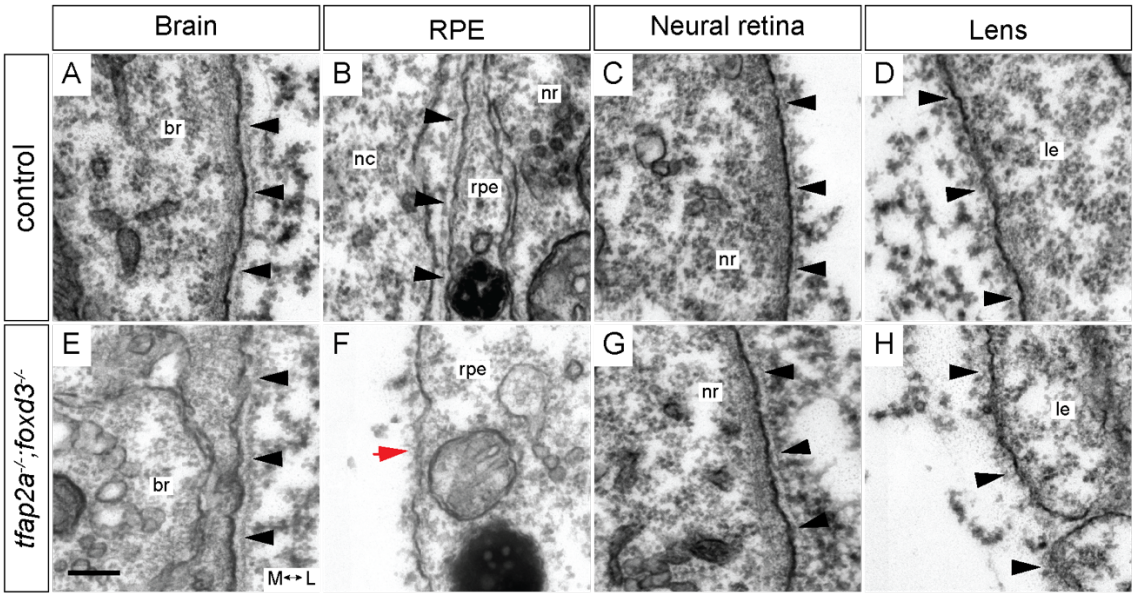

Figure 3.7. The basement membrane around the RPE is disrupted in *tfap2a;foxd3* double mutants. Transmission electron microscopy was used to visualize the basement membranes around the brain, RPE, neural retina, and lens in 24 hpf control (A-D) and *tfap2a;foxd3* double mutant embryos. The basement membrane around the RPE of *tfap2a;foxd3* mutant embryos appears disorganized (F, red arrow), while all other basement membranes appear normal (black arrowheads). Scale bar, 200 nm. br, brain; nc, neural crest cell; nr, neural retina; rpe, retinal pigment epithelium; le, lens. All images are transverse sections, anterior views. M, medial; L, lateral.

Figure 3.8. Dominant-interfering nidogen disrupts optic cup morphogenesis. (A) Protein schematics of full length (WT-Nid1a) and dominant-interfering (DI-Nid1a) forms of nidogen 1a. (B-D') Dorsal view, single confocal sections. *Tg(bactin2:EGFP-CAAX)* females were outcrossed to either *hs:WT-Nid1a* (B-C') or *hs:DI-Nid1a* (D, D') transgenic males. Control embryos (B, B') were not heat-shocked and show no lyn-mCherry expression, while experimental embryos were heat-shocked from 12-13 hpf (C-D'). (E) Quantification of invagination angles, measured as shown in the inset diagram. *P<0.005 using the student's t-test. (F, G) Lateral view, 3D renderings. *sox10:GFP* transgenic females were outcrossed to were outcrossed to either *hs:WT-Nid1a* (F) or *hs:DI-Nid1a* (G) transgenic males, embryos were heat-shocked from 12-13 hpf. GFP-positive neural crest cells migrate into the optic fissure in both conditions (white arrowheads). Scale bar, 50 μm. M, medial; L, lateral; N, nasal; T, temporal.

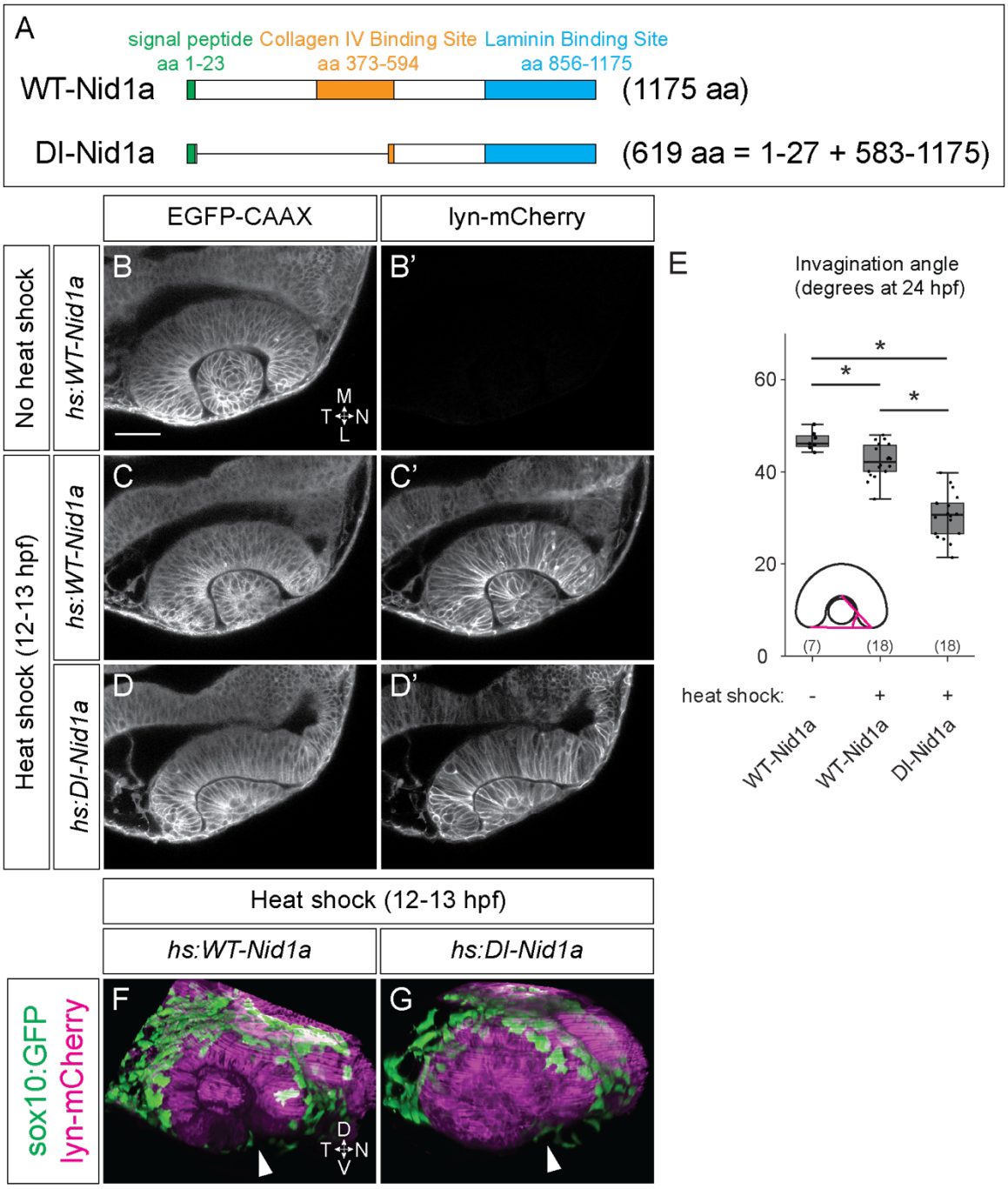
A
signal peptide
aa 1-23
Collagen IV Binding Site
aa 373-594
Laminin Binding Site
aa 856-1175
WT-Nid1a
(1175 aa)
Dl-Nid1a
(619 aa = 1-27 + 583-1175)
EGFP-CAAX
lyn-mCherry
No heat shock
hs:WT-Nid1a
Heat shock (12-13 hpf)
hs:WT-Nid1a
hs:Dl-Nid1a
B
B'
C
C'
D
D'
M
T
N
L
E
Invagination angle
(degrees at 24 hpf)
60
40
20
0
*
*
*
(7)
(18)
(18)
heat shock: - + +
WT-Nid1a
WT-Nid1a
Dl-Nid1a
Heat shock (12-13 hpf)
hs:WT-Nid1a
hs:Dl-Nid1a
sox10:GFP
lyn-mCherry
F
G
D
T
N
V

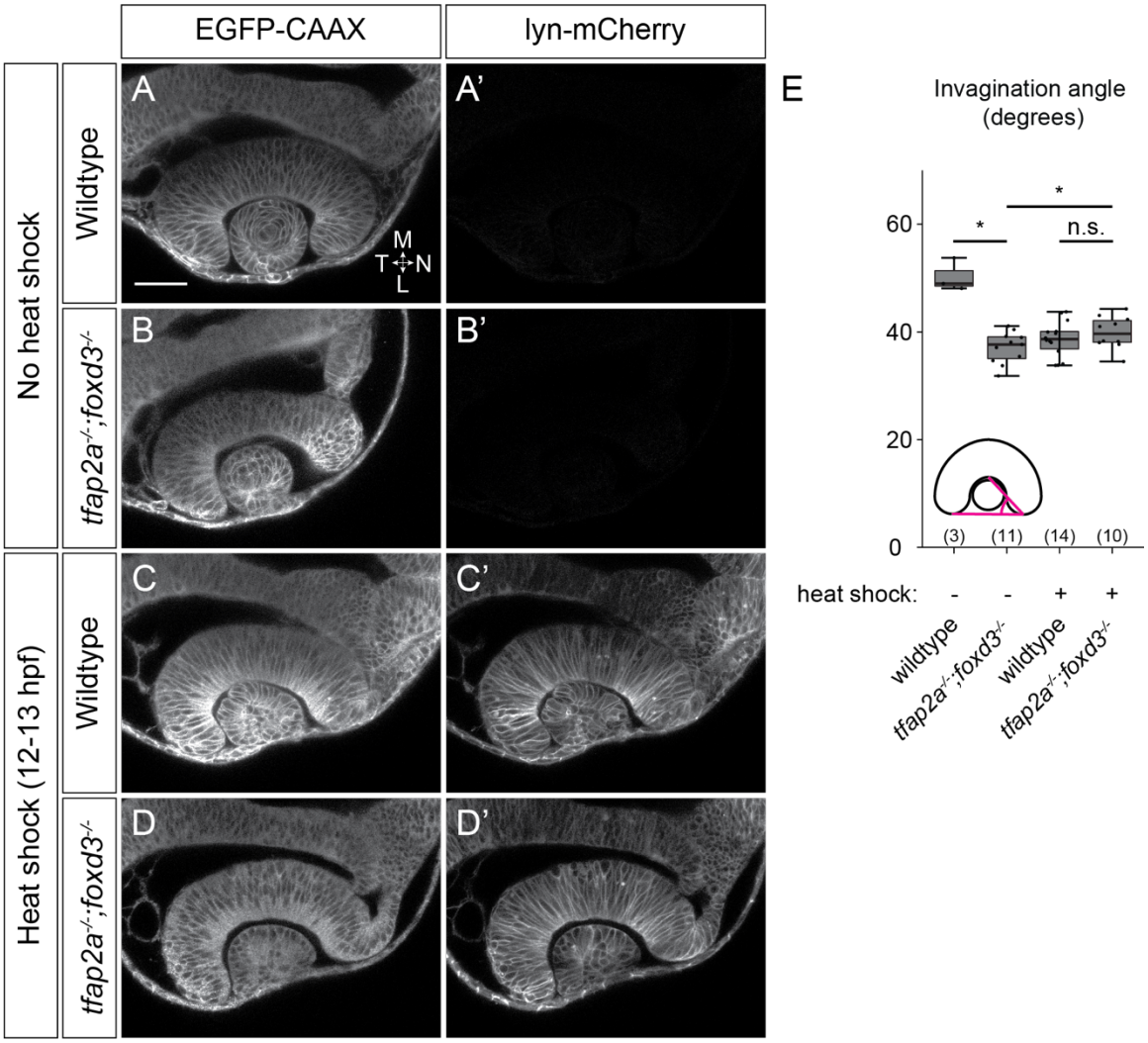

Figure 3.9. Overexpression of Nid1a partially rescues optic cup morphogenesis in *tfap2a;foxd3* double mutants. Dorsal view, single confocal sections from 24 hpf *Tg(hs:WT-Nid1a)*-positive embryos.(A-B') EGFP-CAAX and lyn-mCherry channels from wildtype (A, A') and *tfap2a;foxd3* double mutant (B, B') embryos which were not subjected to a heat-shock. (C-D') EGFP-CAAX and lyn-mCherry channels from wildtype (C, C') and *tfap2a;foxd3* double mutant (D, D') embryos which were heat-shocked from 12-13 hpf. (E) Quantification of invagination angles, measured as shown in the inset diagram. *P<0.05 using the student's t-test; n.s., not significant [P=0.34]. Scale bar, 50 μm. M, medial; L, lateral; N, nasal; T, temporal.

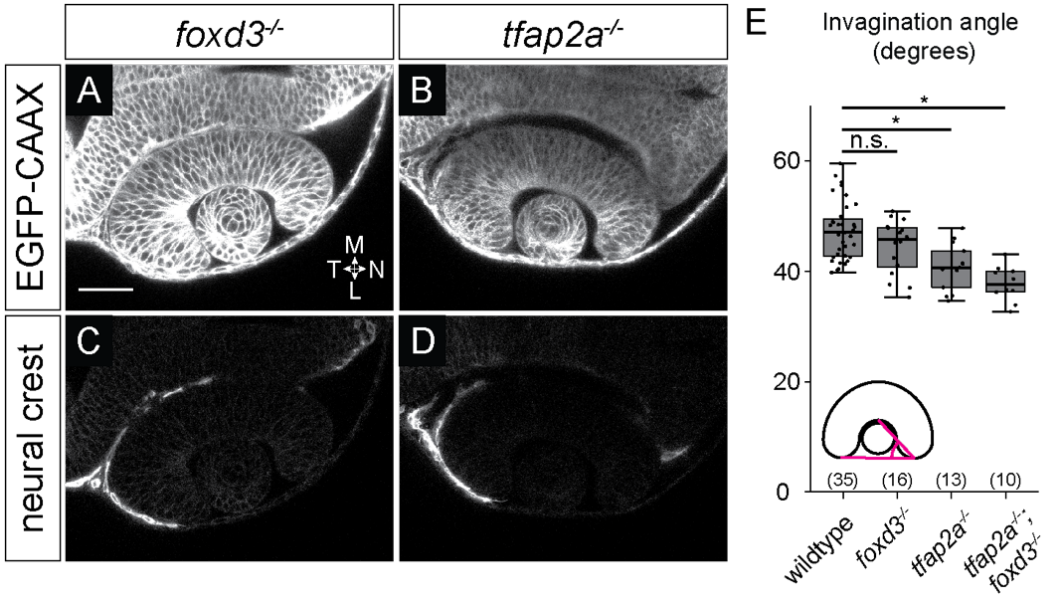

Figure S3.1. Invagination is disrupted in *tfap2a* but not *foxd3* single mutants. (A-D) Dorsal view, single confocal sections of 24 hpf *Tg(bactin2:EGFP-CAAX);Tg(sox10:memRFP)* double transgenic *foxd3* (A, C) and *tfap2a* (B, D) mutant embryos. Sections shown are at the dorsal/ventral midpoint of the lens. (E) Quantification of invagination angles, measured as shown in the inset diagram. *P<0.001 using the student's t-test. Scale bar, 50 μm. M, medial; L, lateral; N, nasal; T, temporal.

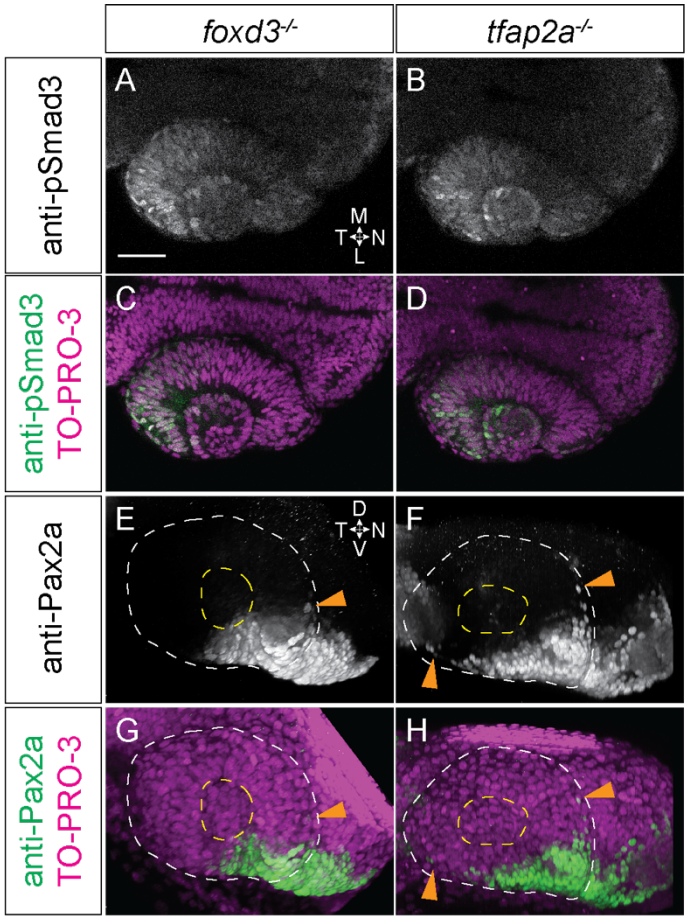

Figure S3.2. At 24 hpf, *tfap2a* and *foxd3* single mutants display normal TGF-beta signaling, while Pax2a expression expands into the RPE. (A-D) Dorsal view, single confocal sections of 24 hpf *foxd3* mutant (A, C) and *tfap2a* mutant (B,D) optic cups stained with anti-phospho-Smad3. Sections shown are at the dorsal/ventral lens midpoint. (E-H) Lateral view, 3D renderings of 24 hpf *foxd3* mutant (E, G) and *tfap2a* mutant (F,H) optic cups stained with anti-Pax2a. White dashed circles denote the boundary of the optic cup, yellow dashed circles display the boundary of the lens. Orange arrowheads in (E-H) indicate RPE cells which ectopically express Pax2a. Nuclei were counterstained with TO-PRO-3 (magenta); merges shown in (C, D, G, H). M, medial; L, lateral; D, dorsal; V, ventral; N, nasal; T, temporal.

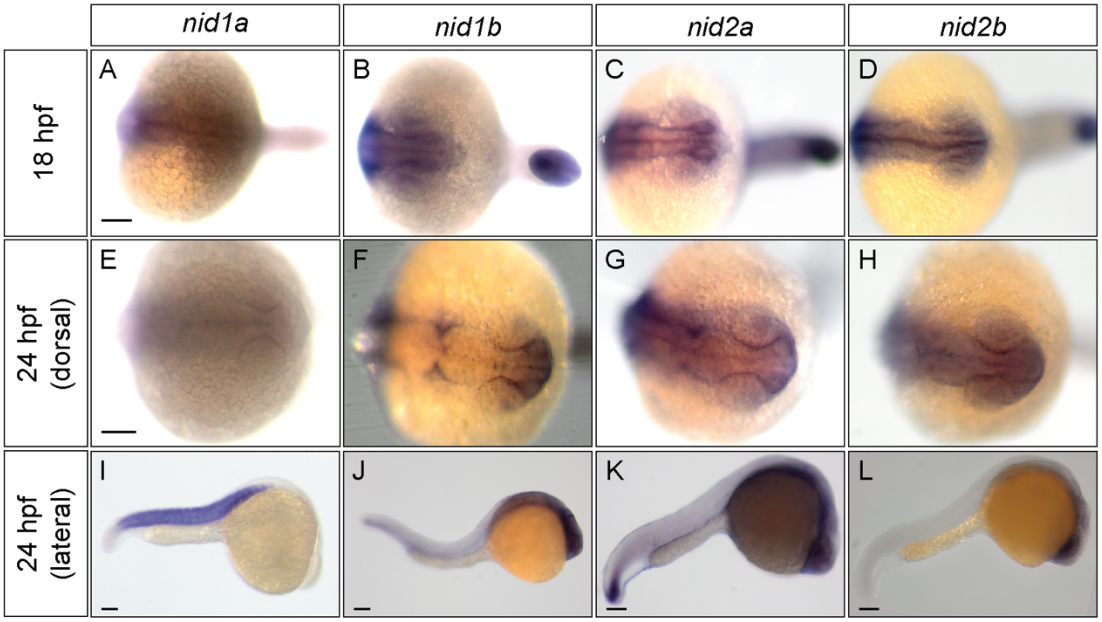

Figure S3.3. Zebrafish nidogen mRNA expression patterns at 18 and 24 hpf. Scale bars, 100 μm.

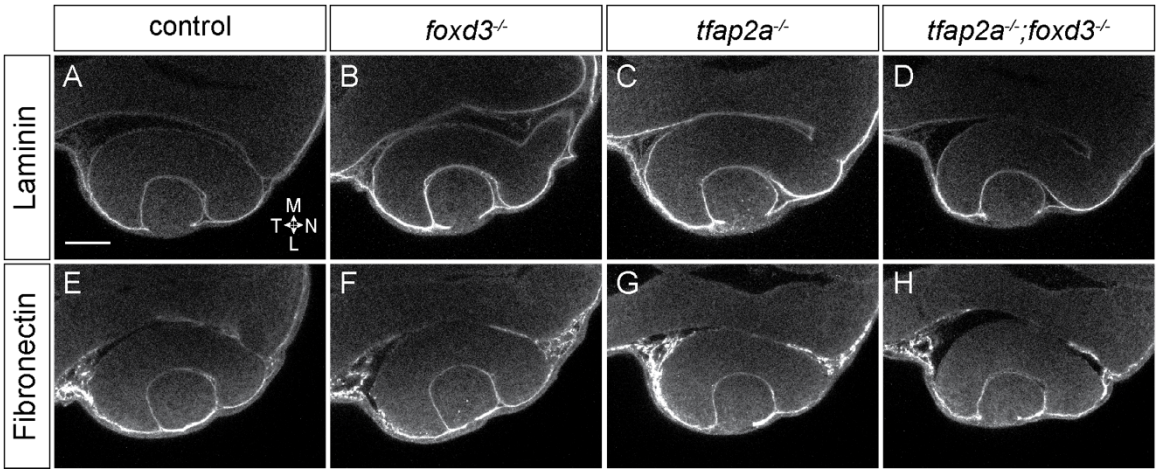

Figure S3.4. Laminin and fibronectin localization are unaffected in *tfap2a;foxd3* double mutants. At 24 hpf, both laminin (A-D) and fibronectin (E-H) are found around the developing optic cup in all genotypes shown. Dorsal view, single confocal sections. Scale bar, 50 μm. M, medial; L, lateral; N, nasal; T, temporal.

References

Akanuma, T., Koshida, S., Kawamura, A., Kishimoto, Y., Takada, S., 2007. Paf1 complex homologues are required for Notch-regulated transcription during somite segmentation. EMBO Rep. 8, 858–863. https://doi.org/10.1038/sj.embor.7401045

Anderson, J.R., Jones, B.W., Watt, C.B., Shaw, M. V, Yang, J.H., Demill, D., Lauritzen, J.S., Lin, Y., Rapp, K.D., Mastronarde, D., Koshevoy, P., Grimm, B., Tasdizen, T., Whitaker, R., Marc, R.E., 2011a. Exploring the retinal connectome. Mol Vis 17, 355–379.

Anderson, J.R., Mohammed, S., Grimm, B., Jones, B.W., Koshevoy, P., Tasdizen, T., Whitaker, R., Marc, R.E., 2011b. The Viking viewer for connectomics: Scalable multi-user annotation and summarization of large volume data sets. J. Microsc. 241, 13–28. https://doi.org/10.1111/j.1365-2818.2010.03402.x

Arduini, B.L., Bosse, K.M., Henion, P.D., 2009. Genetic ablation of neural crest cell diversification. Development 136, 1987–1994. https://doi.org/10.1242/dev.033209

Bader, B.L., Smyth, N., Nedbal, S., Baranowsky, A., Mokkapati, S., Miosge, N., Murshed, M., Nischt, R., Baranowsky, A., Mokkapati, S., Murshed, M., Nischt, R., 2005. Compound genetic ablation of nidogen 1 and 2 causes basement membrane defects and perinatal lethality in mice. Mol. Cell. Biol. 25, 6846–6856. https://doi.org/10.1128/MCB.25.15.6846

Bassett, E.A., Williams, T., Zacharias, A.L., Gage, P.J., Fuhrmann, S., West-Mays, J.A., 2010. AP-2a knockout mice exhibit optic cup patterning defects and failure of optic stalk morphogenesis. Hum. Mol. Genet. 19, 1791–1804. https://doi.org/10.1093/hmg/ddq060

Bohnsack, B.L., Kasprick, D.S., Kish, P.E., Goldman, D., Kahana, A., 2012. A zebrafish model of Axenfeld-Rieger syndrome reveals that pitx2 regulation by Retinoic Acid is essential for ocular and craniofacial development. Investig. Ophthalmol. Vis. Sci. 53, 7–22. https://doi.org/10.1167/iovs.11-8494

Böse, K., Nischt, R., Page, A., Bader, B.L., Paulsson, M., Smyth, N., 2006. Loss of nidogen-1 and -2 results in syndactyly and changes in limb development. J. Biol. Chem. 281, 39620–39629. https://doi.org/10.1074/jbc.M607886200

Bryan, C.D., Chien, C. Bin, Kwan, K.M., 2016. Loss of laminin alpha 1 results in multiple structural defects and divergent effects on adhesion during vertebrate optic cup morphogenesis. Dev. Biol. 416, 324–337. https://doi.org/10.1016/j.ydbio.2016.06.025

Cretekos, C.J., Grunwald, D.J., 1999. Alyron, an insertional mutation affecting early neural crest development in zebrafish. Dev. Biol. 210, 322–38. https://doi.org/10.1006/dbio.1999.9287

Czopka, T., Lyons, D.A., 2011. Dissecting mechanisms of myelinated axon formation using zebrafish, in: The Zebrafish: Disease Models and Chemical Screens. Elsevier Inc., pp. 25–62. https://doi.org/10.1016/B978-0-12-381320-6.00002-3

Dong, L.J., Chung, A.E., 1991. The expression of the genes for entactin, laminin-a, laminin-B1 and laminin-B2 in murine lens morphogenesis and eye development. Differentiation 48, 157–172.

Dutton, J.R., Antonellis, A., Carney, T.J., Rodrigues, F.S., Pavan, W.J., Ward, A., Kelsh, R.N., 2008. An evolutionarily conserved intronic region controls the spatiotemporal expression of the transcription factor Sox10. BMC Dev. Biol. 8, 105. https://doi.org/10.1186/1471-213X-8-105

Eberhart, J.K., He, X., Swartz, M.E., Yan, Y.L., Song, H., Boling, T.C., Kunerth, A.K., Walker, M.B., Kimmel, C.B., Postlethwait, J.H., 2008. MicroRNA Mirn140 modulates Pdgf signaling during palatogenesis. Nat. Genet. 40, 290–298. https://doi.org/10.1038/ng.82

Eiraku, M., Takata, N., Ishibashi, H., Kawada, M., Sakakura, E., Okuda, S., Sekiguchi, K., Adachi, T., Sasai, Y., 2011. Self-organizing optic-cup morphogenesis in three-dimensional culture. Nature 472, 51–56. https://doi.org/10.1038/nature09941

Ekblom, P., Ekblom, M., Fecker, L., Klein, G., Zhang, H.Y., Kadoya, Y., Chu, M.L., Mayer, U., Timpl, R., 1994. Role of mesenchymal nidogen for epithelial morphogenesis in vitro. Development 120, 2003–2014.

Fox, J.W., Mayer, U., Nischt, R., Aumailley, M., Reinhardt, D., Wiedemann, H., Mann, K., Timpl, R., Krieg, T., Engel, J., 1991. Recombinant nidogen consists of three globular domains and mediates binding of laminin to collagen type IV. EMBO J. 10, 3137–46.

Frisch, S.M., Francis, H., 1994. Disruption of epithelial cell-matrix interaction induces apoptosis. J. Cell. Biol. 124, 619–626. https://doi.org/10.1083/jcb.124.4.619

Fuhrmann, S., Levine, E.M., Reh, T.A., 2000. Extraocular mesenchyme patterns the optic vesicle during early eye development in the embryonic chick. Development 127, 4599–4609.

Gage, P.J., Rhoades, W., Prucka, S.K., Hjalt, T., 2005. Fate maps of neural crest and mesoderm in the mammalian eye. Investig. Ophthalmol. Vis. Sci. 46, 4200–4208. https://doi.org/10.1167/iovs.05-0691

Grocott, T., Johnson, S., Bailey, A.P., Streit, A., 2011. Neural crest cells organize the eye via TGF-β and canonical Wnt signalling. Nat. Commun. 2, 266–269. https://doi.org/10.1038/ncomms1269

Halfter, W., Oertle, P., Monnier, C.A., Camenzind, L., Reyes-Lua, M., Hu, H., Candiello,

J., Labilloy, A., Balasubramani, M., Henrich, P.B., Plodinec, M., 2015. New concepts in basement membrane biology. FEBS J. 282, 4466–4479. https://doi.org/10.1111/febs.13495

Hayes, J.M., Hartsock, A., Clark, B.S., Napier, H.R.L., Link, B.A., Gross, J.M., 2012. Integrin 5/Fibronectin1 and focal adhesion kinase are required for lens fiber morphogenesis in zebrafish. Mol. Biol. Cell 23, 4725–4738. https://doi.org/10.1091/mbc.E12-09-0672

Heermann, S., Schütz, L., Lemke, S., Krieglstein, K., Wittbrodt, J., 2015. Eye morphogenesis driven by epithelial flow into the optic cup facilitated by modulation of bone morphogenetic protein. Elife 4, 1–17. https://doi.org/10.7554/eLife.05216

Hendrix, R.W., Zwaan, J., 1975. The matrix of the optic vesicle-presumptive lens interface during induction of the lens in the chicken embryo. J. Embryol. Exp. Morphol. 33, 1023–49.

Hero, I., 1990. Optic fissure closure in the normal cinnamon mouse: An ultrastructural study. Investig. Ophthalmol. Vis. Sci. 31, 197–216.

Hero, I., Farjah, M., Scholtz, C.L., 1991. The prenatal development of the optic fissure in colobomatous microphthalmia. Investig. Ophthalmol. Vis. Sci. 32, 2622–2635.

Hilfer, S.R., 1983. Development of the eye of the chick embryo. Scan. Electron Microsc. 1353–69.

Huang, J., Rajagopal, R., Liu, Y., Dattilo, L.K., Shaham, O., Ashery-Padan, R., Beebe, D.C., 2011. The mechanism of lens placode formation: A case of matrix-mediated morphogenesis. Dev. Biol. 355, 32–42. https://doi.org/10.1016/j.ydbio.2011.04.008

Ivanovitch, K., Cavodeassi, F., Wilson, S.W., 2013. Precocious acquisition of neuroepithelial character in the eye field underlies the onset of eye morphogenesis. Dev. Cell 27, 293–305. https://doi.org/10.1016/j.devcel.2013.09.023

James, A., Lee, C., Williams, A.M., Angileri, K., Lathrop, K.L., Gross, J.M., 2016. The hyaloid vasculature facilitates basement membrane breakdown during choroid fissure closure in the zebrafish eye. Dev. Biol. 419, 262–272. https://doi.org/10.1016/j.ydbio.2016.09.008

Johnston, M.C., Noden, D.M., Hazelton, R.D., Coulombre, J.L., Coulombre, A.J., 1979. Origins of avian ocular and periocular tissues. Exp. Eye Res. 29, 27–43. https://doi.org/10.1016/0014-4835(79)90164-7

Kadoya, Y., Salmivirta, K., Talts, J.F., Kadoya, K., Mayer, U., Timpl, R., Ekblom, P., 1997. Importance of nidogen binding to laminin γ1 for branching epithelial morphogenesis of the submandibular gland. Development 124, 683–691.

Kettleborough, R.N.W., Busch-Nentwich, E.M., Harvey, S.A., Dooley, C.M., De Bruijn, E., Van Eeden, F., Sealy, I., White, R.J., Herd, C., Nijman, I.J., Fényes, F., Mehroke, S., Scahill, C., Gibbons, R., Wali, N., Carruthers, S., Hall, A., Yen, J., Cuppen, E., Stemple, D.L., 2013. A systematic genome-wide analysis of zebrafish protein-coding gene function. Nature 496, 494–497. https://doi.org/10.1038/nature11992

Kheradmand, F., Rishi, K., Werb, Z., 2002. Signaling through the EGF receptor controls lung morphogenesis in part by regulating MT1-MMP-mediated activation of gelatinase A/MMP2. J. Cell Sci. 115, 839–48.

Kimmel, C.B., Ballard, W.W., Kimmel, S.R., Ullmann, B., Schilling, T.F., 1995. Stages of embryonic development of the zebrafish. Dev. Dyn. 203, 253–310. https://doi.org/10.1002/aja.1002030302

Kirby, B.B., Takada, N., Latimer, A.J., Shin, J., Carney, T.J., Kelsh, R.N., Appel, B., 2006. In vivo time-lapse imaging shows dynamic oligodendrocyte progenitor behavior during zebrafish development. Nat. Neurosci. 9, 1506–1511. https://doi.org/10.1038/nn1803

Kudoh, T., Tsang, M., Hukriede, N.A., Chen, X., Dedekian, M., Clarke, C.J., Kiang, A., Schultz, S., Epstein, J.A., Toyama, R., Dawid, I.B., 2001. A gene expression screen in zebrafish embryogenesis. Genome Res. 11, 1979–1987. https://doi.org/10.1101/gr.209601

Kwan, K.M., 2014. Coming into focus: The role of extracellular matrix in vertebrate optic cup morphogenesis. Dev. Dyn. 243, 1242–1248. https://doi.org/10.1002/dvdy.24162

Kwan, K.M., Fujimoto, E., Grabher, C., Mangum, B.D., Hardy, M.E., Campbell, D.S., Parant, J.M., Yost, H.J., Kanki, J.P., Chien, C. Bin, 2007. The Tol2kit: A multisite gateway-based construction Kit for Tol2 transposon transgenesis constructs. Dev. Dyn. 236, 3088–3099. https://doi.org/10.1002/dvdy.21343

Kwan, K.M., Otsuna, H., Kidokoro, H., Carney, K.R., Saijoh, Y., Chien, C.-B., 2012. A complex choreography of cell movements shapes the vertebrate eye. Development 139, 359–372. https://doi.org/10.1242/dev.071407

Langenbacher, A.D., Nguyen, C.T., Cavanaugh, A.M., Huang, J., Lu, F., Chen, J.N., 2011. The PAF1 complex differentially regulates cardiomyocyte specification. Dev. Biol. 353, 19–28. https://doi.org/10.1016/j.ydbio.2011.02.011

Langenberg, T., Kahana, A., Wszalek, J.A., Halloran, M.C., 2008. The eye organizes neural crest cell migration. Dev. Dyn. 237, 1645–1652. https://doi.org/10.1002/dvdy.21577

Lauritzen, J.S., Anderson, J.R., Jones, B.W., Watt, C.B., Mohammed, S., Hoang, J. V.,

Marc, R.E., 2013. ON cone bipolar cell axonal synapses in the OFF inner plexiform layer of the rabbit retina. J. Comp. Neurol. 521, 977–1000. https://doi.org/doi: 10.1002/cne.23244

Lauter, G., Söll, I., Hauptmann, G., 2014. Sensitive whole-mount fluorescent in situ hybridization in zebrafish using enhanced tyramide signal amplification. Methods Mol. Biol. 1082, 175–185. https://doi.org/10.1007/978-1-62703-655-9

Lee, J., Gross, J.M., 2007. Laminin beta 1 and gamma 1 containing laminins are essential for basement membrane integrity in the zebrafish eye. Investig. Ophthalmol. Vis. Sci. 48, 2483–2490. https://doi.org/10.1167/iovs.06-1211

Leerberg, D.M., Sano, K., Draper, B.W., 2017. Fibroblast growth factor signaling is required for early somatic gonad development in zebrafish. PLOS Genet. 1–28. https://doi.org/10.1371/journal.pgen.1006993

Li, Z., Joseph, N.M., Easter, S.S., 2000. The morphogenesis of the zebrafish eye, including a fate map of the optic vesicle. Dev. Dyn. 218, 175–188. https://doi.org/10.1002/(SICI)1097-0177(200005)218:1<175::AID-DVDY15>3.0.CO;2-K

Lupo, G., Gestri, G., O'Brien, M., Denton, R.M., Chandraratna, R.A.S., Ley, S. V, Harris, W.A., Wilson, S.W., 2011. Retinoic acid receptor signaling regulates choroid fissure closure through independent mechanisms in the ventral optic cup and periocular mesenchyme. Proc. Natl. Acad. Sci. U. S. A. 108, 8698–8703. https://doi.org/10.1073/pnas.1103802108

Marc, R.E., Anderson, J.R., Jones, B.W., Sigulinsky, C.L., Lauritzen, J.S., 2014. The AII amacrine cell connectome: A dense network hub. Front. Neural Circuits 8, 1–13. https://doi.org/10.3389/fncir.2014.00104

Marc, R.E., Jones, B.W., 2002. Molecular phenotyping of retinal ganglion cells. J. Neurosci. 22, 413–427. https://doi.org/22/2/413 [pii]

Marc, R.E., Jones, B.W., Watt, C.B., Anderson, J.R., Sigulinsky, C., Lauritzen, S., 2013. Retinal connectomics: Towards complete, accurate networks. Prog. Retin. Eye Res. 37, 141–162. https://doi.org/10.1016/j.preteyeres.2013.08.002

Martinez-Morales, J.R., Rembold, M., Greger, K., Simpson, J.C., Brown, K.E., Quiring, R., Pepperkok, R., Martin-Bermudo, M.D., Himmelbauer, H., Wittbrodt, J., 2009. Ojoplano-mediated basal constriction is essential for optic cup morphogenesis. Development 136, 2165–2175. https://doi.org/10.1242/dev.033563

Miner, J.H., Yurchenco, P.D., 2004. Laminin functions in tissue morphogenesis. Annu. Rev. Cell Dev. Biol. https://doi.org/10.1146/annurev.cellbio.20.010403.094555

Neff, M.M., Neff, J.D., Chory, J., Pepper, A.E., 1998. dCAPS, a simple technique for the genetic analysis of single nucleotide polymorphisms: Experimental applications in Arabidopsis thaliana genetics. Plant J. 14, 387–392. https://doi.org/10.1046/j.1365-313X.1998.00124.x

Nelson, D.A., Larsen, M., 2015. Heterotypic control of basement membrane dynamics during branching morphogenesis. Dev. Biol. 401, 103–109. https://doi.org/10.1016/j.ydbio.2014.12.011

Nguyen, C.T., Langenbacher, A., Hsieh, M., Chen, J.N.O., 2010. The PAF1 complex component Leo1 is essential for cardiac and neural crest development in zebrafish. Dev. Biol. 341, 167–175. https://doi.org/10.1016/j.ydbio.2010.02.020

Nicolás-Pérez, M., Kuchling, F., Letelier, J., Polvillo, R., Wittbrodt, J., Martínez-Morales, J.R., 2016. Analysis of cellular behavior and cytoskeletal dynamics reveal a constriction mechanism driving optic cup morphogenesis. Elife 5, 1–24. https://doi.org/10.7554/eLife.15797.001

Peterson, P.E., Pow, C.S., Wilson, D.B., Hendrickx, A.G., 1995. Localisation of glycoproteins and glycosaminoglycans during early eye development in the macaque. J. Anat. 186 (Pt 1, 31–42.

Picker, A., Cavodeassi, F., Machate, A., Bernauer, S., Hans, S., Abe, G., Kawakami, K., Wilson, S.W., Brand, M., 2009. Dynamic coupling of pattern formation and morphogenesis in the developing vertebrate retina. PLoS Biol. 7. https://doi.org/10.1371/journal.pbio.1000214

Pollard, S.M., Parsons, M.J., Kamei, M., Kettleborough, R.N.W., Thomas, K.A., Pham, V.N., Bae, M.K., Scott, A., Weinstein, B.M., Stemple, D.L., 2006. Essential and overlapping roles for laminin α chains in notochord and blood vessel formation. Dev. Biol. 289, 64–76. https://doi.org/10.1016/j.ydbio.2005.10.006

Provost, E., Rhee, J., Leach, S.D., 2007. Viral 2A peptides allow expression of multiple proteins from a single ORF in transgenic zebrafish embryos. Genesis 45, 625–629. https://doi.org/10.1002/dvg.20338

Pujuguet, P., Simian, M., Liaw, J., Timpl, R., Werb, Z., Bissell, M.J., 2000. Nidogen-1 regulates laminin-1-dependent mammary-specific gene expression. J. Cell Sci. 113, 849–858. https://doi.org/10.1111/j.1600-6143.2008.02497.x.Plasma

Reinhardt, D., Mann, K., Nischt, R., Fox, J.W., Chu, M.L., Krieg, T., Timpl, R., 1993. Mapping of nidogen binding sites for collagen type IV, heparan sulfate proteoglycan, and zinc. J. Biol. Chem. 268, 10881–10887.

Schier, A.F., Neuhauss, S.C., Helde, K.A., Talbot, W.S., Driever, W., 1997. The one-eyed pinhead gene functions in mesoderm and endoderm formation in zebrafish and

interacts with no tail. Development 124, 327–342.

Schmitt, E.A., Dowling, J.E., 1994. Early eye morphogenesis in the zebrafish, Brachydanio rerio. J. Comp. Neurol. 344, 532–42. https://doi.org/10.1002/cne.903440404

Schook, P., 1980. Morphogenetic movements during the early development of the chick eye. A light microscopic and spatial reconstructive study. Acta Morphol. Neerl. Scand. 18, 1–30.

Sedykh, I., Yoon, B., Roberson, L., Moskvin, O., Dewey, C.N., Grinblat, Y., 2017. Zebrafish zic2 controls formation of periocular neural crest and choroid fissure morphogenesis. Dev. Biol. 429, 92–104. https://doi.org/10.1016/j.ydbio.2017.07.003

Semina, E. V, Bosenko, D. V, Zinkevich, N.C., Soules, K.A., Hyde, D.R., Vihtelic, T.S., Willer, G.B., Gregg, R.G., Link, B.A., 2006. Mutations in laminin alpha 1 result in complex, lens-independent ocular phenotypes in zebrafish. Dev. Biol. 299, 63–77. https://doi.org/10.1016/j.ydbio.2006.07.005

Senior, R.M., Griffin, G.L., Mudd, M.S., Moxley, M.A., Longmore, W.J., Pierce, R.A., 1996. Entactin expression by rat lung and rat alveolar epithelial cells. Am. J. Respir. Cell Mol. Biol. 14, 239–247.

Shawky, J.H., Davidson, L.A., 2015. Tissue mechanics and adhesion during embryo development. Dev. Biol. 401, 152–164. https://doi.org/10.1016/j.ydbio.2014.12.005

Sidhaye, J., Norden, C., 2017. Concerted action of neuroepithelial basal shrinkage and active epithelial migration ensures efficient optic cup morphogenesis. Elife 6, 1–29. https://doi.org/10.7554/eLife.22689

Soules, K.A., Link, B.A., 2005. Morphogenesis of the anterior segment in the zebrafish eye. BMC Dev. Biol. 5, 12. https://doi.org/10.1186/1471-213X-5-12

Svoboda, K.K., O'Shea, K.S., 1987. An analysis of cell shape and the neuroepithelial basal lamina during optic vesicle formation in the mouse embryo. Development 100, 185–200.

Thesleff, I., 2003. Epithelial-mesenchymal signalling regulating tooth morphogenesis. J. Cell Sci. 116, 1647–1648. https://doi.org/10.1242/jcs.00410

Thisse, B., Thisse, C., 2004. Fast release clones: A high throughput expression analysis. ZFIN Direct Data Submiss.

Thisse, C., Thisse, B., 2008. High-resolution in situ hybridization to whole-mount zebrafish embryos. Nat. Protoc. 3, 59–69. https://doi.org/10.1038/nprot.2007.514

Tuckett, F., Morriss-Kay, G.M., 1986. The distribution of fibronectin, laminin and

entactin in the neurulating rat embryo studied by indirect immunofluorescence. J. Embryol. Exp. Morphol. 94, 95–112.

Walls, G.L., 1942. The Vertebrate Eye and its Adaptive Radiation. Hafner Publishing Company.

Wan, Y., Otsuna, H., Chien, C. Bin, Hansen, C., 2009. An interactive visualization tool for multi-channel confocal microscopy data in neurobiology research. IEEE Trans. Vis. Comput. Graph. 15, 1489–1496. https://doi.org/10.1109/TVCG.2009.118

Wang, W. Der, Melville, D.B., Montero-Balaguer, M., Hatzopoulos, A.K., Knapik, E.W., 2011. Tfap2a and Foxd3 regulate early steps in the development of the neural crest progenitor population. Dev. Biol. 360, 173–185. https://doi.org/10.1016/j.ydbio.2011.09.019

Weiss, O., Kaufman, R., Michaeli, N., Inbal, A., 2012. Abnormal vasculature interferes with optic fissure closure in lmo2 mutant zebrafish embryos. Dev. Biol. 369, 191–198. https://doi.org/10.1016/j.ydbio.2012.06.029

Wells, K.L., Gaete, M., Matalova, E., Deutsch, D., Rice, D., Tucker, A.S., 2013. Dynamic relationship of the epithelium and mesenchyme during salivary gland initiation: the role of Fgf10. Biol. Open 2, 981–9. https://doi.org/10.1242/bio.20135306

Willem, M., Miosge, N., Halfter, W., Smyth, N., Jannetti, I., Burghart, E., Timpl, R., Mayer, U., 2002. Specific ablation of the nidogen-binding site in the laminin γ1 chain interferes with kidney and lung development. Development 129, 2711–2722.

Williams, A.L., Bohnsack, B.L., 2015. Neural crest derivatives in ocular development: Discerning the eye of the storm. Birth Defects Res. Part C - Embryo Today Rev. https://doi.org/10.1002/bdrc.21095

Zhu, P., Ma, Z., Guo, L., Zhang, W., Zhang, Q., Zhao, T., Jiang, K., Peng, J., Chen, J., 2017. Short body length phenotype is compensated by the upregulation of nidogen family members in a deleterious nid1a mutation of zebrafish. J. Genet. Genomics 44, 553–556. https://doi.org/10.1016/j.jgg.2017.09.011

CHAPTER 4

INVESTIGATIONS INTO THE CELL BIOLOCAL PROCESSES UNDERLYING OPTIC CUP INVAGINATION

Abstract

Tissue morphogenesis is regulated by a wide variety of cell biological processes and signaling pathways. Vertebrate optic cup morphogenesis utilizes many of the same mechanical programs as other tissues, such as actomyosin mediated constriction and adhesion to the extracellular matrix. The extracellular matrix protein laminin is required for proper morphogenesis of the optic cup, and disruptions to cell-matrix adhesions result in severe malformations of the eye. We sought to understand which laminin receptors are required for optic cup morphogenesis and how laminin-mediated adhesions signal to the developing eye to drive morphogenetic movements. Laminin is required to establish proper apicobasal polarity within the optic cup, and mutants lacking laminin develop ectopic specification of apical polarity throughout the eye. Double mutants lacking both laminin and core components of the apical polarity complex still exhibit severe morphogenesis defects, indicating that the formation of ectopic polarity is not the underlying cause of these defects. We also attempted to bypass a requirement for laminin in basal constriction of the developing retina using mutants that exhibit excessive myosin activation; these experiments were inconclusive but suggest that laminin is

absolutely necessary for basal constriction and cannot be bypassed. Finally, in our search to identify new cell biological processes required for morphogenesis, we identified and characterized the genetic lesion in a separate mutant where the lens and retina do not properly separate.

Introduction

Development of every organ depends on a myriad of cell biological processes which coordinate dynamic cellular and tissue movements. Disruptions to any of these processes can alter the cellular behaviors that are critical for formation of a functional organ or entire portions of an organism. However, the extent to which any given process, pathway or individual molecule contributes to a developmental program is often not well understood. While many of the pathways that are required for optic cup morphogenesis are known, much is yet to be discovered regarding how the vertebrate eye takes its functional, semispherical shape.

We and others have shown previously that development of the optic cup is dependent on the presence of the extracellular matrix protein laminin-1 (Bryan et al., 2016; Ivanovitch et al., 2013; Sidhaye and Norden, 2017). Laminin is required for many phases of morphogenesis, and its absence causes defects in both early and late morphogenetic movements. At a molecular level, laminin affects integrin-mediated cell-ECM adhesion in divergent, site specific fashions. During optic cup elongation, laminin promotes cell-ECM adhesion at the optic stalk furrow between the brain and optic vesicle. In contrast, at the lens-neural retinal interface during invagination, laminin appears to prevent excess adhesion to the ECM. Laminin is also required to establish

apicobasal polarity in the optic vesicle (Ivanovitch et al., 2013), and mutants lacking laminin establish ectopic apical domains throughout optic cup morphogenesis, indicating that apicobasal polarity does not revert to a normal state in the absence of laminin (Bryan et al., 2016).

The apical polarity complex is comprised of the three main proteins Par3, Par6 and aPKC, and is involved in many cell biological processes, including membrane trafficking (Bryant et al., 2010), oriented cell divisions (Bergstralh et al., 2013), and cell differentiation (Blasky et al., 2014), among others. The apical polarity complex can also regulate morphogenesis, both on a tissue-wide scale (Horne-Badovinac et al., 2001; Wang et al., 2012) and at a subcellular scale (Jones and Metzstein, 2011). Since the apical complex is involved in tissue morphogenesis, we suspected that aberrant optic cup morphogenesis that occurs in the absence of laminin may be due to the establishment of incorrect apical polarity domains within the optic cup, and set out to test this possibility through mutant analysis and epistasis experiments.

Several sites throughout the optic cup undergo specific constriction events which are primarily localized to the basal, ECM interacting surface of the neuroepithelium; this is in contrast to most epithelial contraction events which primarily undergo apical constriction (Martin and Goldstein, 2014). These basal constriction events are contingent on ECM attachment (Bogdanović et al., 2012; Gutzman et al., 2008; Martinez-Morales et al., 2009; Nicolás-Pérez et al., 2016), and are dependent on nonmuscle myosin II activity (Gutzman et al., 2015; Nicolás-Pérez et al., 2016). Cell-ECM attachments drive myosin activation through integrin-dependent focal adhesions (Akhtar and Streuli, 2013; He et al., 2010; Khyrul et al., 2004), which are disrupted in the developing optic cup of laminin

mutants. We sought to test whether hyperactivation of myosin could drive basal constriction events in the absence of the laminin ECM.

In addition to the cellular events which occur within the neuroepithelium itself, we also have described a role for extraocular tissues in regulating optic cup morphogenesis. The migratory cranial neural crest is required for the correct tissue movements that shape the eye, and we therefore sought to determine whether there were discrepancies in neural crest migration in the absence of laminin which could account for the severity of optic cup morphogenesis defects in the laminin mutant.

While many of the cellular processes that regulate optic cup morphogenesis have been described, other aspects have yet to be identified or explained. For example, physical connections between the neural retina and lens placode are required for lens morphogenesis; these are mediated by extracellular matrix molecules such as fibronectin (Huang et al., 2011) or through cytoskeletal elements such as filopodia (Chauhan et al., 2009). While adhesions and physical connections are necessary for these tissues to develop correctly, it is also important for these tissues to separate at the correct time in order for their development to proceed properly. Here we describe the *O15* mutant which does not undergo proper de-adhesion of the lens and retina during optic cup morphogenesis, and identify the precise genetic lesion in this mutant.

Results

Dystroglycan is not required for polarization of the optic cup

The *lama1*^{UW1} mutant zebrafish displays variable disruptions to apical polarity, with the most common being establishment of ectopic apical surfaces throughout the

embryonic optic cup (Bryan et al., 2016). There are two primary receptor complexes which link epithelia to the laminin extracellular matrix: integrin-containing focal adhesions, and the dystroglycan complex. Deletions of focal adhesion components such as ILK and integrin-β1 have been observed to disrupt epithelial polarization (Akhtar and Streuli, 2013). Additionally, deletions of dystroglycan have been observed to affect apical-basal polarity in *Drosophila* oocytes and chick neuroepithelia (Deng et al., 2003; Schröder et al., 2007). Therefore, we hypothesized that the disruptions to apical polarity we observed in the absence of laminin were due to an absence of signaling through either of these receptor complexes, either alone or acting in concert.

To test the role of dystroglycan in establishing apical-basal polarity, we turned to the *dag1*^{sa11376} mutant allele. This allele contains a point mutation that results in a premature stop codon (Kettleborough et al., 2013), and thus we predicted these mutants would not express any functional, full length dystroglycan protein. We incrossed heterozygous adult *dag1*^{sa11376} carriers to generate wildtype and mutant embryos, then fixed and stained these embryos at 24 hpf to visualize dystroglycan protein and the apical polarity protein aPKC. Wildtype embryos display essentially uniform distribution of dystroglycan protein around the basal surfaces of the optic cup (Fig 4.1A). As we predicted, *dag1* mutant embryos did not express any detectable dystroglycan protein at 24 hpf (Fig 4.1B). However, apical polarity was unchanged in the *dag1* mutants compared to their wildtype siblings (Fig 4.1A-B), as aPKC expression was still detected at the apical surface of the optic cup and midline of the brain in both conditions. This result indicates that dystroglycan is not required for establishing apical-basal polarity within the optic cup.

Disruptions to the apical polarity complex do not rescue the *lama1* mutant phenotype

The *lama1* mutant displays aberrant apical polarity domains at sites throughout the neural retina, as well as at the basal surface of the optic cup. Previous studies have demonstrated a role for the apical polarity complex in regulating morphogenesis, both at a subcellular and a tissue-wide level (Horne-Badovinac et al., 2001; Jones and Metzstein, 2011; Lerner et al., 2013; Martin-Belmonte and Mostov, 2008). Therefore we predicted that the optic cup morphogenesis defects we observed in the absence of laminin were partially due to the ectopic apical surfaces we observed in these mutant embryos. To test this hypothesis, we generated two double mutants with *lama1*^{UW1} and components of the apical polarity complex: *prkci*, which encodes the protein aPKC, and *pard3*.

We used antibody staining against aPKC to observe apical polarity and optic cup development in embryos from a *lama1;prkci* double heterozygote incross at 24 hpf. Sibling control embryos displayed normal apical surfaces within the optic cup (Fig 4.2A), while *lama1*^{UW1} mutants displayed characteristic ectopic apical polarity domains within the center of the neural retina (Fig 4.2C, yellow arrowheads). In 24 hpf *prkci* mutant embryos, we detected lower levels of aPKC protein, but still observed localization of aPKC to normal apical surfaces within the optic cup (Fig 4.2B), in addition to morphologically normal optic cups (Fig 4.2B'). This finding is consistent with the initial characterization of the *prkci*^{m567} mutant which demonstrated that maternally deposited aPKC is present within these embryos and is still detectable beyond 24 hpf (Horne-Badovinac et al., 2001). In *lama1;prkci* double mutant embryos, we detected decreased levels of aPKC protein at the normal apical surface of the optic cup, but to our surprise

did not observe any ectopic apical surfaces in these embryos (Fig 4.2D). However, while the apical surfaces were returned to a normal state in these embryos, we did not observe rescue of the optic cup morphogenesis defects that are characteristic of loss of *lama1*.

Due to the maternal deposition of apical polarity mRNAs and proteins in these embryos, we also used a maternal-zygotic mutant for *pard3* which has no deposition of functional *pard3* mRNA or protein to determine whether complete ablation of the apical complex is capable of rescuing the morphogenesis defects we observe in *lama1* mutants. *pard3*^{fh305} mutant embryos are viable to adulthood and fertile (Blasky et al., 2014), which enabled us to generate *lama1*$^{+/-}$*;pard3*$^{-/-}$ adults, which we then incrossed to generate *lama1;MZpard3* double mutant embryos. We injected mRNA encoding EGFP-CAAX into these embryos, as well as control *MZpard3* embryos to visualize optic cup structure at the end of optic cup morphogenesis at 24 hpf. Surprisingly, *MZpard3* embryos displayed normally formed optic cups at 24 hpf (Fig 4.3A), while the optic cups of *lama1;MZpard3* double mutant optic cups morphologically resembled the optic cups of *lama1* single mutants (Fig 4.3B). Together, these results demonstrate that not only are the ectopic apical surfaces that are generated in *lama1* mutant optic cups not the underlying cause of the disruptions to optic cup morphogenesis we observe in these embryos, but that the apical polarity complex is dispensable for optic cup morphogenesis.

Hyperactivating myosin II does not rescue basal constriction in *lama1* mutants

During normal zebrafish optic cup morphogenesis, the basal surface of the neural retina undergoes actomyosin mediated constriction which helps drive the cellular and

tissue shape changes during invagination. Recent work has demonstrated that basal constriction within the optic cup, as well as at the developing midbrain-hindbrain boundary, depends on the presence of a laminin ECM at both sites, and that actomyosin contractility is lost when laminin is depleted at either site (Gutzman et al., 2015, 2008; Nicolás-Pérez et al., 2016). We hypothesized that since laminin appears to be required for activation of nonmuscle myosin II mediated constriction during optic cup invagination, ectopic activation of that myosin may bypass a need for laminin.

To test this hypothesis, we generated *lama1*^{UW1}*;mypt1*^{hi2653} double mutants. *mypt1* encodes Mypt1 (also known as Ppp1r12a), a subunit of myosin phosphatase, and the *mypt1*^{hi2653} mutant allele contains a retroviral insertion (Amsterdam et al., 2004). Myosin phosphatase regulates the activation state of myosin regulatory light chain, which when phosphorylated is in its active, contractile state. When Mypt1 is lost, myosin phosphatase is rendered nonfunctional, which in turn leads to hyperactivation of myosin (Gutzman and Sive, 2010; Huang et al., 2008). To our surprise, the optic cups of 24 hpf *lama1;mypt1* double mutants appear phenotypically indistinguishable from *lama1* single mutants (Fig 4.4B), while sibling control embryos display normal optic cup morphogenesis (Fig 4.4A), and from this we conclude that loss of Mypt1 is insufficient to drive basal constriction in the absence of laminin.

Laminin is not required for neural crest cell migration

Earlier experiments we conducted showed that neural crest cells migrate over the optic cup throughout optic cup morphogenesis. Neural crest cells are required for optic cup invagination, and are required for proper basement membrane development around

the RPE. While laminin mutations cause optic cup morphogenesis defects earlier than invagination stages (Bryan et al., 2016; Ivanovitch et al., 2013), these defects could be exacerbated by further disruptions to the extraocular environment such as loss of neural crest. Therefore, we wanted to determine whether cranial neural crest migration around the optic cup is dependent on the presence of the laminin ECM.

To visualize neural crest cells, we used the *Tg(sox10:memRFP)*^{vu234} where the neural crest cells are labeled with membrane bound RFP. We generated *lama1*^{UW1}*;Tg(sox10:memRFP)*^{vu234} adults and incrossed them to visualize neural crest cells in *lama1* mutants and their wildtype siblings at 24 hpf; embryos were injected with mRNA encoding EGFP-CAAX to visualize the optic cup. As our previous experiments showed, neural crest cells migrate around the optic vesicle throughout optic cup morphogenesis, starting from the dorsal, posterior region of the optic vesicle, and moving anteriorly, ventrally and laterally such that they surround the optic cup by 24 hpf. In 24 hpf wildtype embryos, neural crest cells are visible around the entire optic cup; representative dorsal, lens-midpoint and ventral sections are shown in (Fig 4.5 A, C, E), respectively. Somewhat surprisingly, neural crest cell migration in the *lama1* mutant appears to be unaffected by the absence of laminin. In *lama1* mutants, neural crest cells are detectable around the optic cup at all positions observed in wildtype embryos (Fig 4.5 B, D, F), demonstrating that by 24 hpf, neural crest cells are capable of migrating to the correct location around the optic cup in the absence of laminin. Therefore, laminin is not required for neural crest migration around the optic cup.

The *O15* deficiency spans over 100 genes on chromosome 5

The *O15* mutation was isolated from a haploid, ENU mutagenesis screen. Both haploid and diploid *O15* mutants display aberrant lens development: at 24 hpf, under brightfield microscopy the lens is not visible (Figure 4.6A, B). Confocal microscopy reveals that the lens is indeed still present in these mutants, but that the lens appears to be in tight contact with the neural retina at 24 hpf. Over the next several days, the lens gradually becomes visible by brightfield microscopy, but these embryos develop other mutant phenotypes and are fully paralyzed by 72 hpf and do not survive to adulthood.

We sought to identify the genetic lesion which was responsible for these phenotypes, and therefore undertook efforts to locate the *O15* mutation in the zebrafish genome. Through rough mapping, the mutation was found to reside on chromosome 5. Further refinement was made possible by performing RNA-seq on wildtype and mutant embryos, and comparing them using the MMAPPR software package pipeline (Hill et al., 2013) using the zebrafish Zv9 genome assembly. Prior uses of MMAPPR identified both known and unknown nonsense point mutations, which is what we expected to find in the *O15* mutant. Much to our surprise, MMAPPR detected a large segment of chromosome 5 where the RNA-seq read depth was depleted, suggestive of a large deletion.

Using genomic DNA from *O15* mutants and wildtype siblings, as well as PCR primers designed against both the 5' and 3' sides of the deletion, we amplified multiple loci in an effort to approach and map across the breakpoint. When we identified primer pairs which amplified using wildtype DNA but failed to amplify from mutant DNA, we reasoned that one of the two primers targeted a sequence which was missing in the deletion. Finally, we identified a primer pair which amplified from mutant DNA but not

wildtype DNA. After TOPO cloning and sequencing this amplicon, we identified a molecular lesion spanning a large portion of chromosome 5 (Figure 4.6C). The 5' end of the amplicon mapped to the first intron of the *si:dkey-245n4.2* gene, while the 3' end of the amplicon mapped over 9 megabase pairs down chromosome 5 within intergenic space between the *slc14a2* and *lnpep* genes. Using the GRCz10 zebrafish reference genome, the 5' end of the *O15* deficiency maps to chromosome 5 at position 42,469,846 bp, and the 3' end maps to 51,532,989 bp for a total deletion of 9,063,143 bp; 22 base pairs are present between these endpoints, and appear to be the product of nonhomologous end joining as they have no homology to any portion of chromosome 5. Over 100 genes are contained within this region of the genome and are lost in the *O15* mutation. With the molecular breakpoint known, we can classify *O15* as a deficiency and hereby notate it as *Df(Chr05:O15)*. Additionally, with the sequence for the genetic lesion, we are able to conclusively genotype any embryo as wildtype, heterozygous or mutant for *Df(Chr05:O15)* (Figure 4.6D).

Discussion

Development of the vertebrate optic cup requires a careful balance of many cell biological processes ranging from precise signaling events across tissues to cytoskeletal remodeling within specific subcellular regions. Understanding how the eye takes its shape necessarily involves taking all these events into account and trying to understand how these processes can feed into each other or act in independent pathways. The broad goal of this work has been to understand how the tissue-wide cell adhesion programs that are required during optic cup morphogenesis feed into intracellular processes such as

apicobasal polarity or myosin activation.

Dystroglycan is not required to establish optic cup polarity

The laminin receptor dystroglycan has previously been shown to play a role in establishing apicobasal polarity in *Drosophila* oocytes (Deng et al., 2003) and breast cancer cells in culture (Muschler et al., 2002). Therefore, we predicted that dystroglycan would be required for apical polarity establishment in the zebrafish optic cup. However, *dag1* mutant zebrafish form phenotypically wildtype optic cups with a normal apical polarity domain. This result does not conclusively demonstrate that dystroglycan is insufficient to polarize the optic cup after laminin binding, but does illustrate that dystroglycan protein is not strictly required for apical-basal polarity. There are two remaining possibilities for how polarity is established in the eye. Integrin-dependent focal adhesion signaling is critical to establish polarity in several cell culture systems (Akhtar and Streuli, 2013; Khyrul et al., 2004), and provides one possible mechanism by which optic cup polarity could be established completely independently of the dystroglycan complex. Alternately, signals downstream of both integrins and dystroglycan could work independently to establish polarity within the eye, and it is possible that the signals from one are sufficient to establish polarity in the absence of the other. To distinguish between these possibilities, it will be necessary to disrupt focal adhesion function, either alone or together with the *dag1* loss of function mutant. It will be interesting to perturb the focal adhesion complex to test its function in regulating apicobasal polarity within the optic cup.

Loss of a myosin deactivator does not rescue basal constriction defects that arise in the absence of laminin

Attachment to the ECM is required for basal constriction within the developing optic cup (Bogdanović et al., 2012; Martinez-Morales et al., 2009; Nicolás-Pérez et al., 2016) and the zebrafish midbrain-hindbrain boundary (Gutzman et al., 2008). Further, basal constriction at both sites requires nonmuscle myosin II activation (Gutzman et al., 2015; Nicolás-Pérez et al., 2016). Therefore, we predicted that the basal constriction events within the developing retina are driven through ECM-attachment mediated activation of these actomyosin networks. We tested whether activation of nonmuscle myosin II through loss of function of *mypt1,* which encodes a myosin phosphatase, could rescue basal constriction in the absence of laminin. However, the *lama1;mypt1* double mutants we generated presented with the *lama1* mutant phenotype at 24 hpf, indicating that the *mypt1* mutation cannot rescue basal constriction in the absence of laminin. This result suggests multiple possibilities: first, that the level of nonmuscle myosin II activation that occurs in the absence of Mypt1 is not sufficient to drive basal constriction of the optic cup of *lama1;mypt1* double mutants. A second possibility is that in the absence of laminin, nonmuscle myosin II is not phosphorylated in the first place, and thus loss of Mypt1 cannot lead to prolonged activation of the myosin regulatory light chain and subsequent contractility. Yet another possibility is that in the double mutants studied here, nonmuscle myosin II localization is not restricted to the correct, basal subcellular compartment required for basal constriction to occur. A careful analysis of antibody staining against phosphorylated myosin, or live imaging using a fluorescently labelled myosin will help distinguish these possibilities.

Laminin is not required for neural crest cell migration

Experiments detailed in Chapters 2 and 3 of this dissertation have demonstrated that optic cup morphogenesis depends on the laminin extracellular matrix, as well as neural crest cells that migrate around the developing optic cup and modify the surrounding ECM. We suspected that some of the optic cup morphogenesis defects we observe in *lama1* mutants could be the result of aberrant neural crest migration. To test this possibility, we crossed *lama1* mutants with *sox10:memRFP* transgenic zebrafish where the neural crest cells are labelled with membrane-bound RFP. To our surprise, neural crest migration appears to be unaffected by loss of laminin: in 24 hpf *lama1;sox10:memRFP* embryos, while the optic cup is severely malformed, neural crest cells have migrated to normal positions around the optic cup. While analysis at the end of optic cup morphogenesis does not rule out the possibility that neural crest cell migration is disrupted at earlier stages of development, the presence of neural crest cells in the correct places around the optic cup at the end of optic cup morphogenesis argues against this.

The *O15* deficiency provides a new tool to study de-adhesion

Cell adhesion is a necessary process for tissues to form correctly, and intertissue adhesion is critical for coordination of lens and retinal development. However, these tissues must separate and generate the correct spacing to accommodate retinal vasculature, as well as to position the lens the correct distance to focus light on the retina. How these tissues lose their attachments and become separated from one another is not understood, and the zebrafish *O15* mutant provides a unique model to study this process.

These mutants have little to no space between the lens and retina, and identifying the gene or genes regulating the spacing between these tissues is necessary to study this process. However, by its very nature as a deficiency, the *O15* mutant makes identifying genes underlying this process somewhat difficult. The *O15* deficiency encompasses over 100 genes on chromosome 5, several of which are expressed in the developing eye during optic cup morphogenesis, and thus are good candidate genes to study their role in this process. For example, the *versican a* (*vcana*) gene is lost in the *O15* deficiency; this gene encodes an extracellular matrix protein known to guide cell migration and serve as a repulsive molecular boundary during neural crest migration (Szabó et al., 2016). During optic cup morphogenesis, *vcana* is expressed from the developing lens (Thisse et al., 2001), and thus may serve as a partitioning factor that could drive separation of the lens and retina. Another candidate in regulating lens-retina de-adhesion is the *col4a3bp* gene. While col4a3bp protein appears to be ubiquitously expressed during optic cup morphogenesis in zebrafish, it is somewhat enriched in the developing eye and *col4a3bp* morphants display microphthalmia (Granero-Moltó et al., 2008). Additionally, preliminary experiments from our lab suggest that injecting col4a3bp mRNA into presumptive *O15* mutants reduces the frequency of the "hidden lens" phenotype by approximately 40% (E.O. Wirick and K.M. Kwan, unpublished data). It is possible that this de-adhesion process depends on multiple genes and thus the "hidden lens" we observe could be the result of several genes required for lens development being absent. Over 100 other genes are absent from the genome in the *O15* deficiency, and through genetic complementation tests with the *O15* mutant we can begin testing the individual role of any of these genes in de-adhesion or any other processes that gene may regulate.

Materials and methods

Zebrafish lines

Embryos from the following mutant and transgenic lines were raised at 28.5-30 °C and staged according to hours post fertilization and morphology (Kimmel et al., 1995).

- Mutant alleles: *dag1*^{sa11376} (Kettleborough et al., 2013); *lama1*^{UW1} (Semina et al., 2006); *prkci*^{m567} (Horne-Badovinac et al., 2001); *pard3*^{fh305} (Blasky et al., 2014); *mypt1*^{hi2653} (Amsterdam et al., 2004); *Df(Chr05:O15)*.
- Transgenic allele: *Tg(sox10:memRFP)*^{vu234} (Kirby et al., 2006).

RNA synthesis and injections

Capped mRNA was synthesized using a linearized pCS2 template (pCS2-EGFP-CAAX), the mMessage mMachine SP6 kit (Ambion), purified (Qiagen RNeasy Mini Kit) and ethanol precipitated. 150 pg of mRNA was microinjected into the cell of one-cell stage embryos.

Antibody staining

Embryos were fixed at the indicated stage in 4% paraformaldehyde, permeabilized in PBST (PBS+0.5% Triton X-100), and blocked in PBST + 2% bovine serum albumin. Antibodies and concentrations are as follows: anti-aPKC (PKC ζ (C-20) Santa Cruz Biotechnology #sc-216) was diluted 1:200; anti-beta dystroglycan (Abcam, ab49515), 1:100. Secondary antibodies used were Alexa Fluor 488 goat anti-mouse (Life Technologies, A-11001), Alexa Fluor 488 goat anti-rabbit (Life Technologies, A-11008),

Alexa Fluor 568 goat anti-rabbit (Life Technologies, A-11011), and incubated at 1:200. Nuclear detection was through incubation with 1 μM TOPRO-3 iodide (Life Technologies, T3605). Embryos were cleared through a series of 30%/50%/70% glycerol (in PBS) for imaging.

Imaging

For live imaging, 24 hpf embryos were embedded in 1.6% low-melt agarose (in E3) in DeltaT dishes (Bioptechs, #0420041500 C), E3 was overlaid and the dish covered to prevent evaporation. For antibody stained imaging, embryos were embedded in 1% low-melt agarose (in PBS) in Pelco glass-bottom dishes (Ted Pella, #14027), PBS was overlaid to prevent evaporation. For all timelapse and antibody imaging, datasets were acquired without knowledge of embryo genotype. Embryos were de-embedded and genotyped after imaging was completed. Confocal images were acquired using a Zeiss LSM710 laser scanning confocal microscope, 2.10 μm z-step, 40x water-immersion objective (1.2 NA). Images were processed using ImageJ.

O15 deficiency mapping and genotyping

Genomic DNA was isolated and pooled from multiple *O15* mutant or control sibling embryos. PCR primers were designed against sequences on either side of the predicted genomic lesion. As much of the sequence around the breakpoints is intronic or intergenic and contained repetitive sequences, extra care was taken to identify primer binding sites that were unique in the zebrafish genome. Platinum Taq polymerase was used for PCRs, which enabled us to perform TOPO cloning with any products generated.

The initial ~2kbp amplicon which spanned the *O15* breakpoint was amplified using the following primers: Forward (5'-GTCACTTCTGCAAGCAAAGCAGAAGATTATT-3'), Reverse (5'-CTAGGCAAGTTATGGGACAACAGTGGTTTG-3'). We subsequently amplified a smaller set of amplicons which can be used to conclusively genotype zebrafish at the *O15* locus as wildtype, heterozygous mutant or homozygous mutant. These amplicons use a common forward primer: (5'-CAGTGTGTGTTACTGCTTACACAACATG-3'). The wildtype amplicon is 774 bp long and is amplified using the reverse primer (5'-GCACTTTTCTACTCACAACACTTGTTTTTGAAG-3'); the mutant amplicon is 497 bp long and uses the reverse primer (5'-GGGAAATATTTGGCAAAGAATCAAATTTTCAAAGCC-3').

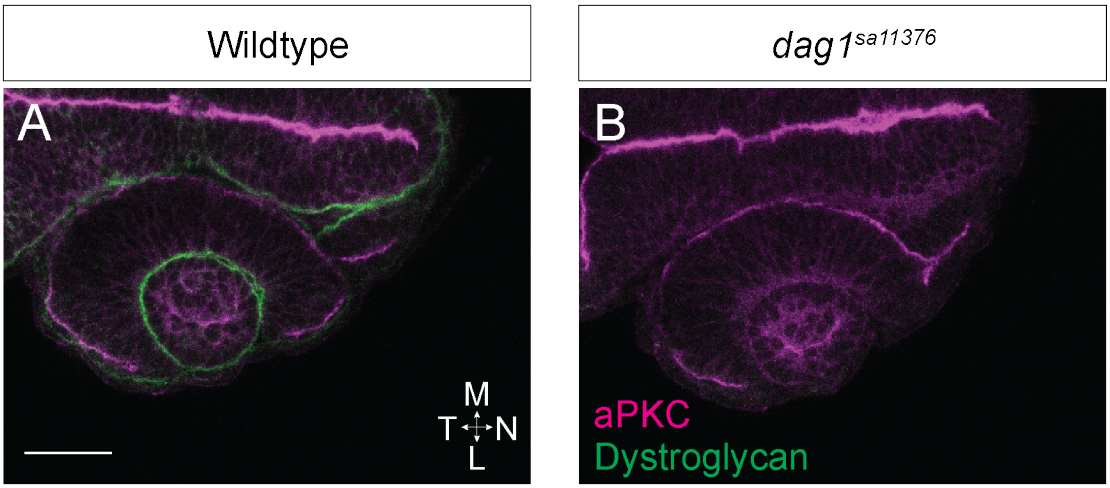

Figure 4.1. Dystroglycan is not required to establish apical polarity within the eye. (A-B) Antibody staining for the apical polarity protein aPKC (magenta) and the laminin receptor dystroglycan (green) in 24hpf wildtype control (A) or *dag1*^{sa11376} mutant embryos (B). Dorsal view, single confocal sections from 4D datasets. Scale bar, 50 μm. M, medial; L, lateral; N, nasal; T, temporal.

Figure 4.2. *prkci* mutations do not rescue optic cup morphogenesis in *lama1* mutants. (A-D) Antibody staining for the apical polarity protein aPKC in 24 hpf control (A), *prkci*^{m567} single mutant (B), *lama1*^{UW1} single mutant (C), and *lama1*^{UW1}*;prkci*^{m567} double mutant (D) embryos. Green arrowheads denote the normal apical surface in the optic cup; yellow arrowheads in (C) indicate ectopic apical surfaces present in the *lama1*^{UW1} mutant. (A'-D') Embryos were counterstained using TO-PRO-3, images in (A'-D') show the nuclear signal corresponding to the images in (A-D). Anterior view, single confocal sections from 4D datasets. Scale bar, 50 μm. M, medial; L, lateral; D, dorsal; V, ventral.

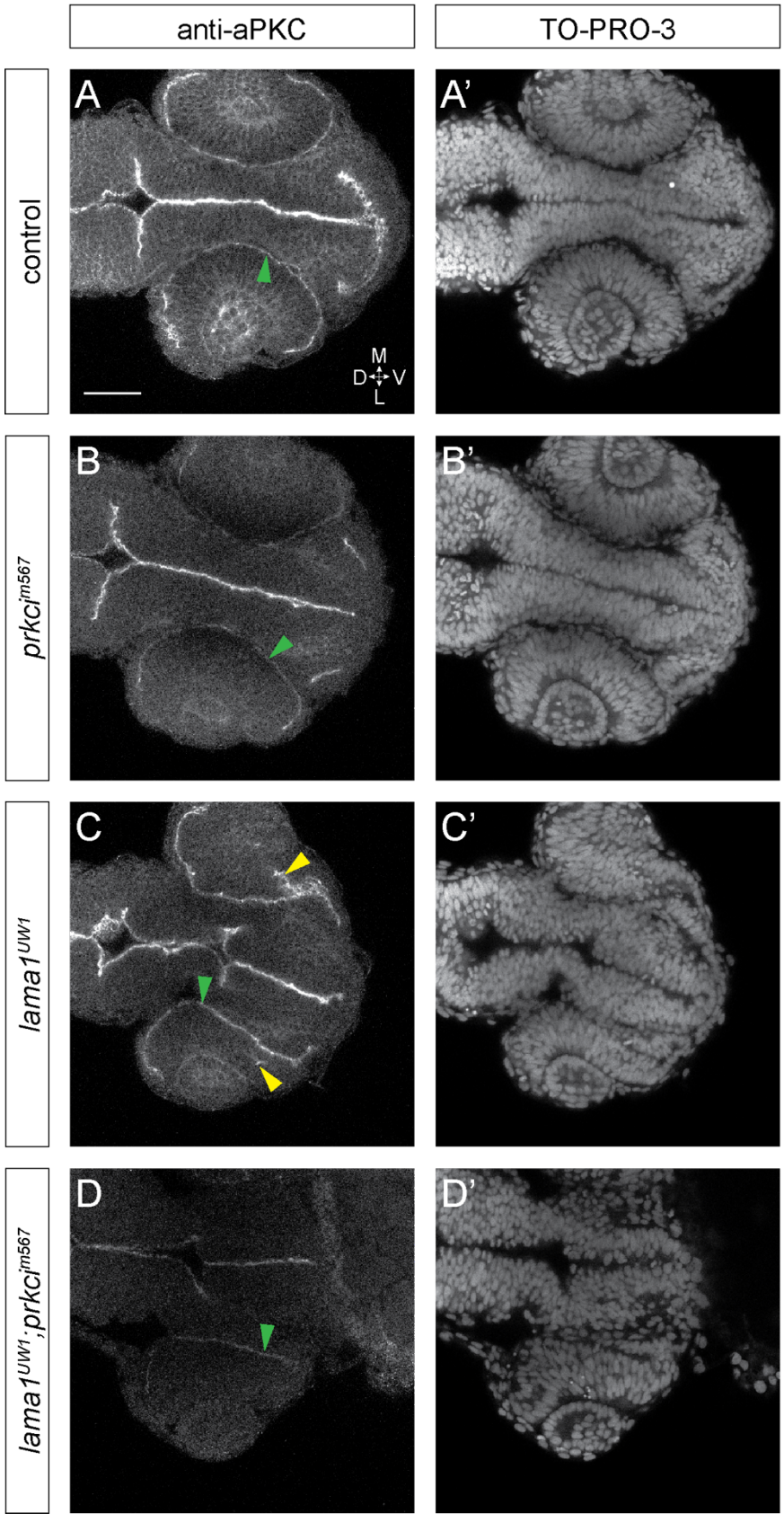
anti-aPKC
TO-PRO-3
control
prkci^m567
lama1^UW1
lama1^UW1;prkci^m567
A
A'
B
B'
C
C'
D
D'
M
D
V
L

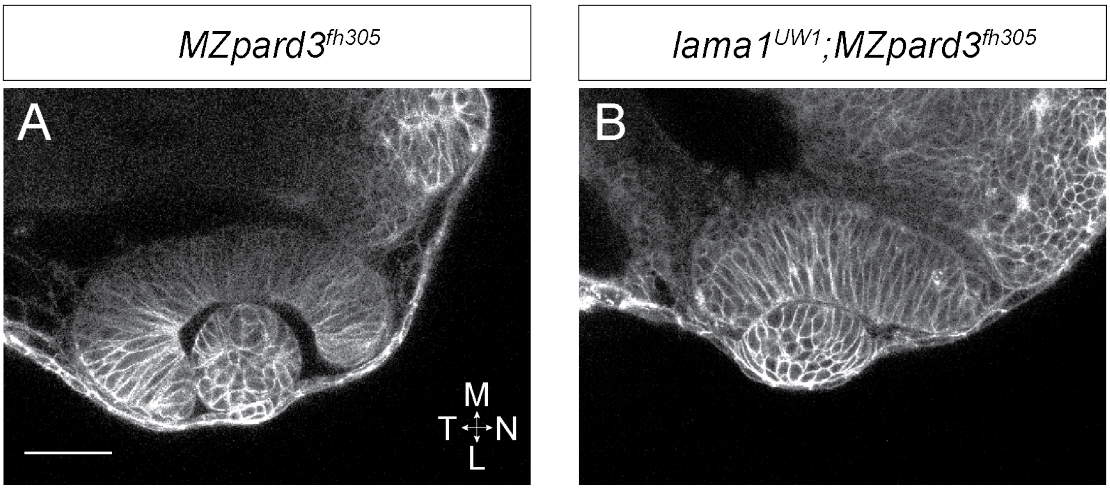

Figure 4.3. Maternal-zygotic loss of *pard3* does not rescue optic cup morphogenesis in *lama1* mutants. (A-B) Dorsal view, single confocal sections from 4D datasets of 24 hpf *MZpard3*^{fh305} single mutant (A) or *lama1*^{UW1}*;MZpard3*^{fh305} double mutant (B) embryos expressing EGFP-CAAX. Scale bar, 50 μm. M, medial; L, lateral; N, nasal; T, temporal.

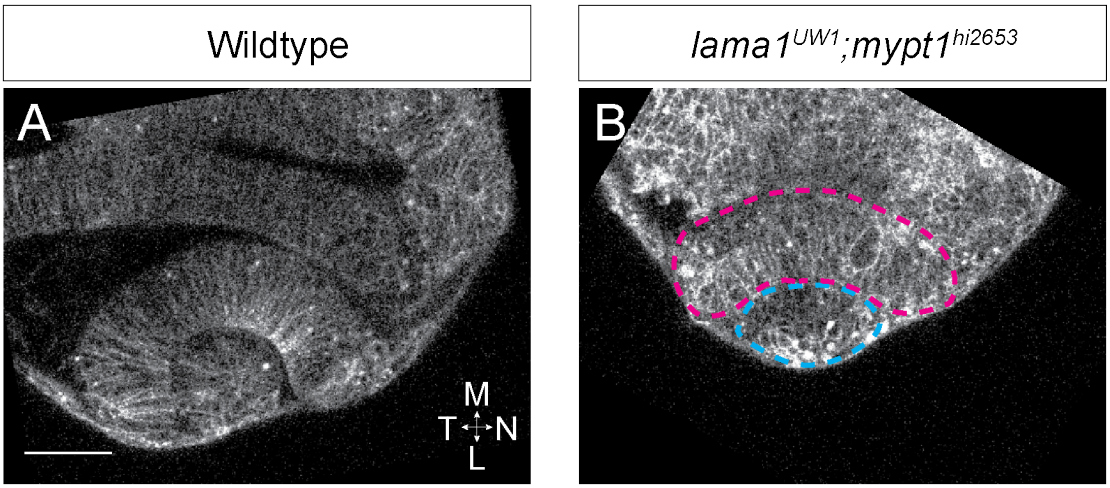

Figure 4.4. Inducing ectopic nonmuscle myosin II constriction does not rescue optic cup morphogenesis in *lama1* mutants. (A-B) Dorsal view, single confocal sections from 4D datasets of 24 hpf wildtype (A) or *lama1*^{UW1};*mypt1*^{hi2653} double mutant (B) embryos expressing lyn-mCherry. The optic cup is outlined in (B) for visual clarity: the lens is outlined in blue, pink outlines the neural retina and RPE. Scale bar, 50 μm. M, medial; L, lateral; N, nasal; T, temporal.

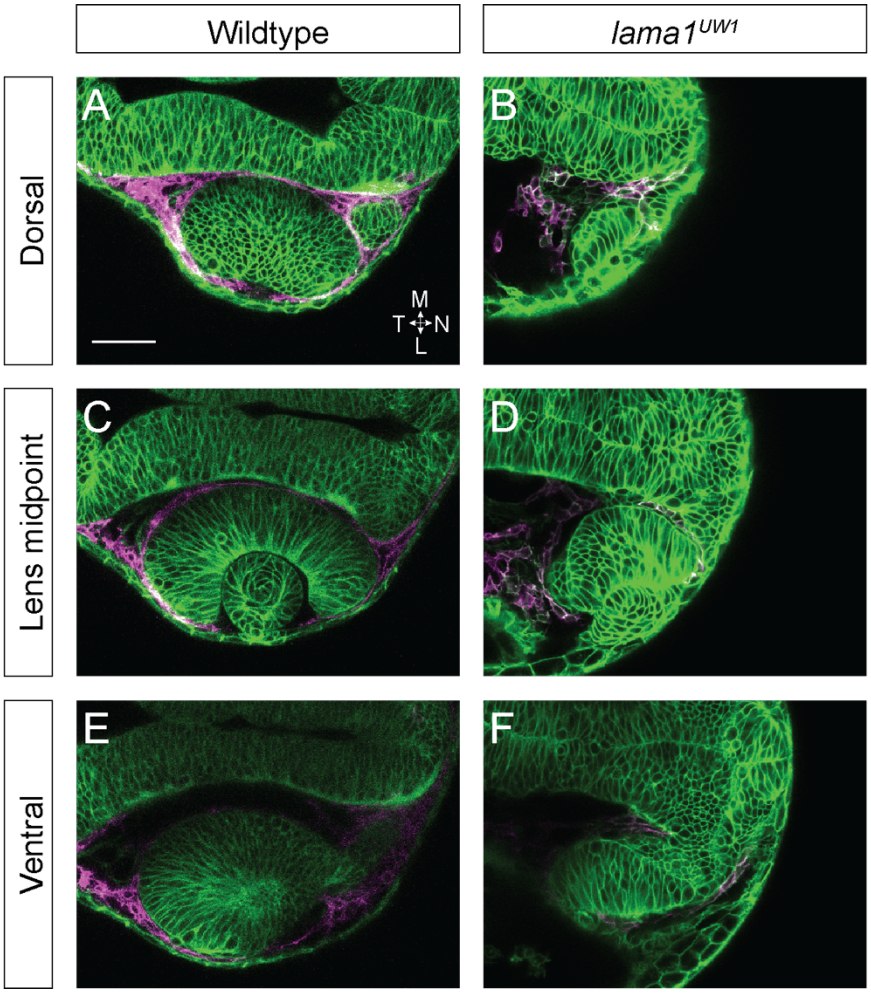

Figure 4.5. Laminin is not required for neural crest migration around the optic cup. (A-F) Representative sections from the dorsal (A, B), lens midpoint (C, D), and ventral (E, F) optic cups of 24 hpf wildtype (A, C, E) and *lama1*^{UW1} mutant (B, D, F) zebrafish expressing the *sox10:memRFP* transgene which labels neural crest cells (magenta). Embryos also expressed EGFP-CAAX to visualize all cell membranes (green). Scale bar, 50 μm. M, medial; L, lateral; N, nasal; T, temporal.

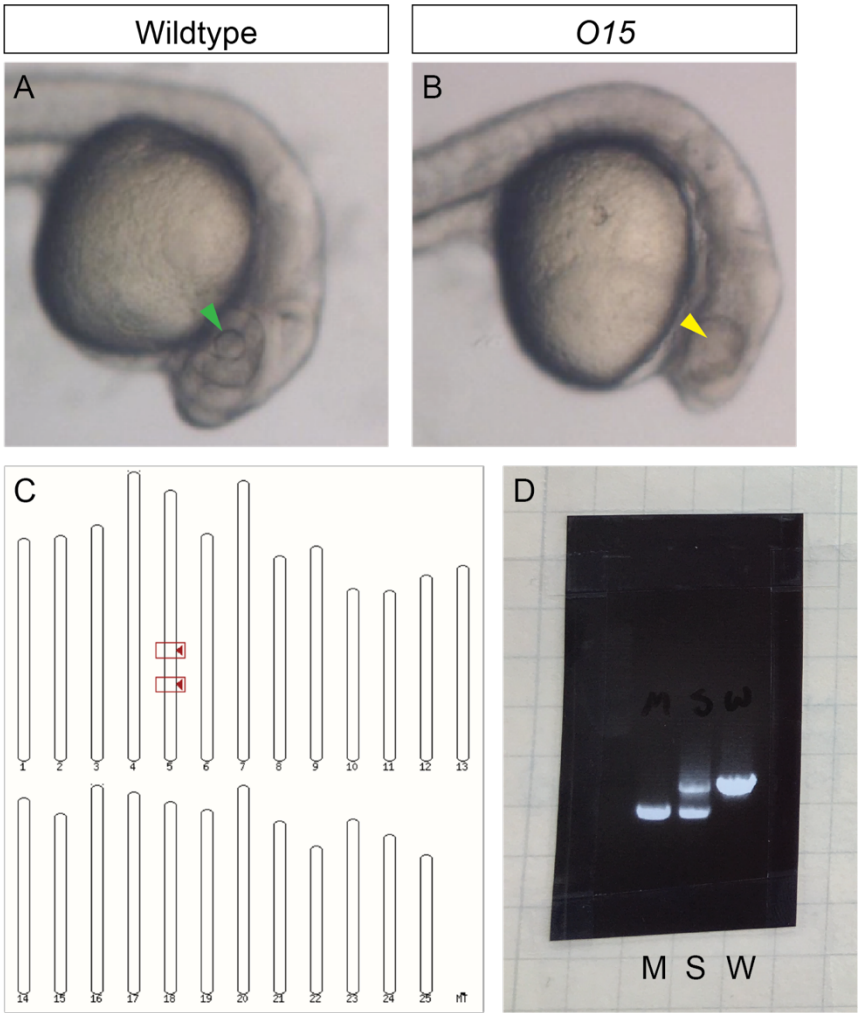

Figure 4.6. The *O15* deficiency phenotype, genomic location, and genotyping amplicon. (A, B) Brightfield images of 24 hpf wildtype sibling (A) and *O15* mutant embryos (B). Green arrowhead in (A) denotes the lens, while the yellow arrowhead in (B) indicates the obscured/hidden lens in the *O15* mutant. (C) Overlaid screenshots of Ensembl BLAT alignment results using either the 5' or 3' end of the sequenced *O15* deficiency. Red arrows bound the deficiency on chromosome 5. (D) Photograph from my lab notebook, dated August 18, 2016. 0.8% TAE gel with results from *O15* genotyping PCRs. M = mutant sample, with a band only at 497 bp. S = heterozygous sibling sample, with bands at both 497 and 774 bp. W = wildtype control sample, with a single band at 774 bp.

References

Akhtar, N., Streuli, C.H., 2013. An integrin-ILK-microtubule network orients cell polarity and lumen formation in glandular epithelium. Nat. Cell Biol. 15, 17–27. https://doi.org/10.1038/ncb2646

Amsterdam, A., Nissen, R.M., Sun, Z., Swindell, E.C., Farrington, S., Hopkins, N., 2004. Identification of 315 genes essential for early zebrafish development. Proc. Natl. Acad. Sci. U. S. A. 101, 12792–7. https://doi.org/10.1073/pnas.0403929101

Bergstralh, D.T., Lovegrove, H.E., St Johnston, D., 2013. Discs large links spindle orientation to apical-basal polarity in drosophila epithelia. Curr. Biol. 23, 1707–1712. https://doi.org/10.1016/j.cub.2013.07.017

Blasky, A.J., Pan, L., Moens, C.B., Appel, B., 2014. Pard3 regulates contact between neural crest cells and the timing of Schwann cell differentiation but is not essential for neural crest migration or myelination. Dev. Dyn. 243, 1511–1523. https://doi.org/10.1002/dvdy.24172

Bogdanović, O., Delfino-Machín, M., Nicolás-Pérez, M., Gavilán, M.P., Gago-Rodrigues, I., Fernández-Miñán, A., Lillo, C., Ríos, R.M., Wittbrodt, J., Martínez-Morales, J.R., 2012. Numb/Numbl-Opo antagonism controls retinal epithelium morphogenesis by regulating integrin endocytosis. Dev. Cell 23, 782–795. https://doi.org/10.1016/j.devcel.2012.09.004

Bryan, C.D., Chien, C. Bin, Kwan, K.M., 2016. Loss of laminin alpha 1 results in multiple structural defects and divergent effects on adhesion during vertebrate optic cup morphogenesis. Dev. Biol. 416, 324–337. https://doi.org/10.1016/j.ydbio.2016.06.025

Bryant, D.M., Datta, A., Rodríguez-Fraticelli, A.E., Peränen, J., Martín-Belmonte, F., Mostov, K.E., 2010. A molecular network for de novo generation of the apical surface and lumen. Nat. Cell Biol. 12, 1035–1045. https://doi.org/10.1038/ncb2106

Chauhan, B.K., Disanza, A., Choi, S.-Y., Faber, S.C., Lou, M., Beggs, H.E., Scita, G., Zheng, Y., Lang, R.A., 2009. Cdc42- and IRSp53-dependent contractile filopodia tether presumptive lens and retina to coordinate epithelial invagination. Development 136, 3657–67. https://doi.org/10.1242/dev.042242

Deng, W.-M., Schneider, M., Frock, R., Castillejo-Lopez, C., Gaman, E.A., Baumgartner, S., Ruohola-Baker, H., 2003. Dystroglycan is required for polarizing the epithelial cells and the oocyte in Drosophila. Development 130, 173–184. https://doi.org/10.1242/dev.00199

Granero-Moltó, F., Sarmah, S., O'Rear, L., Spagnoli, A., Abrahamson, D., Saus, J., Hudson, B.G., Knapik, E.W., 2008. Goodpasture antigen-binding protein and its spliced variant, ceramide transfer protein, have different functions in the modulation of apoptosis

during zebrafish development. J. Biol. Chem. 283, 20495–20504. https://doi.org/10.1074/jbc.M801806200

Gutzman, J.H., Graeden, E.G., Lowery, L.A., Holley, H.S., Sive, H., 2008. Formation of the zebrafish midbrain-hindbrain boundary constriction requires laminin-dependent basal constriction. Mech. Dev. 125, 974–983. https://doi.org/10.1016/j.mod.2008.07.004

Gutzman, J.H., Sahu, S.U., Kwas, C., 2015. Non-muscle myosin IIA and IIB differentially regulate cell shape changes during zebrafish brain morphogenesis. Dev. Biol. 397, 103–115. https://doi.org/10.1016/j.ydbio.2014.10.017

Gutzman, J.H., Sive, H., 2010. Epithelial relaxation mediated by the myosin phosphatase regulator Mypt1 is required for brain ventricle lumen expansion and hindbrain morphogenesis. Development 137, 795–804. https://doi.org/10.1242/dev.042705

He, L., Wang, X., Tang, H.L., Montell, D.J., 2010. Tissue elongation requires oscillating contractions of a basal actomyosin network. Nat. Cell Biol. 12, 1133–1142. https://doi.org/10.1038/ncb2124

Hill, J.T., Demarest, B.L., Bisgrove, B.W., Gorsi, B., Su, Y., Yost, H.J., 2013. MMAPPR: Mutation mapping analysis pipeline for pooled RNA-seq. Genome Res. 23, 687–697. https://doi.org/10.1101/gr.146936.112

Horne-Badovinac, S., Lin, D., Waldron, S., Schwarz, M., Mbamalu, G., Pawson, T., Jan, Y.N., Stainier, D.Y.R., Abdelilah-Seyfried, S., 2001. Positional cloning of heart and soul reveals multiple roles for PKCλ in zebrafish organogenesis. Curr. Biol. 11, 1492–1502. https://doi.org/10.1016/S0960-9822(01)00458-4

Huang, H., Ruan, H., Aw, M.Y., Hussain, A., Guo, L., Gao, C., Qian, F., Leung, T., Song, H., Kimelman, D., Wen, Z., Peng, J., 2008. Mypt1-mediated spatial positioning of Bmp2-producing cells is essential for liver organogenesis. Development 135, 3209–3218. https://doi.org/10.1242/dev.024406

Huang, J., Rajagopal, R., Liu, Y., Dattilo, L.K., Shaham, O., Ashery-Padan, R., Beebe, D.C., 2011. The mechanism of lens placode formation: A case of matrix-mediated morphogenesis. Dev. Biol. 355, 32–42. https://doi.org/10.1016/j.ydbio.2011.04.008

Ivanovitch, K., Cavodeassi, F., Wilson, S.W., 2013. Precocious acquisition of neuroepithelial character in the eye field underlies the onset of eye morphogenesis. Dev. Cell 27, 293–305. https://doi.org/10.1016/j.devcel.2013.09.023

Jones, T.A., Metzstein, M.M., 2011. A novel function for the PAR complex in subcellular morphogenesis of tracheal terminal cells in Drosophila melanogaster. Genetics 189, 153–164. https://doi.org/10.1534/genetics.111.130351

Kettleborough, R.N.W., Busch-Nentwich, E.M., Harvey, S.A., Dooley, C.M., De Bruijn,

E., Van Eeden, F., Sealy, I., White, R.J., Herd, C., Nijman, I.J., Fényes, F., Mehroke, S., Scahill, C., Gibbons, R., Wali, N., Carruthers, S., Hall, A., Yen, J., Cuppen, E., Stemple, D.L., 2013. A systematic genome-wide analysis of zebrafish protein-coding gene function. Nature 496, 494–497. https://doi.org/10.1038/nature11992

Khyrul, W.A.K.M., LaLonde, D.P., Brown, M.C., Levinson, H., Turner, C.E., 2004. The integrin-linked kinase regulates cell morphology and motility in a Rho-associated kinase-dependent manner. J. Biol. Chem. 279, 54131–54139. https://doi.org/10.1074/jbc.M410051200

Kimmel, C.B., Ballard, W.W., Kimmel, S.R., Ullmann, B., Schilling, T.F., 1995. Stages of embryonic development of the zebrafish. Dev. Dyn. an Off. public 203, 253–310. https://doi.org/10.1002/aja.1002030302

Kirby, B.B., Takada, N., Latimer, A.J., Shin, J., Carney, T.J., Kelsh, R.N., Appel, B., 2006. In vivo time-lapse imaging shows dynamic oligodendrocyte progenitor behavior during zebrafish development. Nat. Neurosci. 9, 1506–1511. https://doi.org/10.1038/nn1803

Lerner, D.W., McCoy, D., Isabella, A.J., Mahowald, A.P., Gerlach, G.F., Chaudhry, T.A., Horne-Badovinac, S., 2013. A rab10-dependent mechanism for polarized basement membrane secretion during organ morphogenesis. Dev. Cell 24, 159–168. https://doi.org/10.1016/j.devcel.2012.12.005

Martin-Belmonte, F., Mostov, K., 2008. Regulation of cell polarity during epithelial morphogenesis. Curr. Opin. Cell Biol. 20, 227–234. https://doi.org/10.1016/j.ceb.2008.01.001

Martin, A.C., Goldstein, B., 2014. Apical constriction: Themes and variations on a cellular mechanism driving morphogenesis. Development 141, 1987–98. https://doi.org/10.1242/dev.102228

Martinez-Morales, J.R., Rembold, M., Greger, K., Simpson, J.C., Brown, K.E., Quiring, R., Pepperkok, R., Martin-Bermudo, M.D., Himmelbauer, H., Wittbrodt, J., 2009. Ojoplano-mediated basal constriction is essential for optic cup morphogenesis. Development 136, 2165–2175. https://doi.org/10.1242/dev.033563

Muschler, J., Levy, D., Boudreau, R., Cells, T., Henry, M., Campbell, K., Bissell, M.J., 2002. A role for dystroglycan in epithelial polarization: Loss of function in breast tumor cells. Cancer Res. 7102–7109.

Nicolás-Pérez, M., Kuchling, F., Letelier, J., Polvillo, R., Wittbrodt, J., Martínez-Morales, J.R., 2016. Analysis of cellular behavior and cytoskeletal dynamics reveal a constriction mechanism driving optic cup morphogenesis. Elife 5, 1–24. https://doi.org/10.7554/eLife.15797.001

Schröder, J.E., Tegeler, M.R., Großhans, U., Porten, E., Blank, M., Lee, J., Esapa, C., Blake, D.J., Kröger, S., 2007. Dystroglycan regulates structure, proliferation and differentiation of neuroepithelial cells in the developing vertebrate CNS. Dev. Biol. 307, 62–78. https://doi.org/10.1016/j.ydbio.2007.04.020

Semina, E. V, Bosenko, D. V, Zinkevich, N.C., Soules, K.A., Hyde, D.R., Vihtelic, T.S., Willer, G.B., Gregg, R.G., Link, B.A., 2006. Mutations in laminin alpha 1 result in complex, lens-independent ocular phenotypes in zebrafish. Dev. Biol. 299, 63–77. https://doi.org/10.1016/j.ydbio.2006.07.005

Sidhaye, J., Norden, C., 2017. Concerted action of neuroepithelial basal shrinkage and active epithelial migration ensures efficient optic cup morphogenesis. Elife 6, 1–29. https://doi.org/10.7554/eLife.22689

Szabó, A., Melchionda, M., Nastasi, G., Woods, M.L., Campo, S., Perris, R., Mayor, R., 2016. In vivo confinement promotes collective migration of neural crest cells. J. Cell Biol. 213, 543–555. https://doi.org/10.1083/jcb.201602083

Thisse, B., Pflumio, S., Fürthauer, M., Loppin, B., Heyer, V., Degrave, A., Woehl, R., Lux, A., Steffan, T., Charbonnier, X.Q., Thisse, C., 2001. Expression of the zebrafish genome during embryogenesis [WWW Document]. ZFIN Direct Data Submiss. https://doi.org/cb646

Wang, Y.C., Khan, Z., Kaschube, M., Wieschaus, E.F., 2012. Differential positioning of adherens junctions is associated with initiation of epithelial folding. Nature 484, 390–393. https://doi.org/10.1038/nature10938

CHAPTER 5

SUMMARY

Morphogenesis is the dynamic process that generates the stereotypical shape required for the function of most organs. The movements that drive organ morphogenesis must be tightly regulated, as disruptions to these movements can cause severe defects that impair the function of that organ or, in extreme cases, can cause lethality. The vertebrate eye, while not strictly necessary for viability, is one such organ where even small alterations to the shape can have profound detrimental effects on function. In part due to its positioning close to the exterior of the embryo, the optic cup is an excellent model system to investigate morphogenetic programs. In turn, lessons learned from the optic cup may prove useful to understanding how other organ systems develop.

We seek to understand the foundational events which are required for development of the vertebrate optic cup, and utilize the zebrafish optic cup as a system to study the molecules and interactions required for optic cup morphogenesis. The zebrafish is optically transparent at early stages which enables live microscopic visualization of the cell and tissue movements throughout organ morphogenesis. Zebrafish genetics have reached a point where both forward and reverse genetic approaches are viable options to identify and characterize genes that are required for these processes.

Extracellular matrix (ECM) proteins are found surrounding the vertebrate optic

vesicle, and using a zebrafish *lama1* mutant, we characterized the role of the laminin-α1 protein during optic cup morphogenesis (Bryan et al., 2016). Briefly, laminin-α1 is required for formation and deposition of the heterotrimeric protein laminin-1, and loss of this protein causes severe optic cup morphogenesis defects including an ectopically wide optic stalk, a flattened retina, and an almond shape lens which undergo degeneration at later stages. Laminin-1 normally drives adhesion to the ECM at the constricting optic stalk, and somewhat confoundingly, represses retinal adhesions to the ECM. Laminin is also required for proper lamination of the neural retina as well as establishment of apical-basal polarity within the optic cup.

We attempted to determine the molecular mechanism by which laminin signals to polarize the optic vesicle, and determined that the laminin receptor dystroglycan is not required to establish polarity within this tissue. However, this does not rule out the possibility that dystroglycan could be sufficient to signal to polarize the optic cup in the absence of focal adhesions. Investigating the role of focal adhesions in establishing tissue polarity, both with and without dystroglycan, would address this possibility and conclusively establish which ECM receptors are required for this process. In investigating polarity, we also sought to determine whether the ectopic apical surfaces that form in the *lama1* mutant were the underlying cause of the optic malformations we observed. Compound ablation of *lama1* and the apical complex member *prkci* suggested that these malformations were not directly caused by establishment of ectopic apical polarity, but maternal contributions of aPKC confounded interpretation of these experiments. Instead, we turned to a maternal-zygotic *pard3* mutant which we combined with the *lama1* mutation. This enabled us to test whether complete ablation of functional apical

complexes would have an effect on optic cup morphogenesis, and whether this ablation could in turn rescue the morphogenesis defects we observed in the absence of laminin. To our surprise, we observed no optic cup malformations in *MZpard3* mutants, indicating that the apical polarity complex is indeed dispensable for optic cup morphogenesis. Additionally, we found that *lama1;MZpard3* double mutants displayed the same morphogenesis defects we previously observed in *lama1* single mutants. From these data, we can conclude that laminin is absolutely required for optic cup morphogenesis, and the loss of proper apical polarity seen in *lama1* mutants does not underlie the morphogenesis defects we observe.

In addition to our efforts to understand the role of specific ECM components, we also sought to identify the specific contributions of extraocular tissues during optic cup morphogenesis. In particular, our studies centered on how the neural crest subset of periocular mesenchymal cells regulate optic cup morphogenesis. Mutants lacking neural crest cells display defects in rim movement during optic cup invagination, and aberrant choroid fissure formation with subsequent coloboma. To our surprise, we found that neural crest cells modify the ECM surrounding the optic cup by depositing the ECM protein nidogen. Nidogen primarily serves to crosslink laminin and collagen IV matrices and is critical for formation of most basement membranes. We demonstrate that nidogen is expressed within neural crest cells and not the optic vesicle, and that neural crest cells are required for basement membrane formation along the basal surface of the retinal pigment epithelium, likely through deposition of nidogen. Optic cup morphogenesis is partially rescued when nidogen is ubiquitously expressed in the absence of neural crest cells, which indicates that one of the primary roles of these cells during optic cup

morphogenesis is to modify the ECM.

The work presented in this dissertation demonstrates new and critical roles for the extracellular matrix as a regulator of morphogenesis *in vivo*. The ECM is known to be important for many organs to develop, but how interactions with this dynamic and complex substrate regulate tissue rearrangements and shape changes is just beginning to be understood. Thus, many questions regarding how the optic cup undergoes morphogenesis still remain. The ECM surrounding the optic cup is complex and contains fibronectin and collagen IV, but the function of either protein in regulating optic cup morphogenesis remains unknown. Use of conditional mutant alleles or other interference methods will almost certainly need to be used to study these proteins, but they are very likely to regulate some aspect of early eye development. How the optic cup itself receives and processes the signals from the ECM is also an open question. Actomyosin mediated cytoskeletal remodeling occurs in response to cell-ECM adhesion, but how mechanical forces are transmitted through the ECM and into the cell, and subsequently processed into cellular behaviors, remains to be seen. Finally, an entire population of mesodermal mesenchymal cells interacts with the eye during optic cup morphogenesis, but the role of these cells during this process remain mysterious. New tools and analytical methods, coupled with established mutants, could answer how these cells interact with the developing eye and whether they are required for optic cup development.

References

Bryan, C.D., Chien, C. Bin, Kwan, K.M., 2016. Loss of laminin alpha 1 results in multiple structural defects and divergent effects on adhesion during vertebrate optic cup morphogenesis. Dev. Biol. 416, 324–337. https://doi.org/10.1016/j.ydbio.2016.06.025